Ionotropic receptors (IRs) contribute to temperature synchronization in *Drosophila melanogaster.*

Chenghao Chen

School of Biological and Chemical Sciences,

Queen Mary, University of London

Thesis submitted in fulfillment of

the requirements of the University of London for

the Degree of Philosophiae Doctor (Ph.D.)

September 2013

Declaration

Hereby I certify that the research presented in this thesis are the product of my own work, and that any ideas, quotations or data adaptations from the work of the others, published or otherwise are fully acknowledged and cited according to standard referencing practices of the discipline. I also acknowledge the thorough guidance and support from my supervisor, Professor Ralf Stanewsky.

23th September 2013

Chenghao Chen

Acknowledgement

Completing my PhD was probably the most challenging thing of in the first 30 years of my life, I would never able to accomplish it sanely without the selfless help of the dear friends, especially the following people.

Foremost, I would like to express my sincere gratitude to my supervisor Prof. Ralf Stanewsky for the continuous support of my Ph.D study and research in the last four years, for his patience, motivation, enthusiasm, and immense knowledge. His guidance helped me in all the time of research as well as writing of this thesis. I could not have imagined having a better mentor for my PhD study.

Besides my advisor, I would like to thank the rest of my thesis committee: Prof. Richard Baines and Dr. Joerg Albert, for their encouragement, insightful comments, and hard questions which inspire me. I had a very good time during the viva.

My sincere thanks also go to my panel committee Dr. Angelika Stollewerk and Dr. Fanis Missirlis , for their support, guidance and helpful suggestions in last four years. Their guidance has served me well and I owe them my heartfelt appreciation.

I also thank my labmates in Ralf's Group. Previous members : Niki, Alekos, Carla, Gisela, Joanna and Werner and present members: Maite, Sanne and Min for the friendly atmosphere in the lab and stimulating discussions. Specific thanks to old lab member Ko-fan, for his patient guidance for me at the beginning of my PhD and also for current lab member Adam, who criticized and corrected my grammar mistakes in my thesis. My thanks also go to the mates in London, Zhe, Huijuan, Shuang, Zhen, Costas and other friends for all the fun we have had in the last four years.

Moreover, I would like to thank my teachers and friends in China: Prof. Wei Xie, who first time brings me to the amazing Drosophila world and fully support me to make the decision of studying PhD in abroad. Prof. Junhai Han and Prof.Ming Fang for all the tips in experiments. In particular, I am grateful to Prof. Shanglian Hu for enlightening me the first glance of research.

Last but equally important, I would like to thank my family members: my wife and soul mate Min Xu, who stays on my back all the time and most importantly, bring my pretty angel Sophie to me. My precious daughter Sophie (Xiao Xiao), who brings all the happiness for me to color my life. Also my thanks for my parents Run Chen and Yali Yang, and my parents in law Tongshi Xu and Shicui Li, for all their fully support and

unconditional love, which is always my raw power to motivate me to come to the finishing line.

Abstract

Like most organisms, *Drosophila melanogaster* can synchronize its physiological and behavioural processes by possessing internal circadian clock that regulates. Naturally fluctuating timing cues, like light and temperature (also known as Zeitgebers), synchronize these endogenous and self-sustained clocks with external time. In *Drosophila*, synchronization of the circadian clock by light has been studied in detail, but much less is known about the molecular mechanisms underlying temperature entrainment.

Previous data from our lab shows that Nocte, a Chordotonal organ (Ch organ) located protein, is required for normal temperature entrainment in *Drosophila*. However, neither the function of Nocte in temperature entrainment nor the molecular underlying mechanisms are clear. To address these issues, a proteomics strategy of combing co-immunoprecipitation and MS/MS sequencing was applied to isolate potential interactors of Nocte. IR25a was one of the most promising candidates, which was later confirmed by behavioural tests using RNA interference: Reducing *IR25a* expression in Ch

organ resulted in abnormal behaviour during temperature cycles, similar to what had been described for Nocte mutant.

To further confirm the interaction between Nocte and IR25a, I showed that IR25a physically interacts with Nocte in vivo. Moreover, using an *IR25a-gal4* line, I was able to show that IR25a is expressed in subsets of chordotonal organs (Ch organ) including Johnston's Organs (JO), where Nocte is also highly expressed. These results, along with the behavioural data mentioned above are consistent with the proteomics results and suggest that Nocte and IR25a physically and functionally interact.

IR25a mutants were employed to further investigate the function of IR25a in temperature entrainment. First of all, I found that both central and peripheral clocks in wild type flies can be synchronized to temperature cycles with only two degree differences (12h: 12h, 27 °C: 25 °C). In contrast, synchronization of locomotor activity rhythms in the IR25a null mutants to the same temperature cycles and other TC's with 2°C amplitude was eliminated. Under the same conditions, the oscillations of the core clock proteins TIMLESS (TIM) and PERIOD (PER) that normally occur in fly heads were completely abolished in

IR25a null mutants, suggesting that IR25a is required for temperature entrainment of peripheral clocks. In the central brain pacemaker neurons, the oscillations of TIM in dorsal and lateral neurons were also affected by the IR25a mutants. On the contrary, IR25a is not required for light entrainment and temperature compensation, suggesting that IR25a is specifically involved in temperature synchronization. Moreover, temperature entrainment of the IR25a null mutants can be partially restored by applying larger temperature intervals (29°C: 25°C) indicating that IR25amay function as amplitude detector independent of absolute temperature values. Finally, neuronal activity in $IR25a^{+}$ neurons is crucial for the synchronization of circadian clocks to low amplitude temperature cycles.

Re-constitution of functional olfactory receptors required the assembly of IR25a with IR76a and IR76b. Interestingly, IR76a and IR76b are neither required for temperature entrainment at the behavioural level nor expressed in the Ch organs. To check if other potential IRs interacting with IR25a exist, I screened the expression pattern of most divergent IRs using *IR-gal4/UAS-GFP* flies. IR56a was isolated as a potential partner of IR25a because it is also expressed in the femur chordotonal organs. To investigate the function of IR56a in temperature entrainment, I generated a null mutant of IR56a.

Surprisingly, this gene is not required for synchronizing clocks to a temperature cycle (27°C: 25°C) at the behavioural level. However, the behavioural and molecular phenotypes of IR56a mutant under different temperature cycles need to be further characterized.

Table of Contents

Chapter 3

List of Figures

List of Tables

Abbreviation

per	*period*	Ch	Chordotonal
tim	*timless*	ac	antenna coeloconic
cyc	*Cycle*	TC	Temperature cycles
clk	*clock*	LD	Light-dark cycle
cry	*cryptochrome*	LL	Constant light
dbt	*double time*	DD	Constant darkness
jet	jetleg	ZT	Zeitgeber Time
IR	Ionotropic Receptor	CT	Circadian Time
iGluRs	ionotropic Glutamate receptor	JO	Johnston's Organ
norpA	no receptor potential A	*eys*	*Eyeshut*
TRP	Transient Receptor Potential	M cells	Morning cells
SGG	SHAGGY	E cells	Evening cells
PP2A	PROTEIN PHOSPHATASE 2A	AMMC	antennal mechanosensory and motor center
PP1	PROTEIN PHOSPHATASE 1	DAM	*Drosophila* activity monitor
PDF	Pigment Dispersing Factor	LPN	Lateral posterior neurons
LN	Lateral neurons	QSM	QUASIMODO
s-LNv	Small ventrolateral neurons	DN	Dorsal neuron
l-LNv	Large ventrolateral neurons	*nocte*	no circadian temperature entrainment
SOG	subesophageal ganglion	SCN	suprachiasmatic nuclei
VIP	vasoactive intestinal peptide	AVP	arginine vasopressin
LNd	Dorsolateral neurons	PYX	*pyrexia*

Chapter 1
Introduction

1.1 Circadian rhythm and entrainment in *Drosophila.*

1.1.1 Circadian rhythm and history of Chronobiology

Circadian rhythms are oscillations in biological processes with a period of approximately 24 hours and are present in most living organisms. These rhythms are not only passively driven by environmental timing cues, but also persist under constant environmental conditions for several days or even weeks; therefore indicating that they are generated by self-sustained endogenous oscillators, which has become known as the circadian clock. Canonical Circadian clocks have three basic components: an input pathway that receives environmental cues and transmits them to the core circadian oscillator, a central circadian oscillator that keeps circadian time and activates output pathways, and output pathways that control various metabolic, physiological and behaviour processes (Figure 1.1, reviewed by Hardin,2006).

The first observation of circadian rhythm was performed by French physicist Jacques d'Ortous de Mairan (1678-1771) in 1729, where he

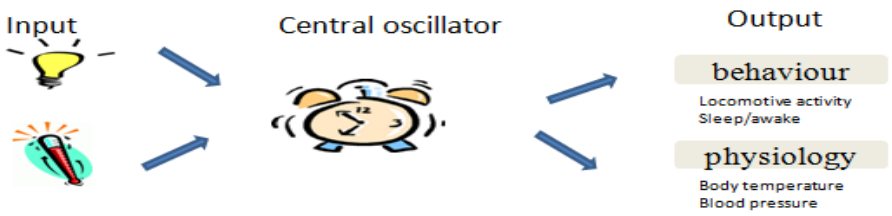

Figure 1.1 The circadian system model.
The components of the input pathway receive the cycling information from the environment and transmit them to the central oscillator. Rhythmic physiological and behavioural processes are then generated via the output pathways.

systematically observed rhythmic leaf movement in the heliotrope plant, *Mimosa pudica*, and that the rhythm was maintained even under constant darkness (free-running period, Figure 1.2). This study implied the existence of an internal biological clock. Following this, many scientists have devoted to this field and revealed that circadian rhythmic behaviour is widespread in biology, from prokaryotes to human beings, which suggests this circadian timekeeping mechanism is conserved through evolution and existed in most living organisms. In the early 20th century, the existence of the circadian clock was further shown by the discovery of its hereditability in runner bean seedlings (*Phaseolus coccineus,* Bunning, 1932; reviewed in McClung, 2006). From the 1950s to 1960s, two dedicated scientists, Collin Pittendrigh (1918-1996) and

Figure 1.2 First description of circadian rhythm in 1729.
Left: the leaves of *Mimosa pudica* are open during the day (left) but curl up at night. Right: Jacques d'Ortous de Mairan(1678-1771)

Jurgen Aschoff (1913-1998) further characterised and defined the key features of circadian clock through a series of behavioural investigations conducted on animals. Their findings led to the development of a new scientific discipline: Chronobiology (Greek, Chronos= time), and most importantly elaborated the three basic criterions of circadian clocks (Menaker, 1996; Daan and Gwinner, 1998; Daan, 2000).

The three criteria of the circadian clocks are: self-sustainability, entrainable to cues and temperature compensated. In detail, self-sustainability means that the circadian clock is able to sustain 24 hour rhythmic behaviour in the absence of any external cues. Therefore it is a self sustained oscillating process. Second, entrainable means the 'time' of the circadian clock can be shifted or resetted by external cues such as light and temperature. In the other words, the circadian clock can be synchronized to external daily rhythms, which helps organisms to adjust to daily and seasonal changes. Therefore, the external cues which are capable of entraining circadian clocks are defined as zeitgebers (German, zeit= time; geber= giver) and zeitgeber time (ZT) is the time at which an organism clock is synchronized to the cycle of the external stimuli. Third, temperature compensation means that the period length of the circadian clock remains the same at different temperatures. Indeed the same period length of the rhythmic eclosion of *Drosophila*

melanogaster was observed in constant darkness at various constant temperatures (Pittendrigh, 1954; Zimmerman et al., 1968). These three properties are the basis of the circadian clock, and were later used to identify clocks in humans (reviewed in Roenneberg and Merrow, 2005).

1.1.2 Circadian clocks in *Drosophila melanogaster*

1.1.2.1 Searching for clock genes

As fruit flies (*Drosophila melanogaster*) have been applied as a powerful genetic tool with the advantages of a relatively short lifespan and easy maintenance, it has become an ideal animal model to apply forward genetic screens in order to investigate the mechanism of circadian rhythms. Using behavioural screening to monitor *Drosophila* eclosion in 1971, Konopka and Benzer found three different alleles which have different circadian phenotypes. In constant darkness the per^{0} mutant showed no rhythmicity, while per^{S} and per^{L} respectively showed shortened and lengthened periods when compared to that of the wild type. All of these mutants were mapped to the same gene locus on the *X* chromosome which was named as *period* (Figure 1.3, Konopka and Benzer, 1971). Cloning and the subsequent analysis of its expression led to the first molecular model of the circadian oscillator, an

auto-regulatory feedback loop in gene expression.

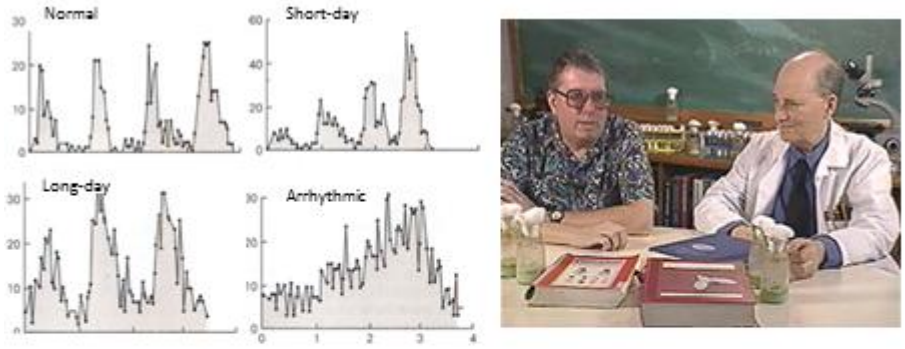

Figure 1.3 The first clock mutants identified by Konopka and Benzer.

Left: Eclosion rhythms in constant darkness, for populations of rhythmically normal and mutant flies. (Taken from Konopka et al., 1971) Right: Ron Konopka (left) and his mentor Seymour Benzer (1921-2007).

1.1.2.2 The transcriptional-translational feedback loop in *Drosophila*

A transcriptional-translational feedback loop model of the *Drosophila* central clock is shown in Figure 1.4. In this model, the transcription of *period* (*per*) and another core clock gene: *timless* (*tim*, Sehgal et al.,1994) are activated by the heterodimers formed by two basic-helix-loop-helix/PAS domain transcription factors known as CLOCK (CLK, Allada et al., 1998) and CYCLE (CYC, Rutila et al., 1998). This occurs via the binding to the E-box elements of the two genes (Kyriacou and Rosato, 2000), which therefore induces an increase of *tim* and *per* mRNA but not in protein level (Hall, 2003). As *tim* and *per* transcription takes place, their transcripts accumulate until their mRNAs reach peak during the early night. TIMLESS protein (TIM) is finally translated and forms

heterodimers with PERIOD (PER)-the complex of which is transported back into the nucleus. In the nucleus, the TIM/PER complexes bind to CLK/CYC, and remove CLK/CYC from the E-box and inhibit the transcription of them. The down-regulation of *per* and *tim* transcription therefore decreases the amount of the PER/TIM dimers and this lead to the next round of transcriptional activation mediated by CLK/CYC. Consequently, this process generates continuous mRNA/protein abundance oscillations of *per* and *tim* products (reviewed by Stanewsky, 2002; Hardin, 2006).

Remarkably, the model mentioned above is a simplified version, both PER and TIM levels in the cytoplasm are precisely controlled by a series of post-translational modification processes (Figure 1.4). For example, Phosphorylation of PER is mainly mediated by the kinase DOUBLE TIME (DBT), which is the homologue of the mammalian casein kinase 1 (Kloss et al., 1998; Price et al., 1998; Syed et al., 2011). DBT promotes the degradation of cytoplasmic PER via an ubiquitin-proteasome pathway mediated by the F-box protein SLIMB (Chiu et al., 2008; Ko et al., 2002) and facilitated by the cytoplasmic localization of PER (Kloss et al., 2001; Muskus et al., 2007; Weber and Kay, 2003). On the other hand, TIM is phosphorylated by SHAGGY (SGG) (Martinek et al., 2001), a homologue of GSK3-beta in mammals, which promotes the nuclear entry of the

dimer by binding to the TIM/PER complex (Cyran et al., 2005; Martinek et al., 2001). Therefore, to speed up the clock can be achieved by overexpressing SGG (Stoleru et al., 2007). Whilst the effect of SGG mediated phosphorylation on TIM protein stability remains unclear, perhaps it is related to the competitive binding of the TIM with another F-box protein JETLAG (JET, Koh et al., 2006). The action of PROTEIN PHOSPHATASE 2A (PP2A) and PROTEIN PHOSPHATASE 1 (PP1) (Sathyanarayanan et al., 2004; Fang et al., 2007) on PER and TIM, respectively, promotes the accumulation and the stability of the protein in the cytoplasm and the subsequent entry of the two to the nucleus. All of these modifications together make sure that the feedback loop continuously cycles based with a 24-hour period.

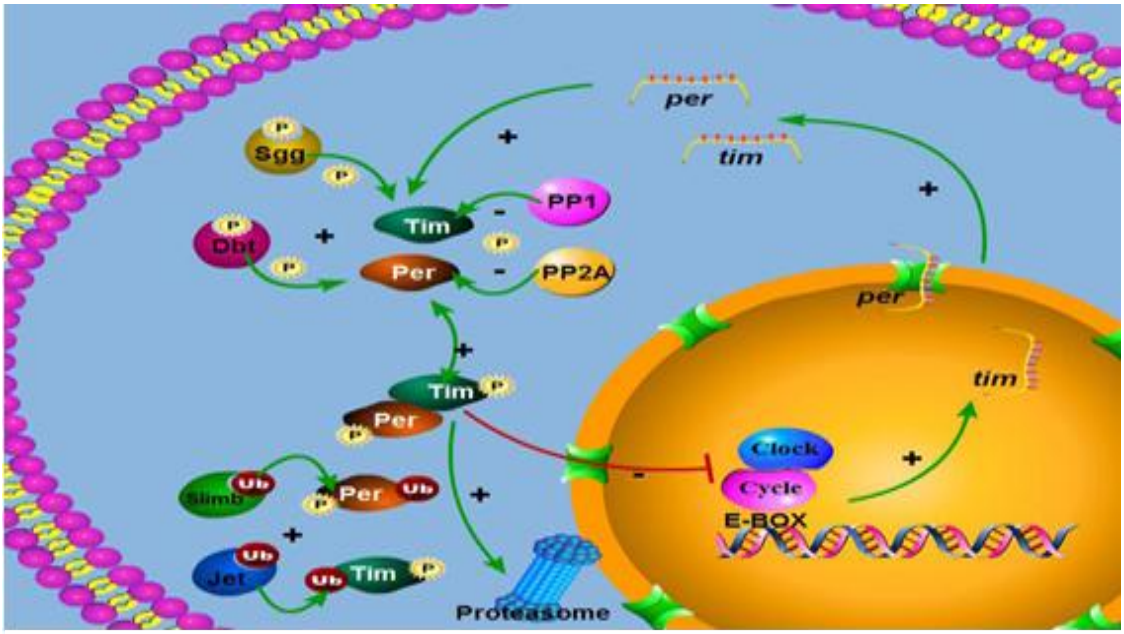

Figure 1.4 The molecular mechanisms in *Drosophila* clock*:* transcription feedback loop. (Taken from Peschel, 2008)

The diagram shows an overview of the important molecular mechanisms in clock cells. The activation of *tim* and *per* transcription and subsequent translation causes the dimerization of the two proteins, the re-entry into the nucleus and inhibition of their own transcription.

1.1.2.3 Light inputs of the *Drosophila* circadian clock at the molecular level

As mentioned before, an entire circadian system not only contains a central oscillator system but also the input and output pathways, which allow *Drosophila* to entrain to environmental cues, such as light (Stanewsky et al., 1998), temperature (Wheeler et al., 1993) and food resources (Xu et al., 2008). Light, working as one of the considerable strongest input factors, modulates oscillations at both molecular and behavioural levels. Transferring of wild type flies from light: dark cycles (LD) to constant light (LL) will lead to the oscillation of clock become arrhythmic not only in locomotor behaviour but also in core clock molecules (Konopka et al., 1989; Mayer et al., 1996; Yoshii et al., 2005).

The basic molecular mechanisms of how light controls behavioural rhythms have been characterized (Fig 1.5). A blue light photoreceptor CRYPTOCHROME (CRY) could be stimulated by light through altering its own structure (Rosato et al, 2001; Fogle et al., 2011), thereby getting the ability to bind to TIM, which then triggers TIM Ubiquitination mediated by JETLAG and degraded via the proteasome (Nadoo et al., 1999; Busza et al., 2004; Koh et al., 2006). When TIM is degraded, the PER/TIM complex cannot be formed and PER is a target of phosphorylation events

by DBT, which thereby leads to PER degradation. These results lead to the disintegration of PER /TIM complex and resetting of their transcription feedback loop (Dunlap, 1999). Thus, the continuous degradation of TIM by CRY occurs when flies expose to LL, which leads to an arrhythmic behavioural phenotype. Although CRY is a major photoreceptor, it is not the only one. Double mutants analysis of *norpA*^{24}*; cry*^{b} revealed that canonical photo transduction is also involved in light entrainment at least at the behavioural level (Stanewsky et al., 1998) and recent study in our lab also demonstrated a novel CRY-independent light input mediated by a ZP domain containing protein, QUASIMODO (QSM), in *Drosophila*. Nevertheless, the molecular degradation mechanism of TIM by QSM is still unclear (Chen et al., 2011).

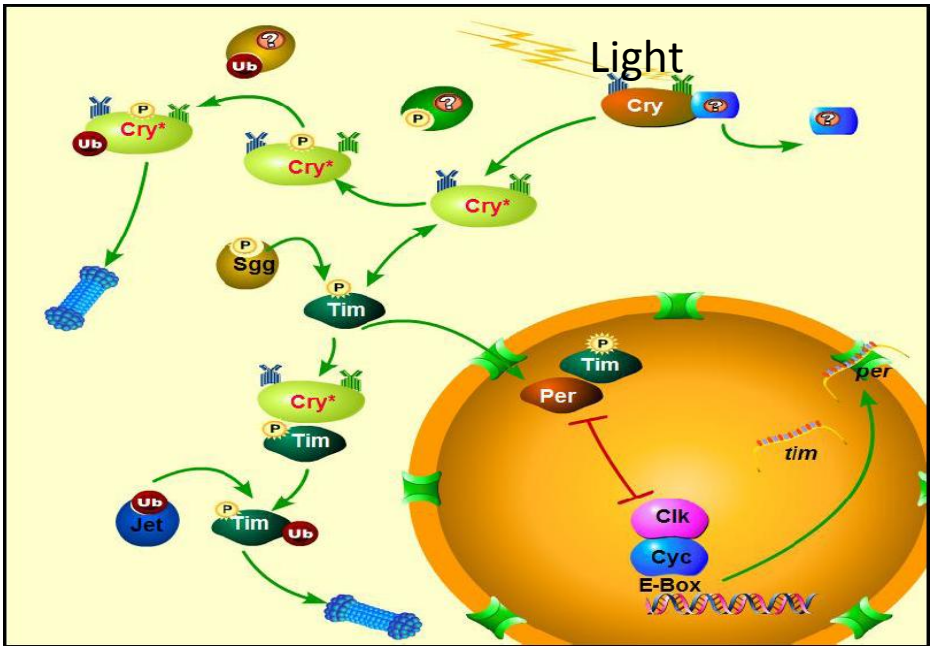

Figure 1.5 The molecular pathway of *Drosophila's circadian photoreception (Taken from Peschel 2008)*

1.1.2.4 Central pacemaker of *Drosophila*

Drosophila circadian core clock is comprised of approximately 150 neurons (75 in each hemisphere) scattered in the brain of the fly. Those so called 'pacemaker neurons' are defined by the presence of PER or TIM (Taghert and Shafer, 2006). According to their anatomic positions, the clock neurons have been divided into two major groups – the dorsal neurons (DNs) and the ventral lateral neurons (LNvs). These DNs and LNvs can be furthermore divided into subgroups (Figure 1.6). The DNs are further divided into DN1s (17 neurons per hemisphere), DN2s (2 neurons), DN3s (40 neurons) and LPN (lateral posterior neurons, 3-4 neurons), while the LNvs are divided into the large ventrolateral neurons (l-LNvs, 4 neurons), the small ventrolateral neurons (s-LNvs, 6 neurons) and the dorsolateral neurons (LNds, 6 neurons) (Helfrich-Forster et al., 2007). Except four core clock genes, genes that are required for light entrainment are also located in subsets of clock neurons. The neuronal peptide pigment dispersing factor (PDF) is expressed in all of the l-LNvs and 4 of the s-LNvs, whereas the expression of CRY is relatively broader (6 DN1, 3 LNds, and all the LNvs). Functional dissection of the sub group of clock neurons revealed that the morning peak in the locomotor behaviour is driven by the PDF-positive LNvs (so called M cells, Figure

1.6), and the evening behaviour of the fly is driven by different clock groups, the LNds, the 5th s-LNv and a subset of DN1 neurons (so called the E cells) (Grima et al., 2004; Rieger et al., 2006; Stoleru et al., 2004). However, this is only a simplified model.

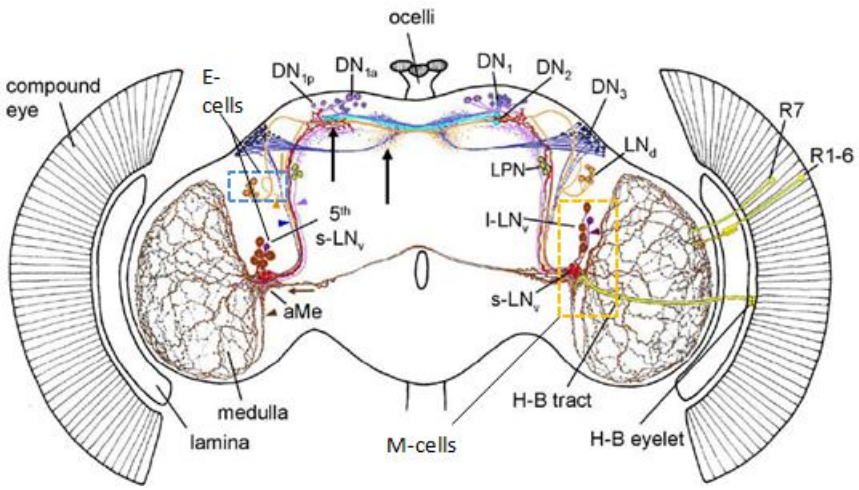

Figure 1.6 Overview of the clock neurons in the adult *Drosophila* brain. (Taken from Helfrich-Forster et al., 2007)
Different groups of clock neurons as well as the light inputs in the adult brain. M-cells (morning cells) and E-cells (evening cells) were highlighted with orange and blue frames respectively.

1.1.3 Temperature synchronization in *Drosophila*

1.1.3.1 Synchronization by temperature cycles in *Drosophila*

Although our understanding of circadian entrainment by light signal is steadily increasing, much less is known about the mechanisms of temperature entrainment. Based on previous research, it is known the

wild-type flies can be robustly synchronized when exposed to temperature cycles (TC) with only 2°C -3 °C amplitude (Wheeler et al., 1993). Locomotor behaviour increases during the warm portion and activity levels reach peak values before cold stage (Yoshii et al., 2005). However, the clock mutant flies such as per^0 could not be entrained with only response to the temperature transition, which indicates that this process needs a functional clock (Wheeler et al., 1993). At the molecular level, PER and TIM in both central (Yoshii et al., 2005; Buza et al., 2007; Gentile et al., 2013; Lee and Montell., 2013) and peripheral clocks (Glaser and Stanewsky, 2005; Yoshii et al., 2005) exhibit rhythmic expression during TC, which is another piece of evidence for that clock genes can be regulated by temperature cycles.

Previous studies also suggest that temperature entrainment interacts with light signals: as discussed before, constant light can lead to arrhythmicity in wild type flies at both the molecular and behavioural level (Emery et al., 2000). Interestingly, temperature entrainment could robustly override this arrhythmicity to rhythmicity (Yoshii T et al., 2002; Glaser and Stanewsky et al., 2005), but the mechanism underlying this process is still unclear.

Like light entrainment, isolated peripheral tissues can be synchronized by

TCs, but isolated brain cannot (Glaser and Stanewsky et al., 2005), indicating that a unknown temperature input pathway located in peripheral tissues is required to synchronize central clocks to TC. The studies in our lab showed that *Drosophila* chordotonal organs (a mechanosensory organ located in the joints of the antenna and limbs), but not the classic thermosensory organs (3rd antennal segment and arista, Sayeed and Benzer 1996), is required for perceiving cycling temperature inputs (Sehadova et al, 2009).

1.1.3.2 Genes involved in temperature entrainment in *Drosophila*

1.1.3.2.1 *nocte*

To investigate genes and molecules involved in temperature entrainment, EMS mutation was generated and screened using *BG-luc* (a transgenic fly with two thirds of PER protein fused with a C-terminal luciferase, Stanewsky et al., 1997) oscillation reporter system and locomotor activity behavioural analysis. A novel 'temperature-mutant' located on the X chromosome, named *nocte* (no circadian temperature entrainment) was isolated (Glaser and Stanewsky, 2005). Using the luciferase reporter system, it has been shown that *nocte* mutants disrupt the rhythmic expression of PER under temperature cycles and constant light when

combined with BG-*luc,* but shows normal rhythmic expression in LD condition. As for behavioural analysis, *nocte*^{1} (a stop codon mutation leading to a truncated protein) shows robust rhythmic locomotor behaviour pattern in LD but not in TC, which suggested that only the temperature entrainment pathway is affected by the mutant (Glaser and Stanewsky, 2005).

Further studies showed that arrhythmic PER and TIM expression in constant light could be restored by temperature cycles in wild-type flies, but not in *nocte*^{1} mutant background, suggesting that the existence of an unknown temperature input pathway synchronized molecular clocks mediated by Nocte (Glaser and Stanewsky, 2005). In addition, using the GAL4-UAS system, driving *UAS-nocte-RNAi* by *F-GAL4* to specifically knock down the expression of *nocte* in periphery sensory organs including chordotonal organs (ChO, Kim et al., 2003), interferes the oscillations of PER under temperature cycles, which indicates that circadian temperature signals transducted from peripheral sensory neurons to central clock neurons is mediated by Ncote (Sehadova et al, 2009). However, the underlying molecular mechanisms are still unclear.

1.1.3.2.2 *norpA*

norpA (no receptor potential A) encodes an Phospholipase C (PLC) which

plays an essential role in the visual phototransduction cascade in fly's photoreceptors (reviewed by Minke and Parnas, 2005). Electrophysiological recording showed that Photo transduction is completely eliminated in the *norpA* null mutants. However, *norpA* alone is not sufficient to abolish the light entrainment in *Drosophila* (Stanewsky et al., 1998; Forster et al., 2001). Glaser and colleagues showed that *norpA* mutants exhibit defects in entrainment of the circadian clock to temperature (Glaser and Stanewsky, 2005). A previous report demonstrated the different splicing patterns of the 3'-UTR region of *per* in *norpA* mutants, which disrupts the normal seasonal circadian rhythms (Collins et al., 2004; Majercak et al., 2004). However, this temperature-dependent splicing event of *per* is not relevant to temperature entrainment, since the two transcripts are expressed at equal levels during TC in wild-type and *norpA* mutants (Glaser and Stanewsky, 2005). It’s also been reported that NORPA is required for temperature preference at the larvae stage (Kwon et al., 2008), and *norpA* mutants lose the ability to distinguish between 18°C and 24°C, but the molecular mechanisms underlying may be different from temperature entrainment.

1.1.3.2.3 TRP channel

Channel proteins are of prime importance for the survival and function of virtually every cell. Transient receptor potential (TRP) channels are a type of Ca^{2+}-permeable channels that are expressed in many tissues and cell types, especially in the neurons of the sensory organs. The name TRP is derived from a spontaneously occurring *Drosophila* mutant lacking TRP that responded to a continuous light with a transient receptor potential (Minke et al., 1975). With the completion of the *Drosophila* genome project, it has become clear that the fly genome contains 13 putative TRP channel genes (Figure 1.7), which are conserved to humans' TRP channels (Harteneck et al., 2000). TRP channels mediate almost all the responses to natural environmental cues, such as light, temperature, humidity, olfaction, pH, and most of the signals used for communication like pheromones (reviewed by Hardie., 2003; Montell., 2001). TRP channels are classified into seven related subfamilies designated TRPC, TRPM, TRPN, TRPV, TRPA, TRPP, and TRPML (reviewed by Montell., 2005) All these TRP subfamilies are represented in the *Drosophila* genome. Among these subgroups, The TRPC class is primarily involved in the visual system via the phototransduction cascade mediated by the PLC (reviewed by Raghua and Hardie., 2009). Channels in TRPV and TRPN are required for the mechanotransduction current in the sensory bristle and mechanosensory organs (Corey et al., 2003). Recently, a study in *Drosophila* gravity sensation also revealed that Painless and PYX in TRPA

are required for negative geotaxis but not for hearing (Sun et al., 2009), indicating the distinct functions for different TRP channels. TrpA1 and PYX in TRPA are reported as temperature sensors mediating temperature preference behaviour (Lee et al., 2005; Kwon et al., 2008; Hamada et al., 2008; Tang et al., 2013), and are recently also shown involved in temperature entrainment (Lee and Montell, 2013 and Wolfgang et al., 2013, highlighted in Figure 1.7). For dTrpA1, the behavioural analysis shows that mutants in dTrpA1 disrupt the clock synchronization to temperature cycles, although the phenotype is subtle in *dtrpA1*^{1} mutant. However, rescue experiments performed using clock cells gal4 other than peripheral clock gal4 suggests dTrpA1 is required for central clock synchronizing to TC. Indeed, a gal4 reporter of *dTrpA1* showed that it is expressed in subsets of almost of the groups of clock neurons especially in LPN, a group of neurons important for temperature entrainment (Yoshii et al., 2005, 2010). The data Indicates that a subset of central pacemaker neurons may contribute to temperature synchronization. On the other hand, behavioural analysis in *pyx* mutants demonstrated this channel is required for low temperature entrainment (20°C: 16°C) but not for the temperature higher than 20°C, indicating the indirect role other than channel function of PYX is involved in, as PYX channel is activated by the temperature over 40°C. These fresh results offer us some new sights about the temperature entrainment, while the

molecular mechanisms underlying are still unclear.

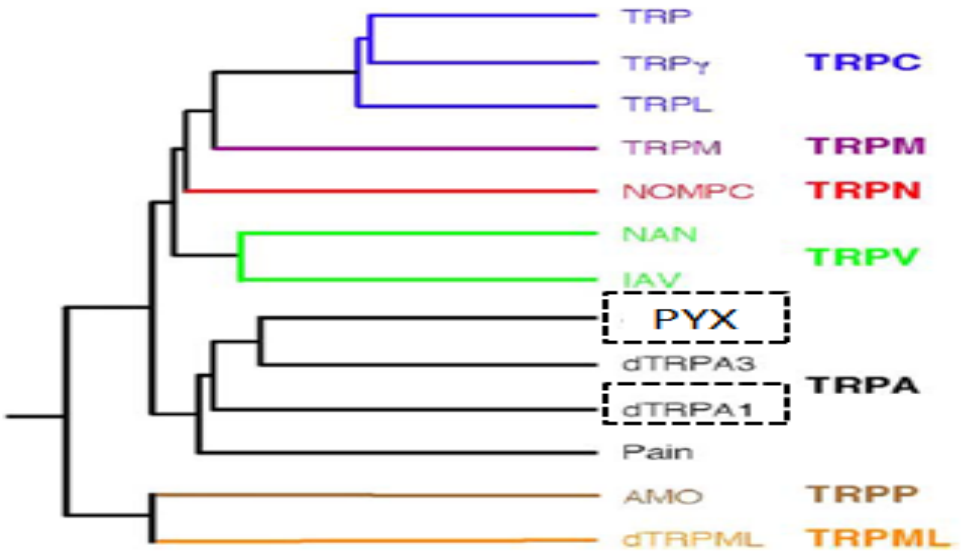

Figure 1.7: Dendrogram of the 13 TRP channel Family in *Drosophila*. (Taken and revised from Montell et al., 2005)
Frames highlight the channels involved in temperature entrainment.

1.1.3.3 Chordotonal organs in *Drosophila* involved in temperature entrainment

In *Drosophila*, it has been shown that down-regulation of the expression of *nocte* in ChO leads to abnormal behavioural pattern during TC (Sehadova et al., 2009). Moreover, many ChO developmental mutants (*eys*^{395}, *tilB*^{1}) show defects in temperature entrainment (Sehadova et al, 2009). All these results highlight the important role of ChO in temperature synchronization. ChO are specialized structures involved in

insect sensory mechanotransduction (Kernan., 2007). In *Drosophila,* ChO are broadly distributed underside of the cuticle where they are found at nearly every joint within the limb and body segments of insects (Kernan., 2007), and the biggest Ch organ in flies is Johnston's organ located in the 2nd antennal segment (Figure 1.8 A Tauber, Eberl., 2003). A major structural unit of ChO is the scolopale, a fluid-filled capsule that encloses the ciliary sensory endings of 1– 3 neurons and is attached at their tips to an extracellular dendritic cap (Figure 1.8 B). Mechanical stimulation that leads to stretching of the sense organ stimulates the neurons, converting the physical signal into neuronal receptor potentials. Functional analysis revealed these mechanotransduction receptors are implicated in sensing several physical stimuli, such as sound, gravity, and wind that impact many complex behaviours in the adult fly (Kamikouchi et al., 2009; Kernan, 2007; Yorozu et al., 2009). The axons of Johnston's organ project to antennal mechanosensory and motor centre (AMMC), a brain region posterior-ventral to the antennal lobe (Figure 1.8 C). JO neurons project broadly throughout the AMMC, forming five spatially segregated zones. Each JO neuron projects to only one of these five zones, zones A to E. Thus, fruit fly JO neurons can be anatomically classified into five subgroups, A to E, according to their targeting AMMC zone in the brain (Kamikouchi et al., 2006). Functional imaging of neural activity in an intact fly ear reveals that JO neuron subgroups A and B (AB

neurons) and JO neuron subgroups C and E (CE neurons) respond to different types of receiver movements (Kamikouchi et al., 2009; Yorozu et al., 2009).

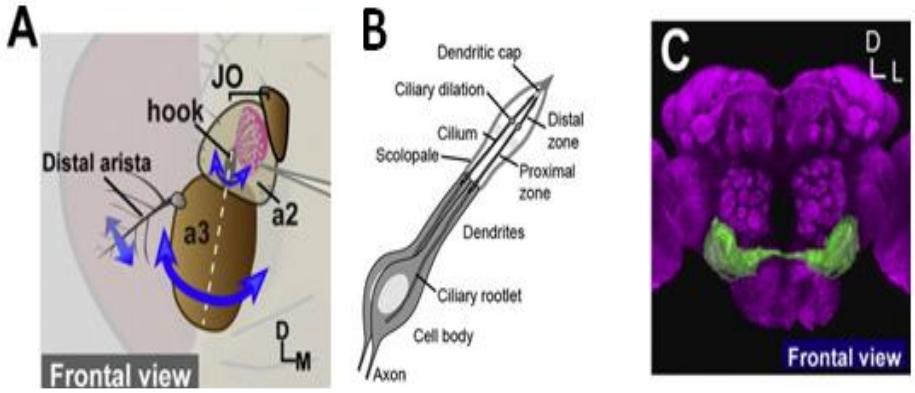

Figure 1.8 Anatomy of the hearing system in fruit flies.
(A) Frontal view of the antennal ear. JO is located within the second segment of the antenna (a2). Vibrations of the third segment of the antenna (a3) are picked up and translated into neural activities by JO neurons, housed in ~200 scolopidia. Arrows indicate the oscillating movement of the receiver. The white broken line indicates a longitudinal axis of the funiculus. (B) A sensory unit in the fly ear. (C) The AMMC, the primary centre for JO neurons. Green fluorescent protein (GFP), expressed in JO neurons using the GAL4/UAS system, visualizes the AMMC (*green*). The brain was counterstained with a neuropil marker, nc82 antibody (*magenta*).

The AB neurons measured together showed a strong response to sinusoidal vibrations at broad frequency ranges as well as pulse-like vibrations, but not to static deflections. In contrast, CE neurons respond more strongly to static deflections than to vibrations.

1.1.4 Molecular components of circadian clock and its entrainment to temperature cycles in mammals

Similar to *Drosophila melanogaster*, there is also a transcriptional

feedback loop existing in the mammalian circadian clock system to maintain the 24-hour rhythmicity. However, it's more complex compared to the one in *Drosophila*. So far, more than 10 genes have been identified as core clock genes in mammals, and most of them are functionally conserved to *Drosophila* clock genes. Briefly, the Basic Helix-Loop-Helix (BHLH) Per-Arnt-Sim (PAS) domain transcription factors, Clock (CLK) and Brain and muscle Arnt-like protein1 (BMAL1), bind as heterodimers to E-box enhancers and activate the expression of the clock-controlled genes (*ccgs*) and clock genes that encode transcriptional repressors, Period 1 and 2 (PER1/2, Gekakis et al., 1998) and Cryptochrome (CRY1/2, Kume et al., 1999). After phosphorylation by casein kinase 1 δ and ε (CK1δ/ε, Lowrey et al., 2000; Camacho et al., 2001) and glycogen synthase kinase 3-beta (GSK3-β, Kurabayashi et al., 2010) respectively, the PERs and CRYs can dimerize in the cytoplasm and translocate back to the nucleus as a complex, which in turn interacts with CLK-BMAL1 to interfere with transcriptional activation, thereby blocking their own expression and so closing the feedback loop (Figure 1.9). In addition, as in *Drosophila*, post-translational modification is also essential for modulating the circadian clock in mammals. Besides the phosphorylation modifications mentioned above, the ubiquitination and subsequent protein degradation of CRYs mediated by the F-box protein FBXL3 (Siepka et al., 2007) and the 26S proteasome play an important role in

terminating the negative repression of PERS/CRYs, and restarting a new cycle of transcription, therefore is the key to resetting the period of clock.

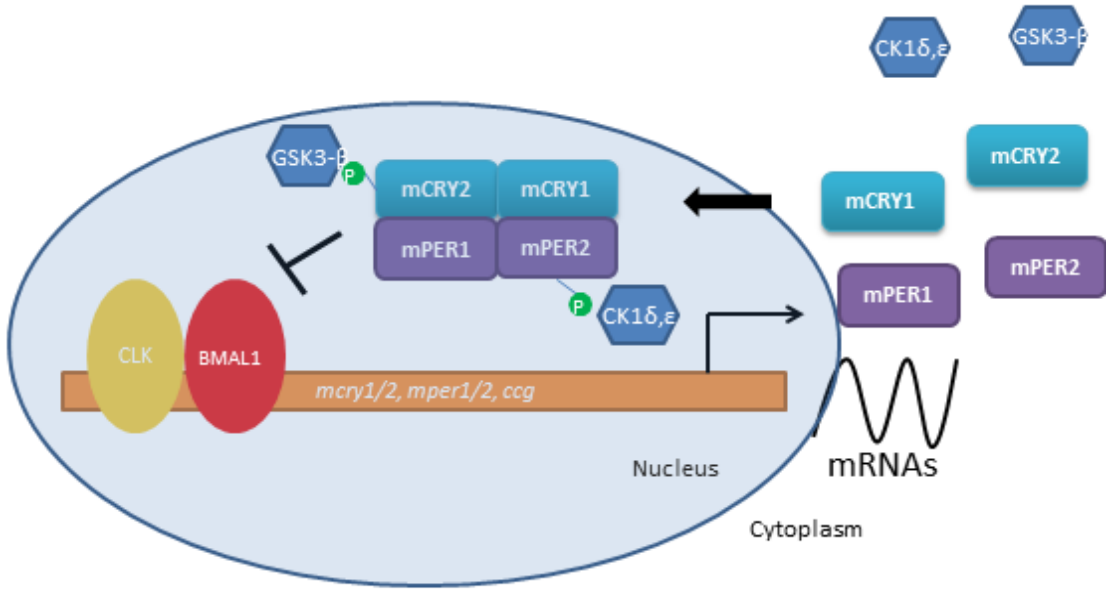

Figure 1.9 Schematic of the molecular clock of mammals.

The simplified model is inferred from in vitro and in vivo experiments discussed in the text. Clock genes (*mcry1/2*, *mper1/2* and other clock controlled genes (*ccgs*)) under regulation are represented as orange tubes. For indicated gene and protein names see text. CLOCK (CLK, yellow):BMAL1 (red) bind to the E-box of the CLOCK targets genes and initiate the transcription of their RNA. The translated PER (purple) and CRY (blue) proteins are phosphorylated by protein kinase CK1δ,ε and GS3K-β respectively and translocate back to the nucleus as heterodimeric and homodimeric complexes, which represses their own transcription by interacting with CLK:BMAL1 conversely. Ps (green) indicate the phosphorylation status of mCRY1/2 and mPER1/2.

In mammals, the suprachiasmatic nuclei (SCN) contain the master circadian clock, which is necessary for the synchronization of the phase among the peripheral tissues to distinct phases. The SCN are paired

structures in the ventral hypothalamus, with each half containing about 10,000 neurons in mice and around 50,000 neurons in humans (Cassone et al., 1988). SCN lesion experiments revealed that the SCN drive circadian rhythms of behaviour such as locomotor activity and physiological parameters such as body temperature fluctuations (Stephan et al., 1972). Like different groups of clock neurons expressing different neuropeptides in *Drosophila*, based on distinct neuropeptide expression, the SCN can be further subdivided into the dorsomedial 'shell' enriched with arginine vasopressin (AVP) expressing neurons and ventrolateral 'core' which has high expression of vasoactive intestinal peptide (VIP, Morin et al., 2007). For light entrainment, different from the clock neurons in *Drosophila*, which are able to perceive light directly via CRY^{+} neurons (Stanewsky et al., 1998), SCN are insensitive to light signals, and need to receive the light signals from melanopsin-expressing retinal ganglion cells as well as the image forming photoreceptors (Guler et al., 2007).

Compared with the knowledge of light entrainment, little is known about the genetic and molecular of the response of the mammalian clock to temperature. Using cultured RAT1 fibroblasts, Brown and colleagues showed that a low-amplitude temperature oscillation within the range of 33°C-37°C, which is the range of the normal oscillation of the body

temperature in mammals, is sufficient to drive the cyclic expression of clock genes at the transcriptional level (Brown et al., 2002). Similar results were also obtained in cultured lung and pituitary cells of mice using real time analysis of PER2:Luc bioluminescense with even lower temperature amplitudes (36°C -38°C, Buhr et al., 2010), although with a slight phase difference between them (Figure 1.9 B). These studies clearly show that peripheral clocks can be entrained by a shallow amplitude temperature cycle in the body temperature range, suggesting that temperature synchronization of peripheral clock is a tissue or cell-autonomous process, which is consistent with the finding in *Drosophila* (Glaser et al., 2005). Further pharmacological investigation reveals that the entrainment of the mammalian molecular clock in peripheral tissues by temperature cycles is regulated by the heat shock factor (HSF) family (Buhr et al., 2010). Blocking HSF transiently with the pharmacological agent KNK437 abolishes the sensitivity of peripheral clocks to small temperature changes (Buhr et al., 2010). However, whether this pathway is also conserved in other species for temperature entrainment is unknown.

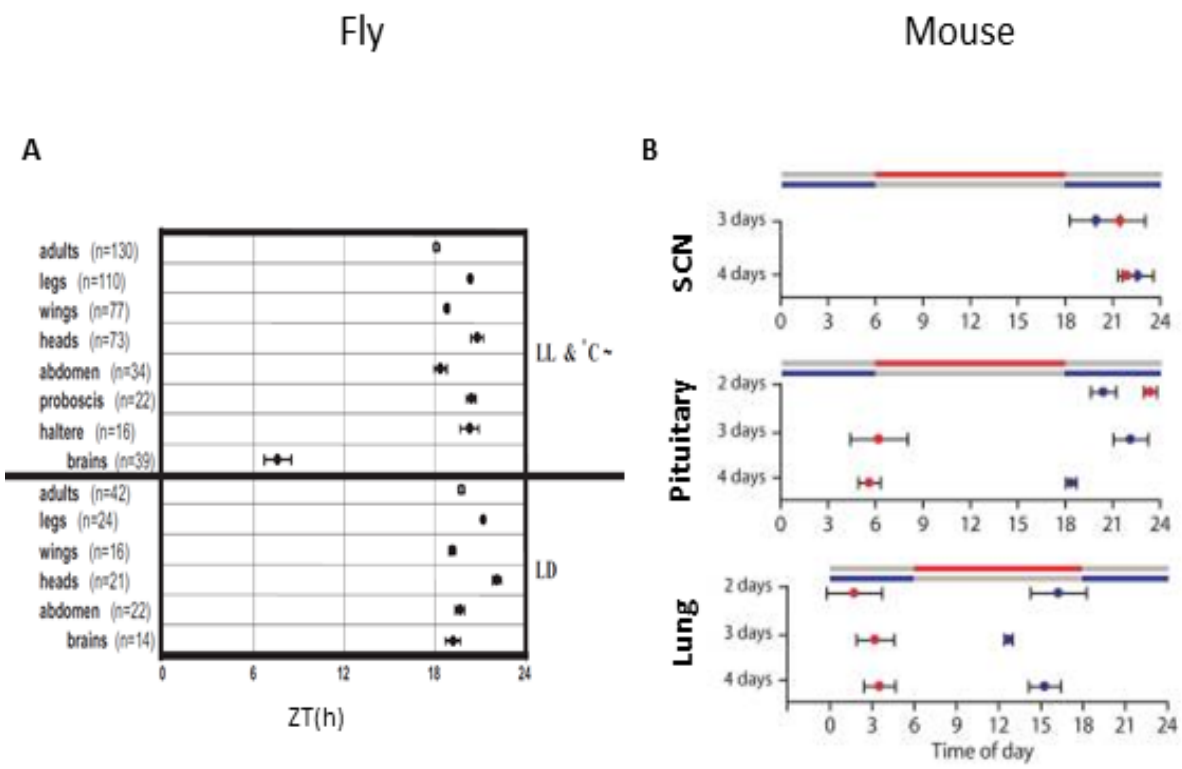

Figure 1.10 comparative view of the properties in temperature entrainment in peripheral and central clocks between flies and mammals.

A. Cultured brains have distinct phase when exposed to temperature (taken from Sehadova et al., 2009). Isolated body parts or whole flies were either kept in light-dark cycles (LD) at 25°C or in constant light and 25° C:16°C temperature cycles (LL& °C~) as indicated in the figure. Phase comparison of bioluminscence peaks obtained from flies carrying XLG-luc construct. See original paper for details about the phase determination. Note that brains exposed to temperature cycles have a distinct phase compared to peripheral tissues.

B. Peripheral tissues, but not SCN are sensitive to temperature changes within the physiological temperature range (taken from Buhr et al., 2010). SCN, pituitary, and lung cultures exposed to opposing square-wave 12hr:12hr 36°C:38.5°C temperature cycles. Phase graphs show time of peak PER2LUC bioluminescence the day after the temperature cycle. Coloured bars above represent the times of warm temperature for the points of corresponding colour below. Data are mean+/− SEM. n=4 for each SCN point and n=5 for each pituitary and lung point.

Remarkably, the master clock SCN cannot be entrained by body temperature rhythms, with no phase difference when exposed to

opposing temperature cycles (Figure 1.10 B). At the molecular level, a few clock genes such as *dbp* (Brown et al., 2002) and *per2* (Buhr et al., 2010) in cultured SCN failed to respond to circadian fluctuating temperatures, but are strongly entrained to temperature cycles in peripheral tissues. Analogous observations are also made in *Drosophila*: isolated brain can synchronize to light-dark but not to temperature cycles, with a distinct phase compared with the phase of the peripheral tissues (Figure 1.10A, Sehadova et al., 2009). Further experiments showed that neural communication among the cells in the SCN is critical for SCN to maintain the resistance to temperature cycles. Interestingly, compared to ectothermic animals, warm-blooded animals exhibit an extremely weak response to environmental temperature changes, which is consistent to with the SCN being resistant to temperature changes. Therefore, in hemothermic animals, peripheral tissues are sensitive to temperature changes, while an intact SCN is able to keep its endogenous phase even in the presence of physiological temperature fluctuations, which suggests that circadian body temperature cycles may be used by SCN to enhance the internal circadian synchronization. However, in order to confirm this hypothesis, further investigations are required for identifying more genes and neural circuits which are involved in temperature entrainment.

To summarize all statements mentioned above, both insects such as *Drosophila* and mammals show similar phenomenona in temperature entrainment, indicating that there is a conserved molecular mechanisms operating in ectothermic and endothermic animals. As a model system, *Drosophila* offers a powerful combination of molecular, genetic, behavioural and cell culture tools, therefore representing an attractive model to explore this issue. The knowledge we achieved in temperature entrainment using *Drosophila* will definitely aid our understanding of human temperature entrainment and related diseases.

1.2 Ionotropic glutamate receptor family (IRs)

Ionotropic Receptors (IRs) are a recently characterized family of olfactory receptors in *Drosophila melanogaster*, that are widely expressed in non-Odorant Receptors (non-OR) Olfactory sensory neurons (OSNs). Unlike the canonical insect Odorant Receptor family (ORs), which are comprised of 44 G-protein coupled receptors (GPCRs) (Vosshall and Stocker. et al, 2007), IRs are derived from ionotropic glutamate receptors (iGluRs), a conserved family of synaptic ligand-gated ion channels. The first description of IRs was in 2009 after a genomic scale bioinformatic screen for novel olfactory genes was performed by Richard Benton (Benton et al., 2007). In this screen, a large and highly divergent family of ionotropic

glutamate receptor (iGluR) related genes that became known as-Ionotropic Receptors (IRs), were identified. The expression pattern analysis that followed revealed that these genes are mainly expressed in the coeloconic cilia of the 3rd antennal segment, where the classic ORs are not expressed. Therefore, these putative IRs were proposed to be the "missing" receptors in the coeloconic cilia, and may complement the function of ORs (Benton et al., 2009). In the last four years, several studies were carried out to characterise the expression pattern (Benton et al., 2009), the molecular architecture (Abuin et al., 2011), the neural circuits (Silbering et al., 2011) of *Drosophila* IRs in olfactory perception, as well as their roles in hearing (Senthilan et al., 2012) and salt sensation (Zhang et al., 2013). Here, I review these IRs focused studies at the molecular, neuronal circuitry and functional levels to provide an overview of them.

1.2.1 Isolation the basic molecular structure of IRs

Genomic analysis has identified 66 IR genes (including 9 putative pseudogenes) in *Drosophila melanogaster* (Benton et al., 2009; Croset et al., 2010) and named them using the same nomenclature conventions as used in *Drosophila* ORs (*Drosophila* Odorant Receptor Nomenclature Committee, 2000). Comprehensive expression analysis of these genes by

RT-PCR, fluorescence RNA in situ hybridization and/or using transgenic reporters has shown that 16 of these are expressed in the antenna. Further studies revealed that ten of these 16 IRs are expressed in selective subsets of coeloconic sensilla OSNs (Benton et al., 2009; Croset et al., 2010 Figure 1.11), either uniquely or co-expressed with other IRs. These 16 antenna expressed IRs are therefore grouped as 'antennal IR', and the other 41 IRs (including co-receptor IR8a and IR25a) are grouped as 'divergent IR', due to the diversity of their expression pattern (Benton et al., 2009). Sequence analysis throughout the whole *Drosophilids* genomes revealed that these 'antennal IRs', other than the 'divergent IRs' are conserved throughout the whole *Drosophilids* genomes, suggesting their conserved function in odour recognition (Croset et al., 2010).

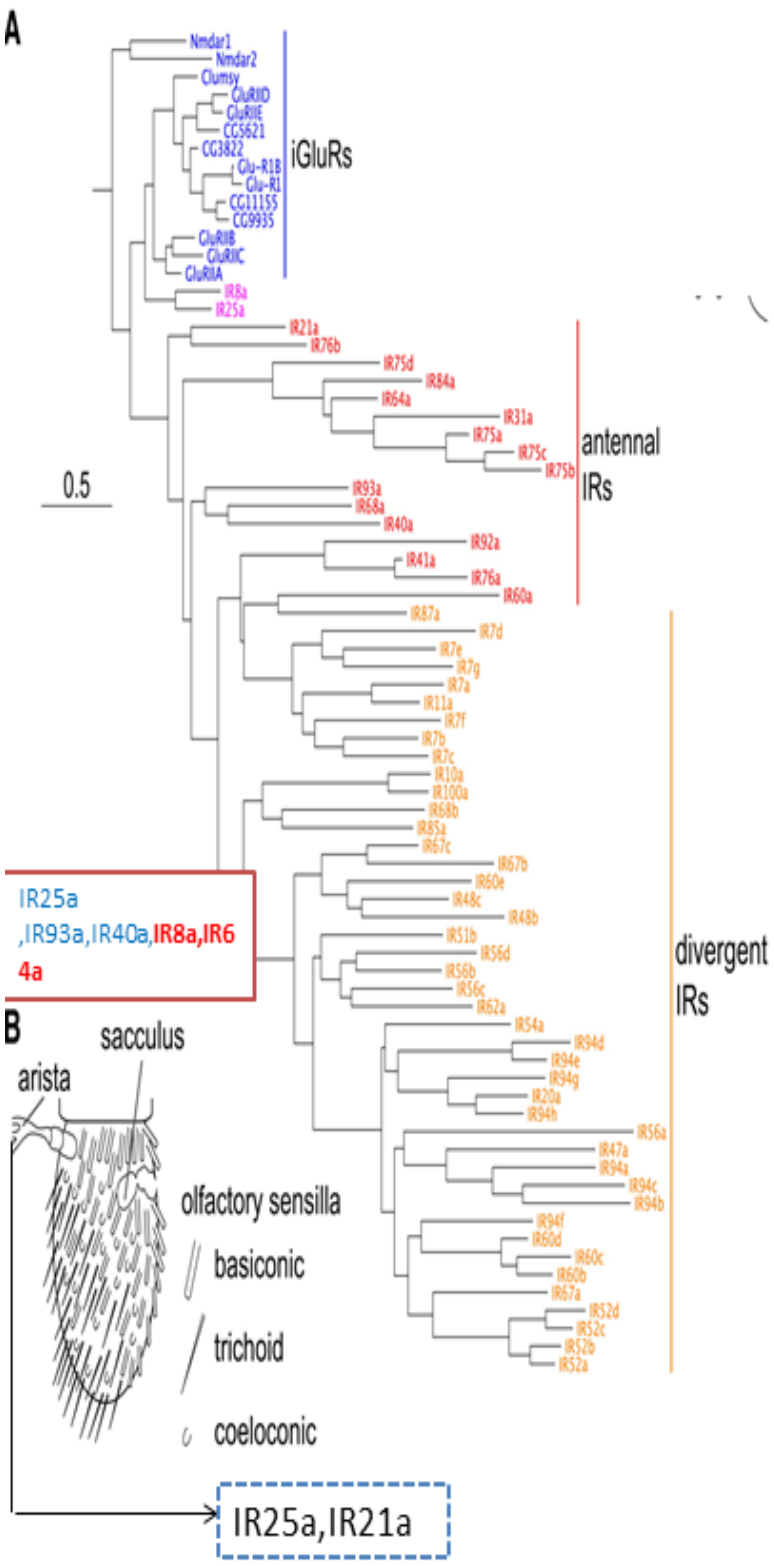

Figure 1.11 **Phylogenetic Relationships of IRs** (Taken and revised from Abuin etal., 2011.) A: Phylogenetic tree of *Drosophila* iGluRs and IRs.). The scale bar indicates the expected number of substitutions per site. B: Schematic of the Drosophila third antennal segment illustrating the different classes of olfactory sensilla and other sensory structures. The sacculus expressed IRs were highlighted in the square and arista IRs were shown in the dotted square.

Throughout the entire IR family, IR8a and IR25a have the highest sequence identity to iGluRs (Figure 1.11) and are conserved across

Protostomia (Croset et al., 2010). Moreover, IR8a and IR25a have broad distribution of their transcripts in antennal IR-expressing OSNs (Benton et al., 2009). These properties suggested that IR8a and IR25a have a conserved and a central role in IRs. Indeed, consistent with the broad expression, these receptors appear to function as co-receptors with several different, selectively expressed IRs (Abuin et al., 2011; Benton et al., 2009).

The homology of IRs to iGluRs aids to the understanding of the molecular mechanisms underlying the location and dendritic targeting of the IRs to the OSN sensory cilia, the specific binding with other ligands. In addition, our deep understanding of the molecular mechanisms of these classic synaptic ligand-gated ion channels give us insight into downstream neuronal responses (Gereau and Swanson, 2008; Mayer, 2011). Like iGluRs, all of the IRs contain a predicted extracellular N-terminus, a bipartite ligand-binding domain (LBD), whose two lobes (S1 and S2) are separated by an ion channel domain, and a short cytoplasmic C-terminal region (Fig. 1.12). Despite this similarity in protein domain organization with iGluRs, the sequence identity of IRs and iGluRs is low (<34% amino acid sequence identity), particularly within the LBD (Croset et al., 2010). Within the *Drosophila* IRs, sequence homology ranges between 10% and 70%, strongly suggesting their

functional diversity (Benton et al., 2009). Indeed, functional domain analysis revealed that by exchange of arginine residue in the IR84a LBD ($IR84a^{317R\rightarrow A}$) that is homologous to an arginine in iGluRs which is in contact with the a-carboxyl group of the glutamate ligand and completely eliminates its odour responsiveness, while no effect is evident for targeting cilia, suggesting that LBD in IR84a is crucial for odour recognition other than just the receptor location (Abuin et al., 2011). In contrast, a mutation of a conserved aspartate residue in the IR8a LBD that is homologous to an aspartate in iGluRs in contacts with a-amino group of the glutamate ligand completely abolished both odour responsiveness and cilia localization, suggesting a different role of the IR8a LBD in receptor localization and odour recognition (Abuin et al., 2011).

Like iGluRs, co-receptors IR8a and IR25a have a large extracellular amino-terminal domain (ATD). Functional and structural studies reveal that ATD in iGluRs is involved in channel assembly and binding to co-factors (Mayer et al., 2011). Domain functional analysis in odour neuronal responses shows that cilia localization and function were abolished with the deletion of the ATD in the IR8a, suggesting a role of this domain in protein folding, IR complex assembly, or cilia targeting (Abuin et al., 2011). In contrast, odor-specific IRs (‘antennal IR’ except

IR8a and IR25a) don't have ATD domain, but the short N-terminal (approximate 200 amino acids) region before LBD in the odor specific IRs have the same function as ATD in co-receptors. A study of odor specific IR84a shows that the normal cilia-targeting and odor responsiveness of the wild-type receptor were abolished with the deletion of this region, suggesting it is important for folding, complex assembly, and/or localization of the receptor (Abuin et al., 2011).

Moreover, the C-terminal cytoplasmic domain also has different functions in IR co-receptors compared to odour specific receptors. In the same study (Abuin et al., 2011), it has been shown that that deletion of the C-terminal cytoplasmic tail of IR84a had no effect on either receptor localization or odour recognition. Whereas co-receptor IR8a has a much longer C-terminal tail than it in odor specific IRs, deletion of this domain strongly reduced cilia-targeting efficiency and odour responses.

The ion channel domain in IRs is the most conserved domain when compared with iGluRs (Croset et al., 2010), indicating that IRs retain their ion-conducting properties. Indeed, studies using ectopic expression of IRs in oocyte expression systems reveal that both the combination of IR84a/IR8a and IR75a/IR8a, but not an individual receptor alone showed odour-evoked inward currents. Further ion conduction property analysis

revealed that the inward currents mediated by both complexes are carried preferentially by monovalent cations (Na^+ and K^+) (Abuin et al., 2011), but that IR84a/IR8a is also slightly permeable to Ca^{2+}. Interestingly, this Ca^{2+}permeability appears to depend upon a glutamine residue in the IR84a channel pore region; this residue (which is absent in IR75a) is also a major determinant of Ca^{2+} permeability in iGluRs (Hume et al., 1991 and Liu and Zukin, 2007). Notably, IRs have distinct pharmacological properties when compared to those of iGluRs. Several classic antagonists of iGluRs including two NMDA pore blockers (memantine andMK-801, Kashiwagi et al., 2002) and an AMPA and Kainate receptor blocker (philanthotoxin, Jones et al., 1990) have no effect on either IR8a/IR84a or IR8a/IR75a (Abuin et al., 2011), which may be caused by the distinct structure of IR complexes compared with iGluRs.

Another study of *Drosophila* salt sensation shows a different ion conduction property of IRs. IR76b, an IR required for low concentration salt attraction, was found to induce current changes due to monovalent cations when IR76b is ectopically expressed in HEK293 cells. However, instead of K^+, this channel is more preferable to Na^+, suggesting IR76b is a Na^+ channel. Moreover, mutation analysis on IR76b also identified that the conserved 293 threonine (T293) residue in the 3rd transmembrane region of the ion channel domain is important for the closed

conformation of the ion channel (Zhang et al., 2013).

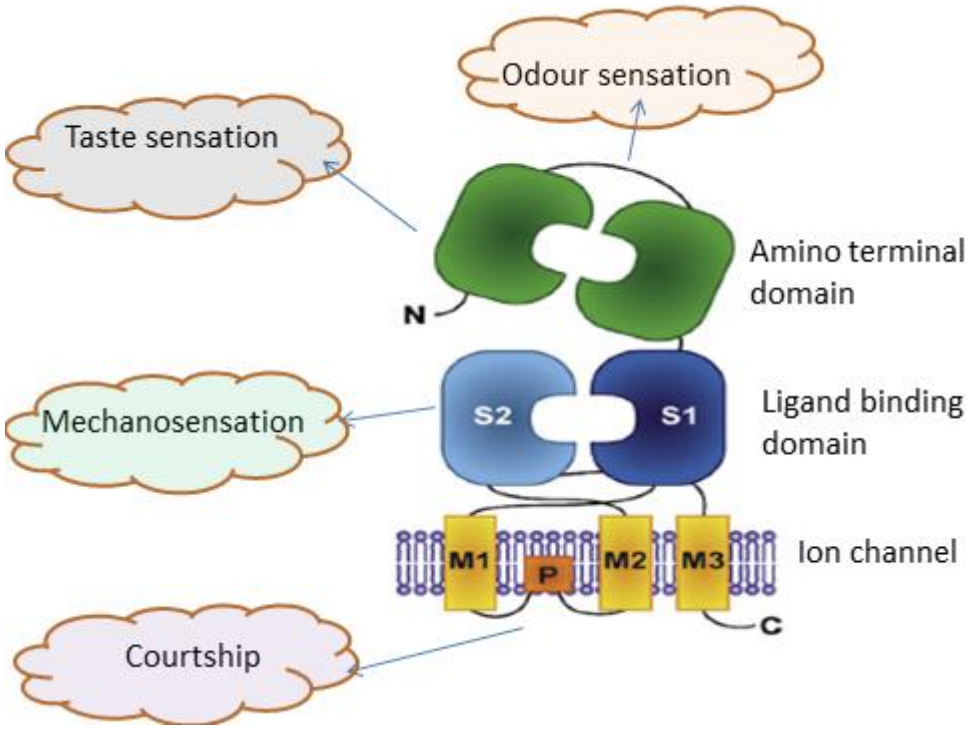

Figure 1.12 The molecular structure of IR (co-receptor) and function involved in. (Taken and revised from Abuin et al., 2011)

1.2.2 Heteromeric complexes formed by IRs

Ion channels and other proteins involved in transmembrane signalling are often composed of several different kinds of subunits in order to form a functional complex. The well-characterized NMDA receptor provides a perfect example. NMDA receptors are members of ionoropic glutamate receptor family that play a fundamental role in neuronal development, synaptic transmission, and synaptic plasticity (Collingridge et al., 2004). They form heterotetrameric channels containing two

obligatory glycine-binding NR1 subunits and two other subunits, either from the NR2 subfamily (2A, 2B, 2C, 2D) or the NR3 subfamily (3A or 3B). The various recombinations of different subunits confer onto the receptor distinct physiological properties that lead to a diversity of NMDA receptor function (Cull-Candy et al., 2004). As homologies of iGluRs, it has also been shown that IRs also function as complexes, but instead of tetramers, they have two different assembled properties based on the different co-receptors (IR8a or IR25a): (A) For the broadly-expressed co-receptor IR8a, electrophysiological studies in Xenopus oocytes and odour-evoked neuronal responses revealed that expression of IR8a was sufficient to confer responses to phenylacetaldehyde when co-expressed with odour specific receptor IR84a (Abuin et al., 2011). Another example in acid detection also demonstrated that co-expression of IR8a with a different receptor, sacculus located receptor IR64a, and conferred responses when a different ligand (acetic acid) was used (Ai et al., 2013). (B) In contrast, IR25a, reconstitution of the OR22a neurons phenylethylamine-sensing receptors, requires the following receptors: the presumed odour-specific IR76a and the broadly expressed IR25a co-receptor IR76b, a receptor which is co-expressed with other IRs in ac1 (antennal cilia), ac2 and ac4 (Abuin et al., 2011.).

The recent study in salt sensation provides another working model of IRs. For IR76b, instead of being coupled with another IR, individual IR76b is sufficient to form a functional receptor that restores low concentration salt sensation (Zhang et al., 2013). Although the mechanism of this difference remains unclear, somehow it must be associated with the functional difference between odour recognition and salt sensation.

1.2.3 Spatial distribution of IRs

Our understanding of the expression pattern of IRs originates mainly from the research on *Drosophila* antenna. The *Drosophila* antenna bears three types of olfactory sensory hairs (sensilla): basiconic, trichoid, and coeloconic. In nature, different types of sensilla respond to different types of odorants, for example, basiconic is responsible for pheromones detection. Nearly all of the OR genes have been mapped in the specific sensilla of basiconic and trichoid by in situ hybridization and RT-PCR (Couto et al., 2005) before the isolation of IRs. But with only one exception (OR35a for food odours), no ORs are expressed in antennal coeloconic sensilla neurons (Yao et al., 2005). The discovery of the IR family fills the hole by showing that some of the IRs are specifically localized to the coeloconic sensilla, as their expressions are eliminated in mutants whose coeloconic sensilla development were disrupted (Benton

et al., 2009).

Pioneering electrophysiological analysis has well identified the existence of four sensilla classes (ac1-ac4) in coeloconic sensilla (Yao et al., 2005). A study using in situ hybridization revealed that IRs have their unique spatial expression pattern in these sensilla classes. For example, IR31a is specifically expressed in ac1 whereas IR84a is specifically located in ac4. Some of the IRs is relatively broadly expressed in more than one type of the ac clusters: IR75d is expressed in both ac1 and ac2. The diverse spatial distribution of IRs suggests their different odour reorganization in different sensilla. For example, IR31a labelled ac1 is activated mainly by ammonia whilst IR84 labelled ac4 is mainly activated by phenylacetaldehyde (Benton et al., 2009).

Two IRs co-receptors, IR8a and IR25a, are expressed at somewhat heterogeneous levels in many of the coeloconic OSNs (Benton et al., 2009). Consistent with this broad expression, these receptors appear to function as co-receptors with several different, selectively expressed IRs (Abuin et al., 2011; Benton et al., 2009). IR25a is additionally weakly expressed in basiconic and trichoid OSNs, but its function in these cells is unclear (Benton et al., 2009). In addition, IR25a is also expressed in arista neurons, together with another non-coeloconic expressed IR (IR21a)

(Benton et al., 2009). Arista is a branched cuticular projection from the antennal surface, which was recently shown to house the thermosensory but not the olfactory neurons. However, the function of thermo-sensation seems to be mediated by a TRP channel gene (*brv*), and the function of IRs in heat sensing remains unknown (Gallio et al., 2011). IR40a, IR64a and IR93a are also not expressed in the coeloconic sensilla but rather in sacculus neurons: IR40a, IR93a (and IR25a) in chambers I and II, nearest the opening on the antennal surface, and IR64a (together with IR8a) in neurons in the deepest chamber III. Sacculus is an internal multi-chambered pocket which is required for olfactory, hygrosensory and thermosensory sensation (Shanbhag et al., 1995). Indeed, $IR8a^{+}$/$IR64a^{+}$ neurons are required for acid sensation (Ai et al., 2010, 2013).

The identification of IR genes has also allowed for the visualization of the olfactory circuits in which they are expressed, by using IR promoter to drive expression of neuroanatomical markers (Ai et al., 2010; Benton et al., 2009; Silbering et al., 2011). Like OR-expressing OSNs (Couto et al., 2005; Fishilevich and Vosshall, 2005), neurons expressing the same IR converge on a single glomerulus within the antennal lobe (Benton et al., 2009; Silbering et al., 2011). However, IR-expressing neurons in the sacculus display some exceptional anatomical properties. For example,

IR64a OSNs project to two distinctive glomeruli, DC4 and DP1m (Ai et al., 2010). Further single neuron labelling experiments showed that individual IR64a neuron projects to either DC4 or DP1m but not both glomeruli at the same time (Ai et al., 2013). IR40a/IR93a-expressing neurons have a complex innovation pattern, comprise of several dispersed subregions of antennal lobe that does not clearly correspond to any previously defined glomerulus (Laissue et al., 1999). Whether this indicates a non-olfactory function of these neurons is unclear.

The study of IR76b showed that it is expressed in gustatory organ (Zhang et al., 2013). Both antibody staining and gal4 reporter systems showed that endogenous IR76b in wild type flies is not co-localized with either bitter receptor Gr66a or sugar-responsive receptor Gr5a (Zhang et al., 2013). Further investigation demonstrated that the axon projection of IR76b from labelum to SOG (subesophageal ganglion) is minimal in its overlap with the projection of these two receptors, indicating that IR76b is a class of GRNs distinct from sugar- or bitter-responsive GRNs (gustatory response neuron).

A microarray screen searching for auditory genes (Senthilan et al., 2012) also isolated 7 IRs enriched in Johnston's organ (Jo organ) in wild type flies but a minimal or no expression in *ato* mutant, which doesn't have

the organ (Jarman et al., 1995). Further study using in situ hybridization and florescent GFP driven by IR-promoter gal4 shows that IR94 envelopes the neurons' somata and anchors them in the second antennal segment, whilst also revealing that IR75d is expressed in the neurons and cilia of Jo organ. It should be noted here that, the projection pattern in the brains of these IRs remains unknown.

1.2.4 The multiple functions mediated by IRs

Studies in odour recognition for IR^+ OSNs have been characterized by screening panels of 168 monomolecular odours by extracellular electrophysiological recordings in coeloconic sensilla (Silbering et al., 2011; Yao et al., 2005). During this screen, several differences in the olfactory responses of IR neurons from ORs have been revealed. First, IR^+ neurons are generally more narrowly-tuned and less sensitive than OR^+ neurons. Only 19 out of 168 chemically diverse odours tested in IR^+ neurons produce increases in firing frequency of >50 spikes/s (about 25% of the maximum neuronal responses observed) (Silbering et al., 2011; Yao et al., 2005). Second, and more importantly, IRs and ORs detect distinct classes of odours (Silbering et al., 2011; Yao et al., 2005). Almost all of these agonists for IRs are amines, carboxylic acids or aldehydes, whereas the ligands for ORs are mainly esters, alcohols and ketones

(Hallem and Carlson, 2006). The strongest IR ligands were detected only weakly or not at all by ORs, on the other hand, the strongest OR ligands did not stimulate any IR neurons (Silbering et al., 2011). The distinction in ligand preferences of OR and IR repertoires suggests the largely complementary odour-sensing functions of IRs and ORs, which could explain the co-existence of two distinct repertoires within the *Drosophila* olfactory system. More and More studies on IRs give us new sights of the diverse function of IRs in nature, suggesting the importance of IR family in Drosophila. A study in IR64a/IR8a showed this complex mediates behavioural aversion to acid (Ai et al., 2010 and 2013). An auditory study revealed that IR64a and IR94b have an indirect function in hearing (Senthilan et al., 2012). A recent work in salt sensation revealed that IR76b alone located in the L6 labellum sensilla is necessary and sufficient for low concentration salt sensation, but not for avoiding high salt (Zhang et al., 2013). However, further genetic and chemical ecological analyses are required to link these behaviours to particular IRs and to understand the underlying molecular mechanisms.

1.3 Aim of this work

By the year of 2009 when I started my PhD, three decades of pioneer studies had provided us a relative clear picture about circadian clock system including the molecular mechanisms of transcription translation feedback loops, the location and function of central pacemaker neurons controlling circadian behaviour, and the mechanisms underlying circadian light entrainment. Nevertheless, concerning about the complexity of the circadian clock, much more open questions remains to be further investigated. In particular, the mechanisms by which temperature cycles synchronize the circadian clock are poorly known. During that time, only two genes (*nocte* and *norpA*) involved in temperature entrainment in *Drosophila* were isolated (Glaser and Stanewsky, 2005). However, the actual roles they played in temperature entrainment were still unknown. Compared with *norpA*, which has a canonical function in G protein cascade, nothing was known about the molecular function as well as the signal pathway involved in of *nocte* gene.

In this thesis, I tried to answer the question about the molecular function of *nocte* by identifying the signal pathway it involved in. Utilizing Co-immunoprecipitation combined with proteomics analysis, I aimed to

isolate novel components interacting with Nocte, further dissecting the functions of these novel proteins will not only broaden our understanding about temperature entrainment but also will benefit the understanding of the role of *nocte* in temperature entrainment in turn. As the basic principals of temperature synchronization may be conserved between insects and mammals, understanding of *Drosophila* temperature entrainment will help us to understand the mechanisms of temperature entrainment in mammalian system and related diseases.

Chapter2

Materials and Methods

2.1 Reagents and Chemicals

All chemicals and solutions if not mentioned were purchased from SIGMA, Fischer, ACROS or BDH. Taq polymerase, restriction enzymes, T4 ligase and cloning related reagents were purchased from New England Biolab (NEB). XL1-Blue *E. coli* strain (Stratgene) was used for all of the transformations in this study.

2.2 Molecular cloning of Nocte-tagged and Nocte^{1}-tagged constructs

The constructs used and generated in this study are listed in table 2.2. To generate the *psp-FSNH* construct, the *FLAG-StrepII-Venus-Strep (FSVS)* fragment was amplified from a construct of *PiggyBac/P-element*

YFP-StrepII-FLAG (gift from K.S.Lilley lab, Rees et al., 2011) using a Phusion High-Fidelity PCR kit, this 900 bp fragment was sub-cloned into a *psp73* cloning vector (Promega) to generate *psp73-FSVS* with Bgl II/ Xhol I sites. To introduce a StrepII tag (Skerra and Schmidt, 2000) at the N-terminal of *nocte cDNA*, a 0.5kb fragment was amplified from *psp73-nocte-HA* (Giesecke and Stanewsky, unpublished) by annealing the StrepII tag directly using PCR (primers see in Table 2.1). This fragment was religated back into the *psp73-nocte-HA* to generate *psp-Strep II-nocte-HA. A 3xFLAG* tag was introduced in the N-terminal of *psp73-Strep II-nocte-HA* by sub-cloning the *Strep II-nocte-HA* fragment into *psp-FSVS* with BstB I/ Xhol I sites replacing the Venus position of *psp-FSVS*.

To generate the *psp-FSN*^{1}construct (the tagged Notce^{1}plasmid), a Site Directed Mutagenesis Kit (Stratgene) was employed to directly introduce a single mutation (C→T) at 5119bp of the *nocte cDNA* (Sehadova et al, 2009). The *psp-FSNH* plasmid was used as the template to create *psp-FSN*^{1}*H* with *nocte* DSM as the primers (Table 2.1). Following purification of the PCR product, DpnI digestion was carried out according to the manufacturers' instructions. Routine transformations and minipreps (QIAGEN) were used

to amplify the plasmid DNA. All of the constructs generated in this study were examined by DNA sequencing (services by Eurofins) using the indicated primers (Table 2.1) before continuing.

2.3 Generation of transgenic flies

To generate transgenic flies, *psp-FSNH* and *psp-FSN*[1] were sub-cloned into the transformation vector *pUAST* (Table 2.2) using Bgl II/ Xhol I sites, the amplified plasmids were then purified by Midi prep kit (QIAGEN). Microinjection was performed according to the standard protocol with a sight modification (Spradling and Rubin, 1982), in that more concentrated DNA (500ug/ml) was injected into each embryos of the strain *y w; +/+; ki, P[ry +,Δ 2-3]/+* (Robertson et al., 1988) using green food dye to aid visualization. The mini-white+ gene from the *pUAST* (Brand and Perrimon, 1993) construct was used as a selectable marker for identification of the transgenic flies. The locations of the insertions were determined genetically by crossing transgenic flies to second and third chromosomal balancers (Figure 2.1). The microinjection was performed by our lab technician MinXu,

QMUL.

Table 2.1 Primers used in this study

Name	Sequence(5'-3')	Tm (℃)	Use	Reference
Nocte interactors(Chapter 3)				
FSVS bglII	GC AGATCT ATG GACTACAAAGAC	72	cloning of FLAG-Strep-Venus	self design
FSVS XhoII	GTC CTCGAG TCA CTTTTCGAACTG	72	cloning of FLAG-Strep-Venus	self design
FLAG bglII bst	GG AGATCT TCGAA AAAGGAGCC ATGAGTACACT	72	cloning of FLAG-Strep-Nocte	self design
nocte bpu10I	TAG CCTGAGC TGCCGGCGTTGTTGTTGCTG	72	cloning of FLAG-Strep-Nocte	self design
psp-FSNH N-sq[A]	GGCATCAGAGCAGATTGTA	60	sequencing of plasmid DNA	self design
psp-FSNH C-sq	CAGGTGGCGGTGGTAGTCAAAC	60	sequencing of plasmid DNA	self design
nocte DSM[B] *sense*	GCCAGCAGCAACAGTAGCAGCACTCGCAA	72	Site mutating of nocte^{513}C→T	self design
nocte DSM antisense	TTGCGAGTGCTGCTACTGTTGCTGCTGGC	72	Site mutating of nocte^{513}C→T	self design
nocte[1] *sense*	CAACACCAGCAAATGCCGCACTA	55	genotyping of genomic DNA	self design
nocte[1] *antisense*	GTGACGCCTGGTAGAATGAAGG	55	genotyping of genomic DNA	self design
nocte[1] *sq*	GAGCCACCACCACCAACAG	60	sequencing of genomic DNA	self design
IR25a(Chapter 4)				
ls-tim	TGGAATAATCAGAACTTTGA	52	genotyping of genomic DNA	Tauber et al., 2007
s-tim	TGGAATAATCAGAACTTTAT	52	genotyping of genomic DNA	Tauber et al., 2007
ls/s-tim	AGATTCCACAAGATCGTGTT	52	genotyping of genomic DNA	Tauber et al., 2007
IR25a^{null} *sense*	ATCACTATACTTCGAATGGCCTCGGG	65	genotyping of genomic DNA	self design
IR25a^{null} *antisense*	CGAACAAGTCCGATGCCAAGG	65	genotyping of genomic DNA	self design
nocteRT sense	AAGAACTACGGCGCGTG	60	RT-PCR	Sehadova et al, 2009
nocteRT antisense	CCAAGGCGTTCATGCTC	60	RT-PCR	Sehadova et al, 2009
IR25aRT sense	CAATCCACTCAGCCATTCAA	60	RT-PCR	Croset et al., 2010
IR25aRT antisense	ACCAGAGGCACTCCTTCAGA	60	RT-PCR	Croset et al., 2010
rp49 RT sense	CGATATGCTAAGCTGTCGCACA	60	RT-PCR	Sehadova et al, 2009
rp49 RT antisense	CGCTTGTTCGATCCGTAACC	60	RT-PCR	Sehadova et al, 2009
IR56a(Chapter 5)				
IR56ajo[C] *sense*	TCCACAAAATGGCGCACGA	58	sequencing of genomic DNA	self design
IR56ajo antisense	CGGTTGCGAAACGAATT	58	sequencing of genomic DNA	self design

A: 'sq' means sequencing. B:DSM: direct site mutation. C: 'jo' means jump out. Underline: digestion sites.

Table 2.2 plasmids generated and used in this study

Name	Description	Back bone	Reference
psp73	commercial cloning vector	*psp73*	Promega
pUAST	plasmid used for generating transgenic	*pUAST*	Brand and Perrimon, 1993
piggy-FSVS[a]	plasmid used for amplifying FLAG and StrepII tag.	p3E1.2[b]	Rees et al., 2011
psp-FSVS	backbone used for introducing FLAG and strepII on nocte	*psp73*	self generated
psp-nocte-HA	nocte cDNA with C-terminal HA tag	*psp73*	Giesecke et al., unpublished
psp-SNH[c]	nocte cDNA with C-terminal HA tag and N-terminal strepII tag	*psp73*	self generated
psp-FSNH[d]	nocte cDNA with C-terminal HA tag and N-terminal FLAG, strepII tag	*psp73*	self generated
psp-FSN[1]	Site mutating of nocte[31 33]C→T based on psp-FSNH	*psp73*	self generated
pUAST-FSNH	transgenic plasmid carrying nocte with N-terminal FLAG and StrepII and C-terminal HA	*pUAST*	self generated
pUAST-FSN[1]		*pUAST*	self generated

a:FSVS is short for FLAG-strepII-Venus-strepII
b: Cary et al., 1989
c: SNH is short for psp-strepII-nocte-HA
d: FSNH is short for FLAG-strepII-nocte-HA

2.4 Fly stains

Drosophila melanogaster were kept and raised in 25°C or 18°C in plastic vials (82x25 mm, B.T.P DREWITT) containing standard fly food, which was prepared as follows: 1 liter of water contains agar 10 g, sucrose 15 g, glucose 33 g, yeast 35g, maize meal 15 g, wheat germ 10g, treacle 30 g, soy flour 1 spoon full, nipagin 10ml and proprionicacid 5ml.Table 2.3-5 lists

majority of the flies that were used in this study.

Table 2.3 Flies used in chapter 3 of this study

Nocte interactors		
Name	**Description and use**	**Reference/source**
y w; Bl/Cyo	2nd chromosome Balancer	Lindsley and Zimm,1992
y w; Dr/TM3	3rd chromosome Balancer	Lindsley and Zimm,1992
y w;+/+; ki, P[ry+, Δ2-3]	transposase, to generate transpenic flies	Robertson et al., 1988
gmr-gal4	gal4 expressed mainly in imaginal discs but also other tissues including leg discs	Freeman, 1996
nocte-gal4	gal4 controlled by upstream DNA sequences of *nocte* highly expressed in Ch organs	Sehadova et al, 2009
tim-gal427	gal4 controlled by upstream DNA sequence of *timeless*.	Kaneko and Hall, 2000
UAS-dicer2;tim-gal4 27	enhance the effect of RNAi under control of *tim-gal4 27*	Semoni et al., unpublished
F-gal4 33-5	gal4 controlled by upstream DNA sequences of *nan* highly expressed in Ch organs	Kim et al., 2003
UAS-FSNH	UAS construct. To over-express FLAG-Strep-Nocte- HA fused protein	self generated
UAS-gfp	UAS construct. To over-express GFP	Kaneko and Hall, 2000
UAS-nocte	UAS construct. To over-express wild type Nocte	Giesecke and Stanewsky, unpublished
UAS-nocteRNAi	RNAi line	Sehadova et al, 2009
UAS-IR25aRNAi(1)	RNAi line, CG15627-1	NIG-FLY
UAS-IR25aRNAi(2)	RNAi line, CG15627-1`	NIG-FLY
UAS-CG9297RNAi(1)	RNAi line, CG9297-1	NIG-FLY
UAS-CG9297RNAi(2)	RNAi line,CG9297-2	NIG-FLY
UAS-CG17097RNAi(1)	RNAi line, GD41244	VDRC
UAS-CG170097RNAi(2)	RNAi line, GD41245	VDRC
UAS-tweekRNAi(1)	RNAi line, KK102639	VDRC
UAS-pknRNAi(1)	RNAi line, CG2055-1	NIG-FLY
UAS-pknRNAi(2)	RNAi line, CG2055-2	NIG-FLY
UAS-CG1440RNAi(1)	RNAi line, CG1440-2	NIG-FLY
UAS-CG1440RNAi(2)	RNAi line, CG1440-3	NIG-FLY
UAS-mcm3RNAi(1)	RNAi line, CG4206-2	NIG-FLY

Table 2.4 Flies used in chapter 4 of this study

IR25a		
Name	**Description and use**	**Resources**
UAS-IR25a	to over-expression IR25a	Abuin et al., 2011
UAS-FSN[1]	to over-expression FLAG-StrepII-Nocte[1]	self generated
IR25a-gal4	600 bp upstream sequence from IR25a start codon fused with gal4	Abuin et al., 2011
UAS-mCD8:GFP;UAS-ds-RED	to over-express membrane GFP and nuclei RFP	Sehadova et al, 2009
nompA-GFP/TM6B	full length nompA fused with GFP, used as dendritic cap maker	Chung et al., 2001
UAS-IR25a:mcherryRFP	IR25a fused with cherry RFP to sub-location of IR25a	Benton et al., unpublished
y w; ls-tim	used to out-crossing mutants to the same genetic background	Peschel et al., 2006
IR25a[2]	IR25a null mutant	Benton et al., 2009
IR25a[1]	IR25a null mutant	Abuin et al., 2011
BAC,IR25a[2]	genomic rescue of IR25a[2]	Benton et al., unpublished
Df(IR25a)/Cyo	deficiency line covering *IR25a* loci	Bloomington
y w per^{01}	*period* arrhythmic mutant	Konopka and Benzer, 1979
y w per^{L}	period mutant with long period	Konopka and Benzer, 1979
IR8a[1]	IR8a null mutant	Abuin et al., 2011
nocte$^{1\,rec25}$	new *nocte* recombinant mutant line	Stanewsky et al., unpublished
UAS-Kir2.1	mammalian inward rectifier K^+ channel, to silence neural activity	Baines et al., 2001

2.5 Genomic DNA extraction and genotyping

DNA was isolated from single fly of each different strain. Each fly was homogenized for 5-10 seconds in 50ul of extraction buffer (10mM Tris-Cl pH8.2, 1mM EDTA, 25mM NaCl and 200ug/ml Proteinase K) and

Table 2.5 Flies used in chapter 5 of this study

IR56a		
Name	**Description and use**	**Resources**
IR76a-gal4	upstream DNA sequences of IR76a fused with gal4	Benton et al., 2009
IR76b-gal4	upstream DNA sequences of IR76b fused with gal4	Abuin et al., 2011
IR76a^{1}	IR76a null mutant	Benton et al., unpublished
IR76a^{2}	IR76a null mutant	Benton et al., unpublished
IR76b^{1}	P-element insertion, BL9824	Bloomington
IR76b^{25}	P-element insertion, BL22729	Zhang et al., 2007
IR7a-gal4	upstream DNA sequences of IR7a fused with gal4	Benton et al., unpublished
IR7c-gal4	upstream DNA sequences of IR7c fused with gal4	Benton et al., unpublished
IR10a-gal4	upstream DNA sequences of IR10a fused with gal4	Benton et al., unpublished
IR11c-gal4	upstream DNA sequences of IR11c fused with gal4	Benton et al., unpublished
IR20a-gal4	upstream DNA sequences of IR20a fused with gal4	Benton et al., unpublished
IR47a-gal4	upstream DNA sequences of IR47a fused with gal4	Benton et al., unpublished
IR52b-gal4	upstream DNA sequences of IR52b fused with gal4	Benton et al., unpublished
IR52c-gal4	upstream DNA sequences of IR52c fused with gal4	Benton et al., unpublished
IR52d-gal4	upstream DNA sequences of IR52d fused with gal4	Benton et al., unpublished
IR56d-gal4	upstream DNA sequences of IR56d fused with gal4	Benton et al., unpublished
IR60c-gal4	upstream DNA sequences of IR60c fused with gal4	Benton et al., unpublished
IR67a-gal4	upstream DNA sequences of IR67a fused with gal4	Benton et al., unpublished
IR56a-gal4	upstream DNA sequences of IR56a fused with gal4	Benton et al., unpublished
IR56a^{Mimic}, *BL37456*	MIMIC transposable element located in IR56a upstream DNA sequence	Venken et al., 2011
y w;sna^{Sco} */SM6a,P{hslLMiT}2.4*	MIMIC transposase, BL 36311	Venken et al., 2011
IR56a^{128}	IR56a jump out deletion	self generated
Df(IR56a)/Cyo	deficiency line covering *IR56a* loci	Bloomington
5-HT1A$^{\Delta 5kb}$*/Cyo,GFP*	5-HT1A receptor null mutant	Yuan et al., 2006

incubated at room temperature for 30 minutes. Finally, the homogenized solutions were placed at 95°C for 1-2 minutes in order to inactivate the Proteinase K (Invitrogen). Following this, general PCR reactions using the necessary primers (Table 2.1) were employed to verify the genotypes of the flies used in both behavioural and immunohistochemistry experiments.

Figure 2.1 Procedure of balancing transgenicflies

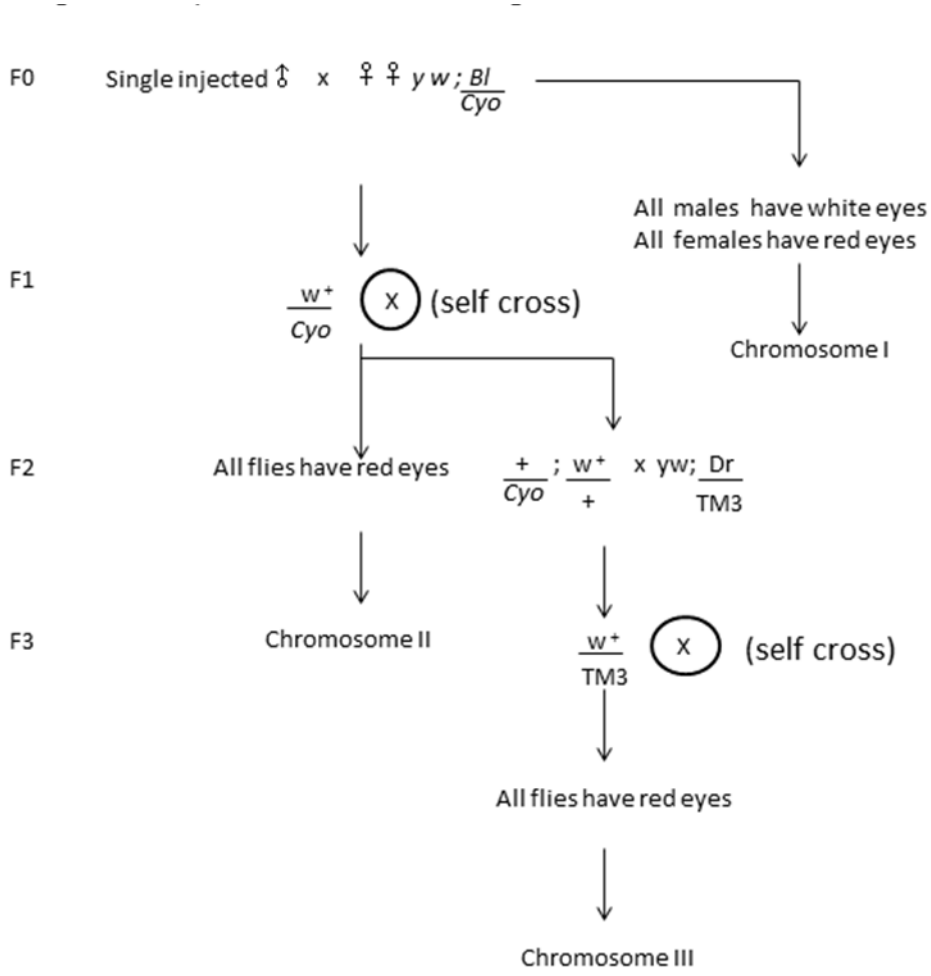

2.6 Co-immunoprecipitation (Co-IP)

Co-IP experiments were performed as described (Rees et al., 2011). For each purification, 200-300mg (wet-weight) of fly heads were collected on dry ice and manually homogenized with a 2ml Dounce homogenizer (Fisher) in 1ml of extraction buffer containing 50mM Tris, pH7.5, 125mM NaCl, 1.5mM MgCl2, 1mM EDTA, 5% Glycerol, 0.4% NP-40, and 0.1% Tween 20 (Rees et al, 2011). To prevent degradation during the lengthy purification steps 2X protease mini EDTA inhibitor mixture (Roche) was added at hourly intervals throughout the procedure. The homogenate was centrifuged at 10,000 rpm for 15min to isolate the soluble fraction used for pull-down.

Each step of the protein pull down protocol is detailed and outlined in Figure3.2. Batches of soluble FSNH tagged protein isolated from the fly heads were purified in parallel; alongside the *gmr-gal4* alone was included as a systematic negative control for both StrepII and FLAG.

For the FLAG pull-down procedure, EZview™ Red ANTI-FLAG® M2 affinity gel (Sigma) was used to bind the FLAG tagged bait and its bound partners.

50ul of pre-washed 50% slurry was added to 1ml of soluble protein and incubated at 4°C for 2h on a rotary mixer. Nonbinding material was removed by centrifugation (8,000×g for 2min) and the resin was washed three times in ice cold extraction buffer. The FLAG tagged protein (along with any associated proteins)was incubated and eluted three times, each time with 50ul (100ug/ml) FLAG peptide (Sigma) in extraction buffer for 30min at 4°C on a rotary mixer. The three eluates were combined and any residual resin was removed by centrifugation at 8,000 rpm for 2min.

For the StrepII pull down procedure, 50ul of prewashed Strep-Tactin Sepharose resin (IBA) was added to 1ml of soluble protein extraction and incubated at 4°C for 2 hours on a rotary mixer. Non binding material was removed by centrifugation (8,000×rpm for 2 min) and the resin was washed three times in ice cold extraction buffer. The StrepII tagged protein (along with any associated proteins), was eluted three times with 50ul of 10mM Biotin (Invitrogen) in extraction buffer for 30min at 4°C on a rotary mixer. The three eluates were combined and any residual resin was removed by centrifugation at 8,000×g for 2min.

2.7 Mass Spectrometry analysis

Protein eluates were precipitated with ice-cold 100% acetone overnight at -80 °C. The precipitate was vacuum dried, and reduced in 2mM dithiotreitol for1 hour at room temperature and alkylated in 10mM iodoacetamide for 30minutes at room temperature. Proteins were digested with 2ug sequencing grade trypsin (Promega, Madison, WI) for 1 hour at 37 °C, followed by a further overnight digestion in another 2ug in order to maximize complete digestion of complex mixtures.

5 or 10ul peptides were loaded onto a 5 cmC18 pre-column, 300 um i.d. (LC packings), the concentrated peptides were subsequently loaded onto a PepMap C18 reverse phase,75 mm i.d., 15 cm analytical column (LC Packings), these were then eluted using an Eksigent nano LC system at a flow rate of 300 nl/min which was attached to a LTQ Orbit rap (Thermo Electron). The gradient described in (Rees et al., 2011) was applied to resolve and elute the peptides into the LTQ ion trap. Two 30 min washes with 85 and65% acetonitrile were carried out to reduce carryover of any residual abundant peptides, such as Actin, that bind non-specifically. The

Mass Spectrometry was performed by Dr. Johanna Rees of the University of Cambridge.

2.8 Western blot

Male flies of the indicated genotypes were selected and maintained in normal fly food at 25°C with 12h:12h light: dark cycles (LD). For LD experiments, flies were collected on the 5th day of light entrainment at the indicated time points. For the temperature experiments, flies were first reared in LL at 25°C for 3 days and then were transferred to either 25°C: 27°C or 25°C: 29°C temperature cycles for either 7 or 14 days, (these are the similar conditions as those used for the behavioural experiments). On the last day of the TC flies were collected at the certain ZT (zeitgeber time). For TIM and PER analysis 30 flies were collected and frozen in liquid nitrogen and stored at -80°C. For each time point 23 fly heads were collected over dry ice. For the testing of the overexpression of tagged Nocte described in chapter3, approximately 50 fly heads were collected. Fly heads were homogenized in 35ul of extraction buffer (20 mM HEPES pH7.5, 100 mM KCl, 5 % Glycerin, 10 mM EDTA, 0.1 % Triton-X 100, 20 mMβ-Glycerophosphat,

0.1 mM Na3VO4, 1x Complete Protease Inhibitor [Roche])(Stanewsky et al., 1997) and centrifuged at 4°C and 13,000 rpm twice. The supernatants containing the protein complexes were separated and boiled with 5X SDS loading buffer (0.3M TRIS,10% SDS, 50% glycerol, 25%β-mercapto-ethanol, 0.01% Bromophenol blue) for 7 minutes before loading and running on 4.5%/6.0% SDS-polyacrylamide gel (Peschel, 2008) for 16 hours at the room temperature at 70V.Proteins were then transferred to Nitrocellulose (Protran Whatman) by use of a Semi-dary electrobloting unit (Fishbrand, Leicestershire, England) at 400 mA for 55 minutes. After blotting, the nitrocellulose membranes were blocked with 5% non-fat milk in TBST (10 mM Tris-Cl,150 mM NaClpH 7.5, 0.05% Tween 20) at room temperature for 2 hours. Ponceau-S staining was used to control for the equal loading and transfer of the proteins. Primary antibodies were diluted in 1% BSA/TBST (5% non-fat milk for FLAG) to their appropriate concentrations (shown in Table 2.6) and incubated with the membranes overnight at 4°C. This was followed by the addition of the secondary antibody (diluted in 5% non-fat milk/TBST) and incubation of the membranes and the secondary antibodies (Table2.6) for a minimum of 2 hours at room temperature. The membranes were then washed with TBST and incubated with chemiluminescent substrate from the

Pierce SuperSignal HRP kit (according to the manual). Finally, X-ray films (Amersham) were developed to the membranes according to the munual.

Table 2.6 antibodies used in this study

1st Antibody				
Name	**Host**	**Ratio (western blot)**	**Ratio (immunohistochemistry)**	**Reference/Source**
Anti-TIM	Rat	1:1,000	1:1,000	Yoshii et al., 2005
Anti-PER	Rabbit	1:10,000	1:15,000	Stanewsky et al., 1997
Anti-IR25a	Rabbit	1:5,000	1:500	Benton et al., 2009
Anti-PDF	Mouse		1:1000	DHSB
Anti-Spam (Anti-21A6)	Mouse		1:20	DHSB
Anti-GFP	Rabbit		1:500	Invitrogen
Anti-FLAG M2	Mouse	1:1,000		Sigma
Anti-Nocte	Genie pig	1:5,000		Carla et al., unpublished
2nd Antibody				
Rabbit-HRP	Sheep	1:16,600		Pierce
Rat-HRP	Sheep	1:12,500		Pierce
Mouse-HRP	Sheep	1:1,000		Pierce
MouseAlexaFluor -488			1:500	Molecular Probes
RatAlexaFluor -594			1:500	Molecular Probes
MouseAlexaFlour -647			1:300	Molecular Probes
RabbitAlexaFlour -594			1:500	Molecular Probes

To quantify band intensity, the pixel intensities (mean gray value) of each lane were determined by Image J software(http://rsb.info.nih.gov/). To

normalize the data, the peak value was set to 1, and the ratio from each of the time points was then divided by the peak value.

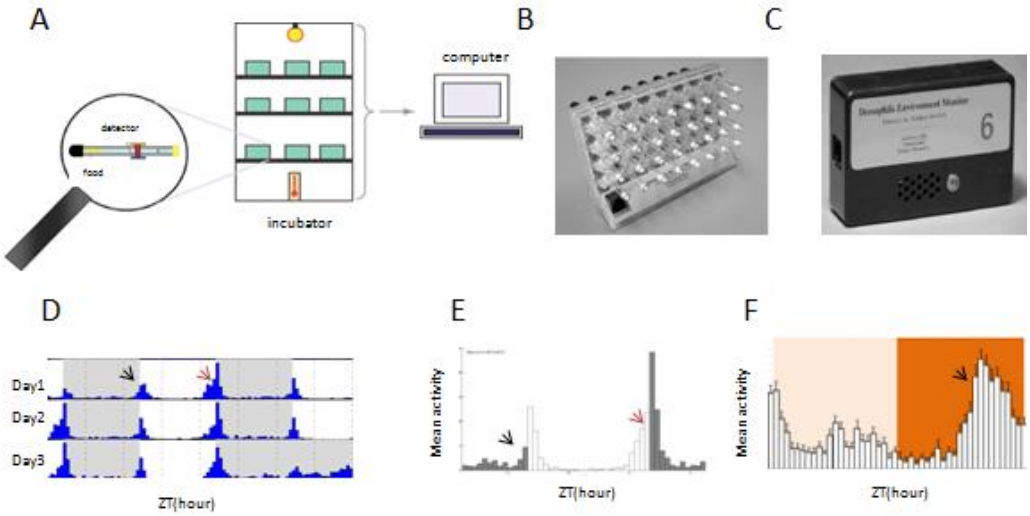

Figure 2.2*Drosophila* Locomotor Activity Monitor System and analysis of data.
A. The working scheme of DAM. B. A monitor used to track locomotor activity . C. An environmental monitor used for recording real time light, temperature and humidity conditions. D. Typical double-plotted actogram of 16 Canton-S flies under LD condition. Blue columns represent the sum of activity in 30 mins with grey and white background standing for darkness and lightness, respectively. Black and red arrows highlight the morning and evening peak. E. Typical daily average (Histogram) of locomotor activity of *Canton-S* flies under the same condition as in D. Black and red arrows indicate morning and evening peaks respectively. Activity during the night (filled bars) and day (open bars) as indicated. F. Locomotor activity of *Canton-S* flies under temperature cycles in constant light. The sum of activity in 30 mins in cool phase (25°C, pink background) and warm phase (27°C, orange background) was plotted in open bars.

2.9 Locomotor activity analysis

The locomotor activity of the flies was monitored using the *Drosophila* Activity MonitorSystem (DAM, Trikinetics Inc., Figure 2.2 A). Male flies (3-5 days old) of the required genotype were placed inside individual glass tubes (5 mm diameter x 65 mm length). Approximately one third of each tube was filled with fly food that comprised of 2% Bacto-agar and 4% sucrose. To prevent the evaporation of the food, one end was sealed with paraffin wax whilst a cotton plug placed at the other end to prevent the fly from escaping. The DAM monitors (Figure 2.2 B), as well as an environmental monitor (Figure 2.2 C, Trikinetics Inc.), were placed inside a light- and temperature-controlled incubator, from where the activity of the flies was monitored. The time that the flies were monitored for and the conditions of the incubator varied depending on the requirements of the experiment. The DAM locomotor monitor measures the individual activity of each of the 32 flies as they walk back and forth along the tube. The movement of each fly is recorded by detecting the amount of times that an infra-red beam is blocked off (Figure 2.2 A). The infra-red beam detectors assign acount of 1 or 0 depending on if it hits the fly or not, this is then automatically recorded by an attached computer. The raw data was sampled every 5 minutes and transformed in the form of every 30 minutes using DAM Filescan

(Trikinetics Inc.) for analysis. The data was analyzed using a signal-processing tool-box (Levine et al., 2002) implemented in Matlab (MathWorks).

The data was represented as an Actogram (Figure 2.2 D), which is a double-plotted representation of activity versus time. As well as in the form of a histogram (Figure 2.2 E), in which the daily average activity of a group of flies during the entrainment conditions is presented. Such analyses were especially useful in analysing light entrainment and free running behaviour. For analysis and quantification of behaviour in temperature cycles, a modified histogram was produced using Excel (Office, Microsoft) (Gentile et al., 2013).Briefly, the activity from the last two days of each temperature cycles was plotted in Excel in 30 minute bins. The activity window was chosen by using the activity between ZT6 and ZT12 (6h before temperature decrease), an 'EI' (Entrainment Index = ratio of total activity occurring during the activity window divide by the activity over the warm phase (ZT0-T12)) was calculated for each of these. Note that, to distinguish the real behavioural peaks from temperature response peaks, a simple filter was applied to the four activity bins for the 2 hours following each

temperature transition. If the bin activity was greater than 1.5 times that of the last bin before the transition, it was replaced by the average of the two previous bins before the transition and the two bins following the bin to be replaced. In this way, only data from genotypes and conditions that did produce a startle response was filtered. The filtered data was only used for calculations, whilst the unfiltered data was used to plot the Histograms.

2.10 Immunohistochemistry

Immunostaining of whole-mount brains was performed according to Yoshii et al.,(2008), with some subtle modifications. Flies were first entrained under the relevant and stated conditions before being collected at theindicated ZT. For LD experiments, flies were fixed on the 5^{th} day of light entrainment at the stated time points. For temperature cycles experiments, flies were first reared in LL at 25°C for 3 days, and then transferred to a 25°C:27°C or 25°C: 29°C temperature cycle for 7 days. Therefore, the conditions are consistent between the samples used for western blots and the flies used for the behavioural experiments. Fly heads were fixed in 4%

paraformaldehyde/PBS at room temperature for 2 hours before being dissected in cold PBS (20.5 mM NaH2PO4, 77.2 mMNa2HPO4, 1.54M NaCl). After being dissected, brains were washed 3-4 times in PBS with 0.1% Triton X-100 (0.1%PBST) at room temperature, following this they were blocked with 5% normal goat serumin 0.5% PBST over night at 4°C. Brains were incubated with the indicated primary antibodies (Table2.6)in blocking buffer at 4°C for 48-72hours. After washing 6 times with 0.5% PBST, the samples were incubated at 4°C for 48 hours with diluted secondary fluorescent antibodies (Table) in 0.5% PBST. Brains were then washed 6 times with 0.5% PBST before being mounted in Vectashield medium(Vector laboratories, Burlingame, Calif.).

In order to observe any endogenous GFP and/or RFP signals, protocol previous described in Sehadova et al (2009) was followed. Briefly, tissues of different fly strains were fixed and dissected in 4% paraformaldehyde/PBS solution as above. Samples were then washed 3 times in 3%PBST at room temperature and finally mounted in Vectashield medium.

Immunostainings on antenna sections was performed as described in Abuin

et al. (2011). 14 µm pre-fixed antennal cryosections in OCT (Tissue-Tek, Sukara) were collected on slides followed by washing for 2 x 10 min in PBS, sections were permeabilized for 30min in PBST and blocked in 5% heat-inactivated normal goat serum in PBST for 30 min. Primary antibodies were diluted in blocking buffer and applied to slides placed horizontally in humidified chambers and left overnight at 4°C. After washing for 3 x 10 min in PBST, slides were re-blocked for 30 min and incubated with secondary antibodies diluted in blocking buffer in humidified chambers in the dark for 2 h. Slides were washed 3 x 5 min in PBST and mounted in Vectashield (Vector Labs).

All samples were later examined using a Leica SP5 confocal microscope. To quantify TIM signals in each brain at different time points, a previous established protocol was applied and modified (Gentile et al., 2013). Pixel intensity(I) of neurons and background staining (B) in each neuronal group was measured by Image J software. The background was subtracted (I'=I-B) and an average staining intensity was calculated from all clock neurons within each neuronal group for each hemisphere separately. For each group of clock neurons, at least 6 hemispheres from each genotype were checked

and measured. The data was normalized by setting the peak value to 1, the ratio from each time point was then divided by the peak value.

2.11 RNA isolation and RT-PCR

For the extraction of RNA from the fly's femur parts, 30-50 flies of each genotype were collected and pooled in 2ml of RNALater (Ambion), 100ul of 0.1%PBST was added to facilitate the penetration of the RNALater into the tissues. After 48 hours at 4°C, femurs from around 200 fly legs were quickly dissected in cold RNALater. Total RNA was extracted using RNAEasy kit (QIAGEN) according to the manufacturers' instructions. Total RNA was finally eluted in Rnase free water and stored at -80°C.

The synthesis of cDNA was performed using the Reverse Transcription Reagents Kit (Applied Biosystems) in 10 ul reaction with 1 ug of total RNA as the template according to the manufacturer's instructions.

In order to verify the mRNA expression levels of both *IR25a* and *nocte* in the femur, various dilutions of cDNA were amplified by PCR using the primers

shown in the Table2.1, and PCR products were then separated and visualised by DNA electrophoresis on 1.5% agarose gels.

To quantify the expression level of each gene for the indicated strains, the pixel intensities (mean gray value, VI) of each lane on the DNA gel were determined by Image J software(http://rsb.info.nih.gov/). As a control for cDNA loading variances, *rp49* (ribosomal protein 49) was also measured and quantified. The inputs (Vr) andratios (R=VI/Vr) were calculated and plotted using Graphpad Prism (GraphPad Software, San Diego California, United States).

2.12Generation of the *IR56a* deletion through imprecise excision

y w; IR56a^{Mimic} (*y+*, as the wild type yellow gene is fused in the MIMIC construct, Table 2.5) was used in the excision of *IR56a* DNA sequence of the 2ndchromosome. This was done by using a transgenic source of transposase under the control of a heat-shock promoter (*y w;P{hsILMiT}*) (Table 2.5).Mobilization and excision of the MIMIC element was as described in

Figure 2.3. The heat shock was carried out for 2 hours and was performed daily from the embryonic stage till the flies hatched in a water bath at 37 °C. Excision events were identified by screening for (*y*).Males with excision events (*y*) were subsequently balanced with *yw; Bl/Cyo*. Approximately 200 independent excision lines were screened by the PCR using genomic DNA amplified by the primersIR56ajo (Table 2.1).

Figure 2.3 Procedure for excision of *IR56a*^{Mimic}

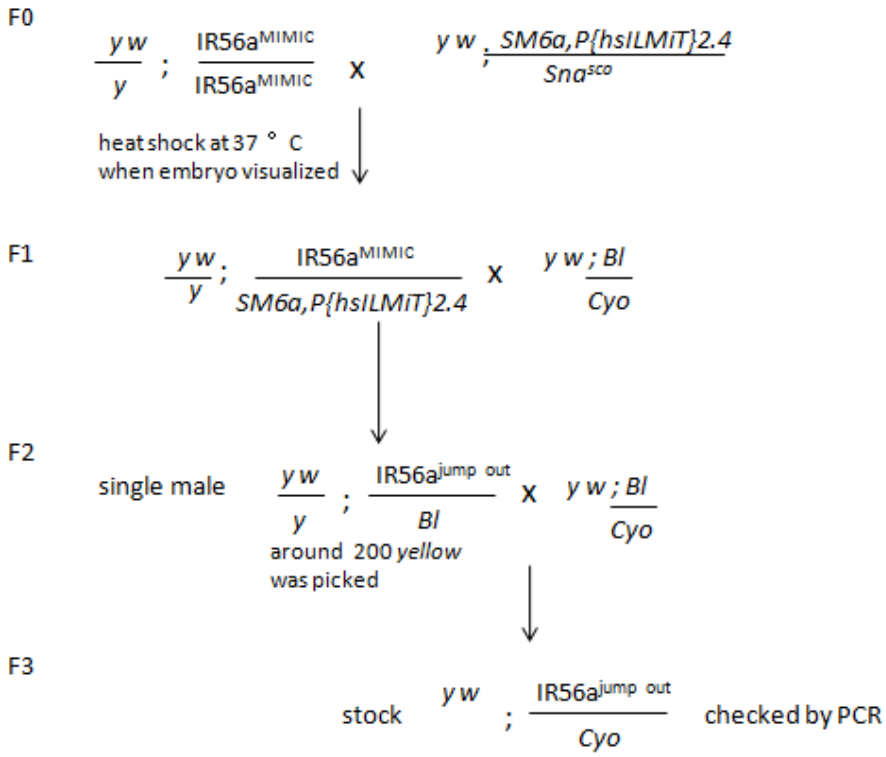

2.13 Statistical analysis

For the statistical analysis of the RT-PCR quantification, the cell numbers calculation and the western blot experiments discussed in chapter 4, one-way ANOVA (Kruskal-Wallis nonparametric test) and Student t-tests(Mann-Whitneynonparametric test)were performed using GraphpadPrism (GraphPad Software Inc). Significance levels are described in the figure legends.

For the quantification of behavioural data during temperature cycles, one-way ANOVA followed by Bonferroni post-hoc test was used to find differences between groups (Gentile et al, 2013), Significance as indicated in the figure legends.

Chapter 3
Isolating novel genes interacting with *nocte* involved in temperature synchronization of the *Drosophila* circadian clock

3.1 Background

As mentioned in chapter1, circadian clocks in *Drosophila melanogaster* coordinate many biological and physiological processes in order to guarantee that they occur at a beneficial time for the flies. It's now widely accepted that the PER/TIM: CLOCK/CYC transcriptional feedback loop is the basis for maintaining the important precise 24 hour rhythmicity of the fly even without external time cues (Stanewsky, 2002; also see details in chapter1). However, both the central and the peripheral circadian clocks also need to be synchronized to the natural environment. This synchronization is based on predictable and recurrent changes in the environment such as the daily light: dark (LD) and temperature cycles (TC), which are known as 'zeitgebers'. The most predominant zeitgeber is light which resets the circadian clock mediated primarily via CRY induced TIM degradation (Stanewsky et al., 1998; Emery et al., 1998; Ceriani et al., 1999). As well as this, several novel light-input routes have been identified (Emery et al., 2000;

Helfrich-Förster et al., 2001; Veleriet al., 2007; Chen et al., 2012 and Szular et al., 2012). Compared to our understanding of how light mediates clock entrainment, however, our understanding of temperature as a zeitgeber is relatively poor. It has been shown that daily temperature fluctuations with amplitude of only 2-3°C in either constant darkness (DD, Wheeler et al., 1993) or light (LL, Yoshii et al., 2005; this study)can robustly synchronize behavioural rhythms in *Drosophila*. This does not only occur at the behavioural level: recently a series of studies have also shown that TC can synchronize central clock neurons either in DD (Busza et al., 2007; Lee et al., 2013) or LL (Gentile et al., 2013; this study). However, it is still unclear how temperature resets the central and peripheral clocks.

In order to broaden our understanding of the processes underlying temperature entrainment, a forward genetic screen utilizing EMS-induced single site mutation mutants was performed in our lab (Glaser and Stanewsky, 2005). Two temperature entrainment mutants that exhibit clear defects at both the molecular and behavioral level in entraining to temperature cycles were isolated. One mutant is linked to the *norpA* gene, which encodes a Phospolipase C (PLC-β) protein that is a crucial factor in the invertebrate phototransduction cascade and is also involved in thermosensation (details in chapter1).The other EMS

induced mutation affects the novel gene *nocte* (*CG17255*), which encodes a glutamine rich protein (Sehadova et al., 2009). Further study revealed that the Nocte protein is highly expressed in the chordotonal organs (Ch organs), which are mechanosensory structures that function as stretch receptors in *Drosophila*. Knock down of *nocte* expression via RNA interfence (RNAi) in Ch organs disrupts the ability of the fly to synchronize its circadian clock to temperature cycles. However, the molecular function of the Nocte protein is still unknown, because bioinformatical analysis of its amino acid sequence failed to identify any functional domains. This difficulty was further compounded by the lack of apparent homology to any proteins of known function.

Considering that temperature entrainment is an intergral and complicated biological process, it is unlikely that Nocte in itself is sufficient for temperature synchronization. Therefore, isolating the proteins that Nocte interacts with could help us to understand the molecular mechanisms of Nocte mediated temperature entrainment. Affinity purification coupled to mass spectrometry provides a reliable and efficient method for identifying proteins and their binding partners. It is reported that the bait stability and recovery as well as capturing potential interaction partners are improved by performing parallel purifications with the FLAG and StrepII tags other than TAP when using

Drosophila embryos as material (Rees et al., 2011). Therefore, in order to isolate the proteins interacting with Nocte *in vivo*, a novel parallel affinity capture method was employed: the 'bait' protein Nocte was tagged with an N-terminal 3XFLAG and a StrepII tag. These were used for pulling down potential candidates in parallel to minimize protein degradation resulting from the prolonged binding and additional washing steps. The protein complexes were digested with trypsin before being identified by high throughput mass spectrometry (Figure3.2). Candidate proteins that appear on the 'contamination' list, which was generated and based on the negative control (the sample of the *gmr-gal4* line alone) were discounted, the other candidates were further analyzed using behavioural assays. Using this method, I report here that a series of protein complexes potentially interacting with Nocte were isolated by affinity purification and identified by the following MS sequencing. Furthermore, we validated potential candidates via behavioural analysis of *Drosophila* locomotive activity. I show that several mutants affecting genes that are involved in pheromone sensation, calcium binding and transport, proteolysis and ATP binding, disturb temperature synchronization.

3.2 Results

3.2.1 Generation and analysis of transformant lines expressing the Nocteand Nocte[1]proteinswith tags

In order to characterize the novel proteins interacting with Nocte in temperature synchronization, a construct was generated to express the Nocte protein combined with FLAG-tag, StrepII-tag and HA-tag(therefore named FSNH, Figure 3.1 A). The whole *nocte cDNA*(6930 bp) with the tags were sub-cloned into the pUAST vector (details see chapter2), this can be used in expressing the fusion protein in different tissues of the fly *in vivo* using different tissue-specific gal4 lines.

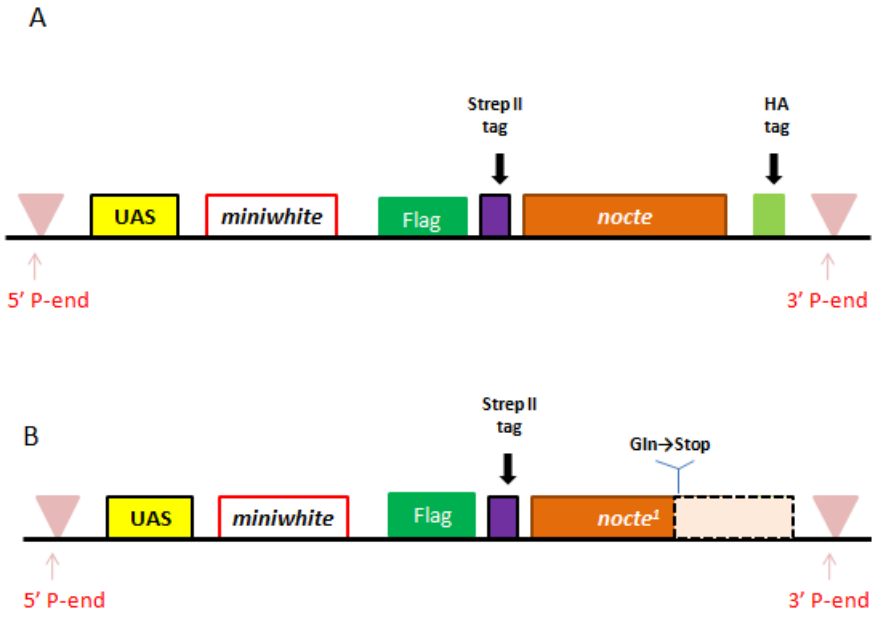

Figure 3.1 The constructs used for Nocte purification.
The constructs FSNH (A) and FSN[1] (B) were generated for Nocte pull-down. Note that the difference between (A) and (B) is an additional HA-tag at the C-terminus of the *nocte* cDNA.

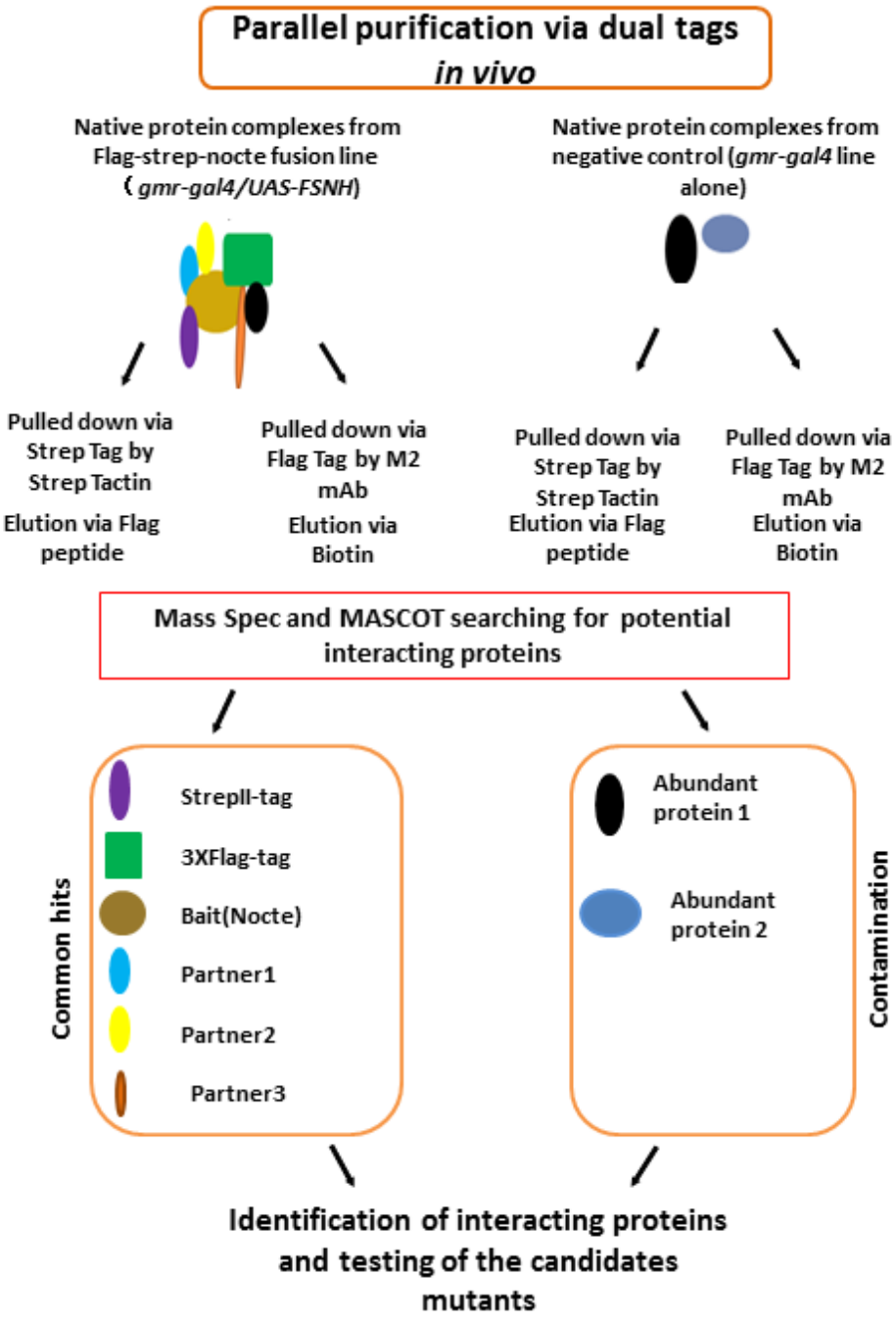

Figure 3.2the outline of parallel purification using the dual-tag strategy.

After micro-injection of the constructs into the embryos of *yw* flies, several transformants with UAS-FSNH or FSN[1] inserted on different chromosomes were isolated (Table 3.1). To determine if these lines can

overexpress the Nocte protein, western blots were performed using 50 fly heads of several transformants driven by *gmr-gal4*.As shown in Figure3.3 A, anti-Nocte serum (bottom) (Gentile et al., unpublished data) detected a protein around 290kDa in both the *gmr-gal4* overexpressing the *UAS-GFP* (negative control), and all of the transgenic lines containing the *tagged nocte* constructs crossed to *gmr-gal4*. However, it is obvious that all of the bands from the over-expression of the FSNH lines are more abundant than that of the *UAS-GFP* line driven by *gmr-gal4*, which shows endogenous Nocte expression only. This was also supported by the quantification (Figure 3.3B). To further confirm the overexpression of the

Table3.1 chromosomal location of the tranformants

Transformant	Chromosomal location	Eye clour
UAS-FSNH1	II	red
UAS-FSNH3	II	red
UAS-FSNH11	III	orange
UAS-FSNH21	III	red
UAS-FSN^{1}6	III	red
UAS-FSN^{1}9	II	red
UAS-FSN^{1}13	II	red

protein derived from *nocte-tagged* constructs, another western blot was carried out but with an anti-FLAG antibody. A protein of similar size to that seen with the anti-Nocte was present in head homogenates of the selected nocte-tagged transformant lines (*FSNH1*,*FSNH3*,*FSNH11* and *FSNH21*, Figure 3.3A top, 3.3 B). On the contrary, the band was absent in the *UAS-GFP* line, which indicates that the transformants can express

abundant levels of the Nocte-tagged proteins with the right molecular size.

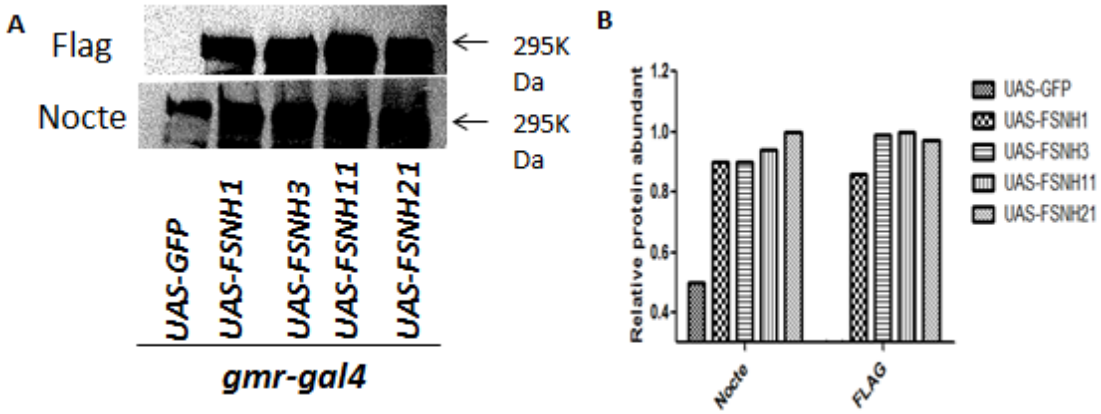

Figure 3.3 Immunodetection of Nocte-tagged protein on Western blots.
(A) The over-expression levels of different transformants were tested by western blots. Different insertion lines were crossed with a pan-retinal *gmr-gal4* driver. The UAS-GFP line served as a negative control. Independently isolated protein extracts were incubated with anti-Flag(top) and anti-Nocte(bottom). (B) Quantification of all the bands shown in A.

In order to determine whether the introduction of multiple tags to the Nocte protein had affect edits normal physiological function, I conducted a series of genetic analyses of the selected transformants by crossing them with different gal4 lines. Based on our previous data, it has been shown that overexpressing the *nocte-cDNA* using a *nocte-gal4*driver (Sehadova et al., 2009) leads to lethality during *Drosophila* early development (Gentile. et al, unpublished, also shown in Table 3.2). This indicates that Nocte is also crucial for the normal development of *Drosophila* besides its function in temperature entrainment. Similar results were found when I used the *nocte-tagged* flies driven by the

same *nocte-gal4* line. By contrast, the lethality phenotype was not observed in the *nocte-gal4/UAS-GFP* flies (Table 3.2), suggesting that the tags localized at *N-terminal* and *C-terminal* of Nocte do not affect its function *in vivo*, at least its function in development, although more experiments such as genetic rescue are necessary to further confirm Nocte-tag can work as Nocte in vivo. Furthermore, both the *nocte-cDNA* and *nocte-tagged* transgenic flies were also crossed with the following tissue specific gal4 lines: pan-neural gal4 (*elav^{c155} –gal4*, Lin and Goodman., 1994), retinal gal4 (*gmr-gal4*, Freeman., 1996) and *F-gal4(33-5)*, which is predominantly expressed in the neurons of the chO (Kim et al.,2003;Sehadova et al., 2009). Progenies of all the drivers carrying *nocte-cDNA* or *nocte*-tagged lines could hatch and survive to adult hood, except the transformant (*FSNH21*) driven by the *elav^{c155}-gal4* line, which leads to lethality, and fails to develop into adult stage. When crossed with *gmr-gal4*, the offspring of the untagged *nocte-cDNA* line has slightly rough eyes, which was not observed in the *nocte-tagged* flies (Table 3.2). This may be caused by different expression levels dependent on the different insertion sites. These results, along with the western blotting data, suggested that the tags we added do not affect the normal physiological function of the Nocte protein. Therefore, it seems promising to use this strategy to identify novel partners of Nocte. Compared with the other three lines, *UAS-FSNH1* has a relatively low

amount of protein expression, and *UAS-FSNH21*results in lethality when crossed to the *elav-gal4*line. Therefore, *UAS-FSNH3* and *UAS-FSNH11* were chosen to do the following parallel affinity purifications, as both of them have a stable abundant protein expression level and similar phenotype compared with untagged *nocte-cDNA*.

Table 3.2. Phenotype analysis of the FSNH transgenic lines

UAS-lines	Chromosome location	Phenotype driven by nocte-gal4	Phenotype driven by elav^{c155}-gal4	Phenotype driven by GMR-gal4	Phenotype driven by F-gal4(33-5)
GFP	II	Viable	Viable	Viable	Viable
nocte-cDNA	II	Lethal	Viable	Viable △	Viable
FSNH1	III	Lethal	Viable	Viable	Viable
FSNH3	III	Lethal	Viable	Viable	Viable
FSNH11	II	Lethal	Viable	Viable	Viable
FSNH21	II	Lethal	**Lethal**	Viable	Viable

△ indicates that the offspring is viable but with abnormal developed eyes.

3.2.2Parallel affinity purification of Nocte interacting proteins

The progenies from the *UAS-FSN3* and *UAS-FSNH11* crossed with *gmr-gal4* were collected along with the *gmr-gal4* line alone, which served as the negative control. The protein complexes were isolated and subjected to pull down experiments following the protocol (outlined in chapter 2). To examine the quality of the purification procedure of both FLAG and StrepII purifications, a serial of protein samples were collected for monitoring the concentration of the bait (Nocte) at the following steps: protein extraction, unbinding protein (shown as ‘unbinding’ in figure 3.4) and elution. The western blotting analysis served to examine

the existence of the bait with anti-FLAG antibody (Figure 3.4 A). The lanes of F1 (*FSNH3* pulled down by FLAG) and F2 (*FSNH11* pulled down by FLAG) at the elution step

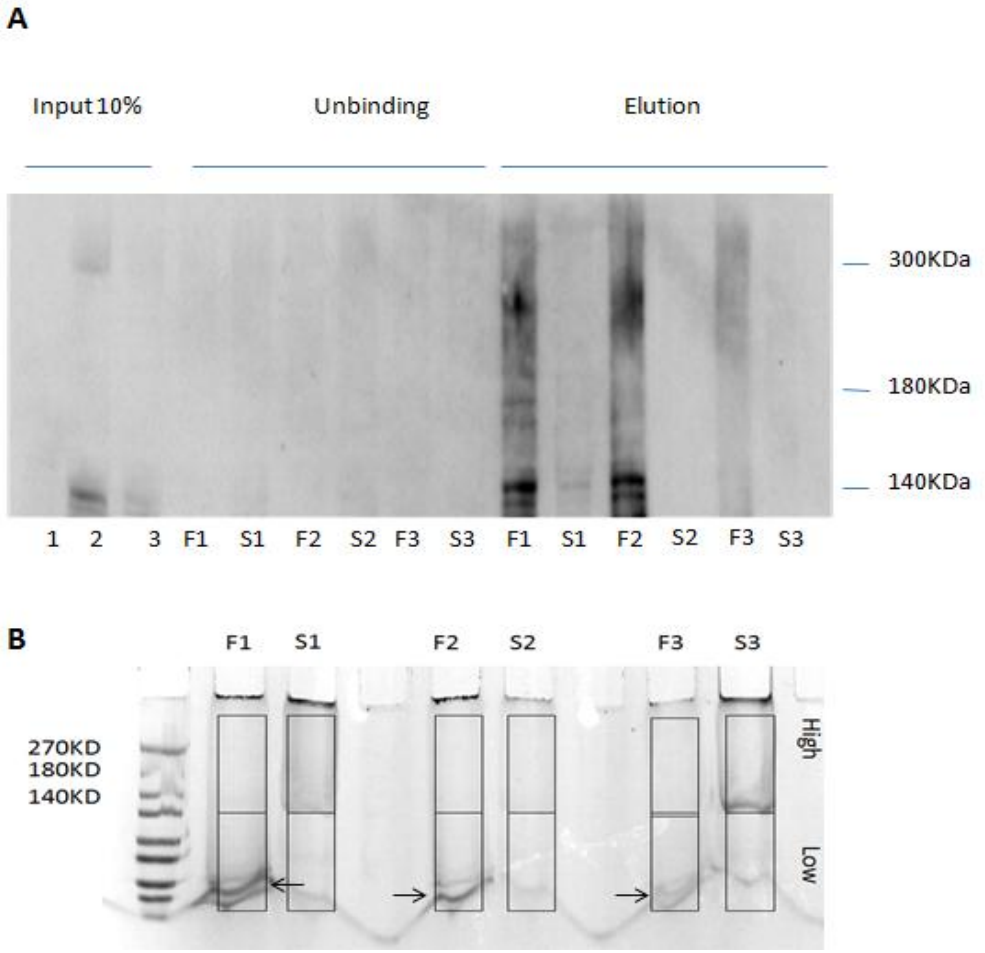

Figure 3.4 Isolation of protein complexes containing Nocte by parallel purification

(A) Western blot assays after parallel purification using anti-Flag serum.1: *gmr-gal4>pUAST-FSNH3*, 2: *gmr-gal4> pUAST-FSNH* 11, and 3 *gmr-gal4* alone (as negative control). F: pulled down by Flag tag. S: pulled down by StrepII tag. For example, F1 means the protein extraction from *gmr-gal4>pUAST-FSNH3* and purified using Flag-tag attached.

(B) Coomassie blue staining the 10% PAGE gel shows the pull-down proteins which will be used in the MS sequencing. Note that the lanes containing S1 and S2 have barely visible protein bands compared with the lanes containing F1 and F2. The frames of High and Low indicate that every lane of the PAGE gel was cut in High molecule and Low molecule parts based on the molecular weight to reduce the contamination during the MS sequencing.

are relatively denser than the lanes of the input and unbinding samples respectively, and both the lanes of F1and F2 at the elution step are also accumulated more than the lane of F3 (*gmr-gal4* alone pulled down by FLAG, serving as the negative control), which suggested that the bait was enriched after the tag purification step and the pull-down by FLAG tag was effective. Unfortunately, I didn't observe the similar phenomenon for StrepII pull down. The bands in S1 (*FSNH3* pulled down by StrepII) or S2 (*FSNH11* pulled down by StrepII) at the elution step were very weak, and therefore not processed further for mass spectrometry analysis.
A similar phenomenon showing the abundant proteins after FLAG pull-down but not with StrepII was also found in the PAGE gel after the Coomassie blue staining (Figure 3.4 B). In addition to the bait, we also detected other bands that corresponded to putative associated components in the Coomassie blue stained gel (Figure 3.4 B, arrows). Based on the data mentioned above, we therefore decided to only use the eluted protein samples pulled down by the FLAG tag to carry out the following mass spectrometry analysis.

3.2.3 Mass spectrometry analysis of Nocte interacting proteins

The whole protein complexes in the lanes of F1,F2 and F3 (Figure 3.4) were digested with trypsin, and then analyzed by liquid chromatography

followed by tandem mass spectrometry (LC-MS/MS). Resulting mass values were collected and searched by the MASCOT (Matrix Science) search engine against a database containing the FlyBase *Drosophila melanogaster* genome (version 5.9) with a total of 21,064 proteins (the mass spectrometry and preliminary peptides analysis was performed by Dr. Joanna Rees, Cambridge Centre of Proteomics). 24 different putative proteins with the different ratios of mass to charge (m/z value, mascot score) were identified in all of the samples (Table 3.3). A confidence score system, which is defined as below, was introduced to evaluate the credibility of the candidates (Table 3.3). A protein seen in both *FSNH3* pull-down (F1) and *FSNH11* pull-down (F2) but not in the *gmr-gal4* alone (F3) control would be assigned a score of 100, a protein seen in either *FSNH3* pull-down or *FSNH11* pull-down but not in F3 would be assigned a score of 50. Proteins that present in F3 were assigned a score of 0, and were treated as false positive contaminations. For example, *Synapsin* in table 3.3 would not be considered as a positive candidate since it appeared in the F3 list, although it has the highest scores in mascot and 6 unique identified peptides. Strikingly, 8 identical proteins were isolated in both *FSNH3*(F1) and *FSNH11*(F2) pull-down by FLAG but not in the *gmr-gal4* (F3) pull-down, with average mascot scores above of 30 (Table 3.3). Thus, I picked them as the most promising potential candidates for the following genetic tests.

Table 3.3. the list of the interact proteins for Nocte bait

Gene name	CG number	Confidence score	F1	F2	F3	Mean mascot Score	Unique peptides
IR25a	*CG15627*	100	1	1	0	44	1
CG17097	*CG17097*	100	1	1	0	42	1
ACP36DE	*CG7157*	100	1	1	0	39	1
tweek	*CG15134*	100	1	1	0	37	2
Pkn	*CG2055*	100	1	1	0	45	1
CG9297	*CG9297*	100	1	1	0	435	5
CG1440	*CG1440*	100	1	1	0	40	1
Mcm3	*CG4206*	100	1	1	0	35	1
CG38434	*CG38434*	50	1	0	0	30	1
CG13185	*CG13185*	50	1	0	0	31	1
eIF4B-PE	*CG10837*	50	0	1	0	43	2
Pros45	*CG1489*	50	0	1	0	42	1
Rpt6R	*CG2241*	50	0	1	0	42	1
CG13168	*CG13168*	50	0	1	0	43	1
CG1814	*CG1814*	50	0	1	0	42	1
Pp4-19c	*CG32505*	50	0	1	0	40	1
CG1516	*CG1516*	0	1	0	1	506	10
Synapsin	*CG3985*	0	1	1	1	603	6

3.2.4 Behavioural analysis of the potential interacting partners of Nocte using RNA interference

To further confirm the potential genetic interactions between Nocte protein and its partners isolated from the affinity purifications, a small scale genetic screen was performed to test if the products of these genes are also required for temperature synchronization as the Nocte protein. A batch of RNAi lines (listed in Table 2.3) were employed to validate in

the *Drosophila* locomotive activity assay. A series of the *UAS-RNAi* lines (Table 2.3) were crossed to clock-cell specific gal4 driver *UAS-dicer2; tim27/CyO* (Kaneko et al., 2000) and *F-gal4 (33-5)*, which is predominantly expressed in the neurons of chordotonal organs. Locomotor activity of the F1 progeny (3-4 days old) was recorded during 12h: 12h light: dark (LD) cycle at constant 25°C for 3-4 days. All of the RNAi flies (for some genes two independent RNAi lines were available. Both of them were tested, but only results from one line are shown unless they exhibit a different behavioural pattern) showed robust bimodal activity patterns like wild type (*y w*)(Figure3.5) when combined with either *UAS-dicer2; tim27/Cyo* or *F-gal4 (33-5)* in LD cycles, indicating that none of these knock-down flies impaired the flies ability to synchronize to light. Although activity were shifted when knocking down the expression of *tweek* in clock cells, morning and evening peaks are clear. Interestingly, down-regulation of *CG9297* within the clock-cells (*tim-gal4 27*) leads to lethality in the adult stage, which is similar to the phenotype of the down-regulation of *nocte* (Gentile et al, unpublished data), suggesting both of them have an important role during development.

We next examined the synchronization to temperature cycles in constant light (LL) conditions. After LD entrainment, all experimental flies were

transferred to a 6-hour phase delayed 12h: 12h 25°C:20°C temperature cycle at constant light (LL) for 7 days. It has been reported that

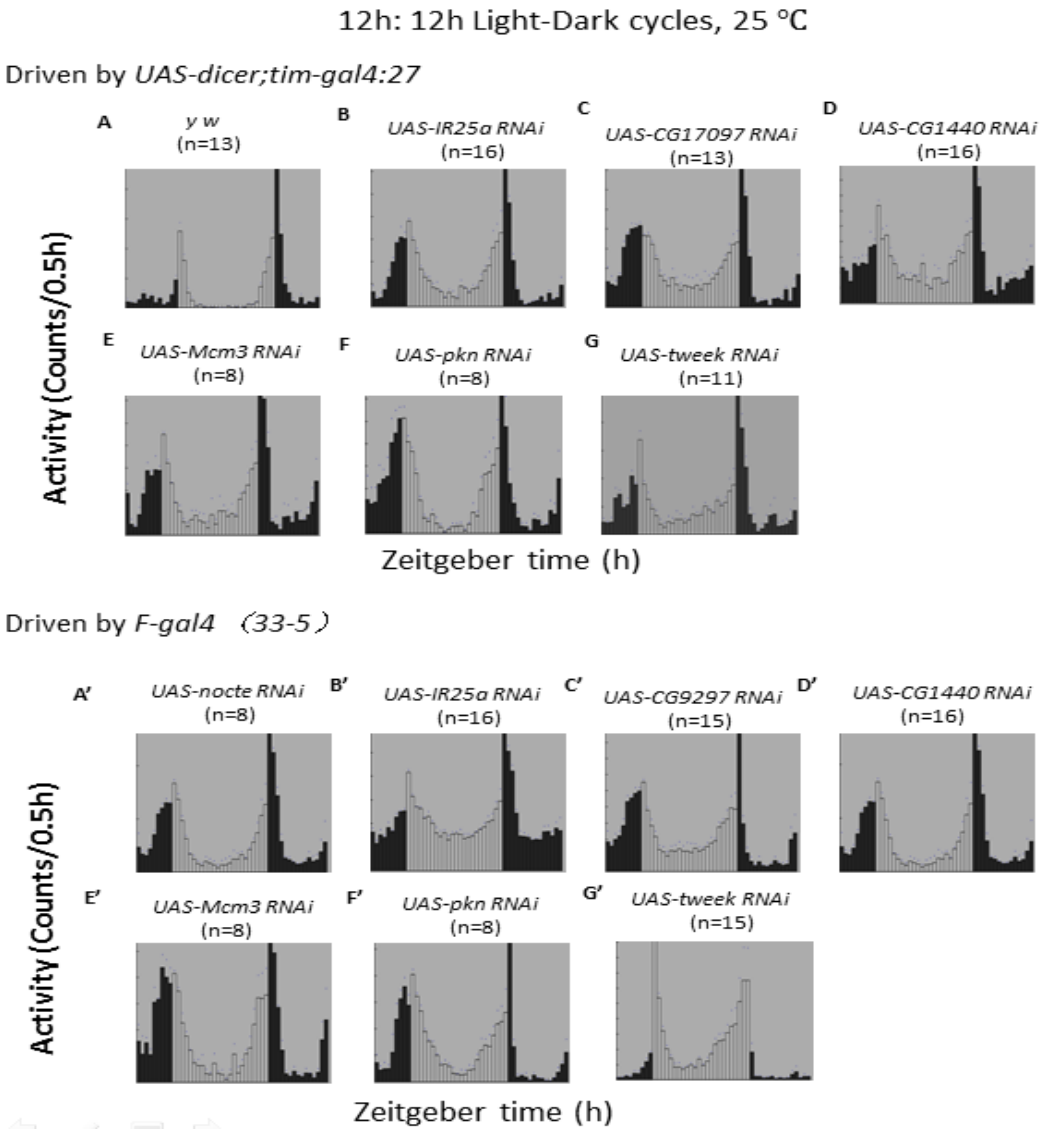

Figure 3.5 Histograms of *Drosophila* locomotor activity patterns of UAS-RNAi lines affected candidate genes driven by *tim-gal4* (A-G) or *F-gal4 (33-5)* (A'-G') under LD cycles.

Black and white columns in each picture represent mean locomotive activity of 30 minutes during the night (black) and day (white), respectively. Note that A (*y w*) is used as positive control without carrying any driver. The genotype of A' is *UAS-nocte RNAi/+;F-gal4/+,* which also served as a negative control. *UAS-CG9297* RNAi driven by *tim-gal4 27* was not shown as progeny fails to develop to adult stage. Number of individual tested is indicated in brackets respectively. *y w* (A) is used as positive control without carrying any driver. The genotype of A' is *UAS-nocte RNAi/+;F-gal4/+,* which served as a negative control. Number of individuals tested is indicated in brackets.

temperature cycles with 12h: 12h 25°C: 16°C in LL are able to synchronize wild type flies but not flies in which *nocte* is down-regulated under the control of *F-gal4* (Glaser and Stanewsky, 2005;Sehadova et al, 2009). Here I show that a 25°C: 20°C temperature cycle is also sufficient to entrain wild type flies with a similar behavioural pattern as in 25°C: 16°C. As shown in the daily average histograms (Figure 3.6), wild-type flies (*y w*) exhibit an entrained behavioural pattern with a robust and well-defined activity peak in the second half of the warm phase, reflecting an anticipation of the transition to cold temperature. In contrast, flies with downregulation of *nocte* in chordotonal organs using the *F-gal4* exhibit distinct behavioural difference to wild type flies: the *nocte RNAi* mutant flies do not show a gradual increase of activity during the warm phase, and instead responsed to the transition of temperature increase and decrease. Furthermore, instead of a gradual locomotor activity increase during the day, the *nocte* mutants were constantly active during the warm phase (Figure 3.6 A'). Strikingly, a severe temperature entrainment defect similar to the *nocte-RNAi/+;F-gal4/+* flies, was observed when crossing *F-gal4* to the *UAS-IR25aRNAi*, the *UAS-CG 9297RNAi*, the *UAS-CG1440RNAi* and the *UAS-Mcm3RNAi* lines (Figure 3.6 B'-E'), whereas behaviour of these flies in LD was normal (Figure 3.5 B'-E'). By contrast, flies in which was down-regulated of the expression of *pkn*, *tweek* and *CG17097* using *F-gal4* behaved normal in

both TC and LD (Figure 3.5 F'-G' and Figure3.6 F'-H'), which indicates that these three genes are not required for either light entrainment or temperature entrainment or poor downregulation effect induced by RNAi, although they may still interact with Nocte and are perhaps involved in *nocte* function. In this study, I only focused on the genes that are involved in temperature entrainment.

To further examine if the temperature entrainment phenotype still occurs after downregulation of the respective genes in clock cells, the same *RNAi* lines were also crossed to cycling *tim-gal4 27* (a clock-cell gal4, Kaneko et al., 2000) and progeny was tested in the same temperature cycling conditions. Strikingly, all of the RNAi flies showed a normal behavioural pattern, similar to wild type flies (*y w*, Figure 3.6 A) in LL and temperature cycles (12h: 12h 25°C: 20°C) (Figure 3.6 B-G). These results demonstrate as previously shown for *nocte* (Sehadova et al, 2009), expression of the new candidate genes in periphery sensory organs (Ch organs) but not in clock cells, is important for their potential role in temperature entrainment. To sum up, all of the behavioural results, along with the proteomics data, indicate that at least 4 candidates (IR25a, Mcm3 and the proteins encoded by *CG9297* and *CG1440*) physically interact with Nocte and therefore constitute

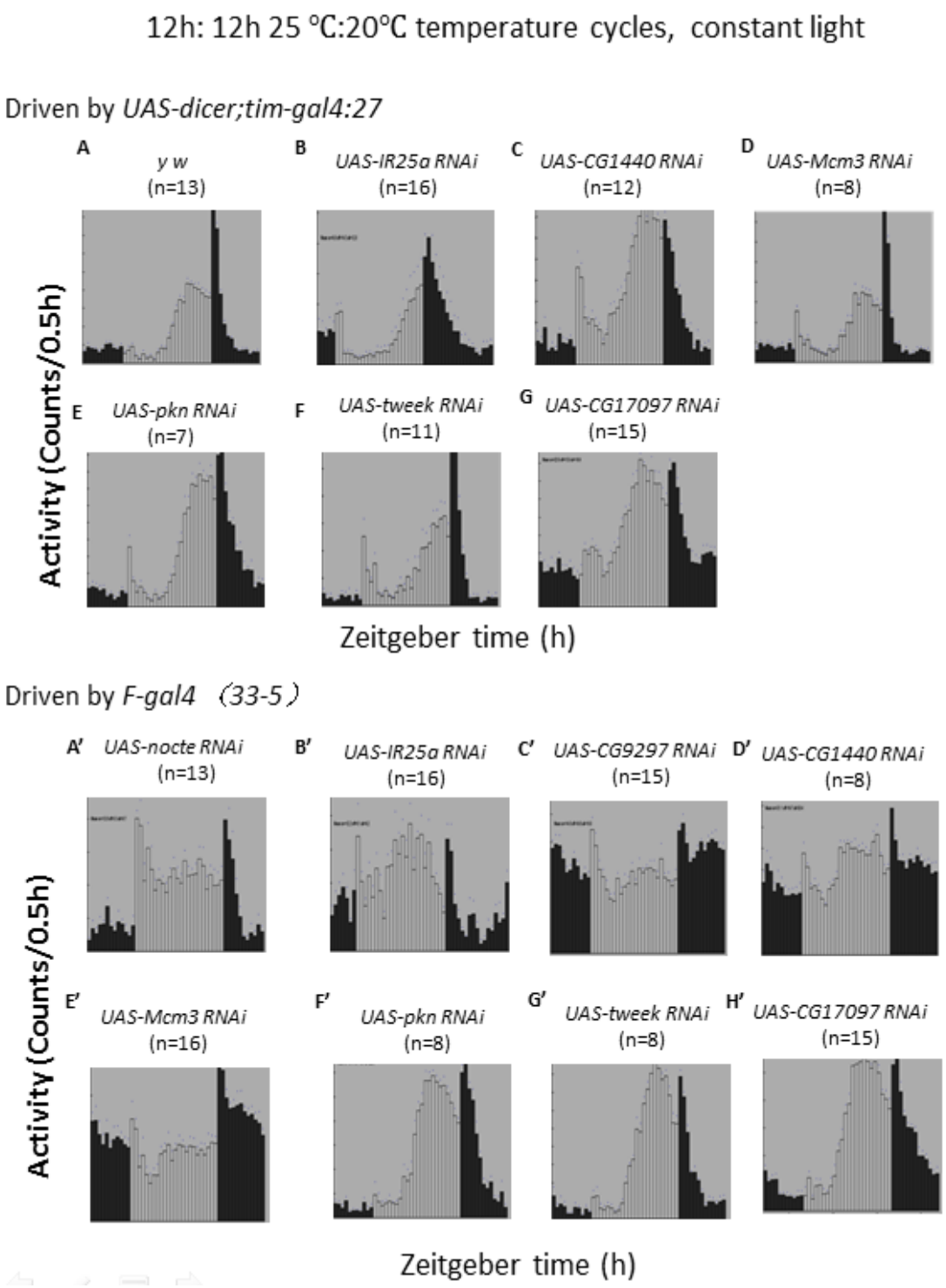

Figure 3.6. Histograms of *Drosophila* locomotor activty patterns of UAS-RNAi lines affected candidate genes driven by *tim-gal4* (A-G) and *F-gal4 (33-5)* (A'-H') under TC in constant light.

Note that black and white columns in each picture represent mean locomtor activity of 30 minutes during the cold (20° C, black) and warm (25° C, white), respectively. *y w* (A) is used as positive control without carrying any driver. The genotype of A' is *UAS-nocte RNAi/+;F-gal4/+,* which served as a negative control. Number of individuals tested is indicated in brackets.

promising new factors involved in temperature entrainment.

3.3 Disscussion

3.3.1Affinity purification combined with mass spectrometry is a reliable and efficient strategy to isolate proteins interacting with Nocte.

Both forward genetics and reverse genetics are powerful strategies to understand the natural world. Forward genetics starts from a phenotype and then characterizing the genetic change that is responsible for that phenotype. Reverse genetics, on the other hand, starts with an interesting gene and then disrupts the function of that gene to produce a phenotype in order to gain insight into the function of this gene, which is also a very efficient method especially for organisms with known genome sequences such as *Drosophila melanogaster.* Before this study, several projects applying forward genetics have already been performed to isolate novel genes required for temperature entrainment in *Drosophila* (Glaser and Stanewsky, 2005;Simoni, 2010). To my knowledge, this is the first sturdy work using reverse genetics strategy to isolate novel genes interacting with a protein involved in temperature synchronization which was isolated by forward genetics: Nocte. As I present here, this method is not only feasible to isolate more interesting

genes to further broaden our knowledge about temperature entrainment. More importantly, most of the genes I isolated have already been annotated, which will help us to understand the potential molecular mechanisms underlining temperature synchronization in *Drosophila*.

It has been known for a long time that temperature can serve as a Zeitgeber to entrain the circadian clock in *Drosophila* (Zimmerman et al., 1968), and Nocte plays an important role in this process (Glaser and Stanesky, 2005; Sehadova et al, 2009). Nevertheless, it is still a long way to identify the genes, protein complexes and signalling mechanisms controlling temperature entrainment. Characterization of native protein interactions could therefore essentially broaden our understanding of novel complex pathways underpinning biological processes, for example, the mechanisms mediating temperature synchronization. Prior to this work, the interactome of Nocte based on high-throughput Y2H (Yeast two Hybrid) interactome mapping for the entire *Drosophila melanogaster* genome has been published (Murali et al, 2010, Figure 3.7 left). Interesting, I could not find any overlap between our affinity capture list and the Y2H list(Figure 3.7), which may be caused by the following two reasons. First of all, one major restriction of Y2H is that interactions are observed out of their *in vivo* context, and may involve

pairs of proteins that never meet *in vivo* as they're located in different cell types, sub-cellular compartments or are expressed at different times in the lifecycle. Subsequently this leads to a high level of false positives (in some cases as high as 90%, Vidalain et al, 2004). In addition, another restriction of Y2H is that this method cannot be used to study the indirect interactions or interactions that involve post-translational modifications. The protein affinity purification can conquer these restrictions and provides more reliable results. So my work is at least complementary to the Y2H approach, which extends our understanding of the Nocte interactome in *Drosophila*. Nevertheless, our original plan was to purify novel proteins interacting with Nocte by both FLAG and StrepII in parallel, and only focus on the candidates which appear in both pull downs. However, it was not possible to carry on with the StrepII pull down because of the low protein yield. To compensate this drawback, Introduced a negative control (the *gmr-gal4* alone) and used two independent transformants (*FSNH3* and *FSNH11*) to perform parallel anti–FLAG pull down. I only focused on candidates identified in both samples and absent from the negative control.

It has been shown that the function of Nocte in temperature entrainment located in the peripheral nervous system--chordotonal organs other than other tissues (Sehadova et al., 2009). It would

therefore be ideal to overexpress tagged Nocte with *F-gal4 (33-5)* and identify the Nocte candidates from isolated legs or Johnston's organs rather than expressing *nocte* in fly heads in this study. However, the pilot experiments showed that the protein isolation from legs was not quantitative enough for the following Mass Spectrometry. Nevertheless, when I confirmed the candidates using behavioural/genetic tests, the candidate genes only induced temperature entrainment defects when knocked-down by *F-gal4 (33-5)*, a chordotonal organ gal4 driver, but not with a clock-cell driver *(tim-gal4)*. This suggests that at least some of the interactions between Nocte and these candidates are real (see chapter4). Nevertheless, it would be more informative if we could repeat the experiments using protein samples from legs with an optimized protein extraction method.

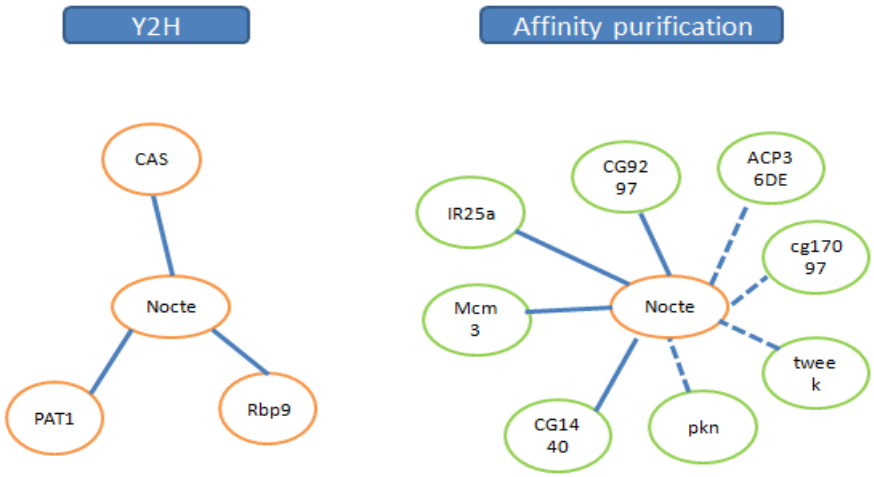

Figure 3.7 The inteactome maps for Nocte based on Y2H and affinity purification data

Nocte interactome map generated by Y2H (left) and Co-IP with MS (right). The thickness of the lines is proportional to the confidence score of the interaction. Dotted lines in the interactome map generated by Co-IP indicate that these interactions could not be confirmed by behavioural tests.

3.3.2Candidates interacting with Nocte are also required for temperature synchronization at the behavioural level.

Although further real-time PCR experiments are required to assay the efficiency of the known-down, behavioural analysis revealed that at least four genes (*IR25a*, *CG9297*, *CG1440* and *MCm3*) may be involved in temperature entrainments. Genes with related function, protein location and phenotypes in the behavioural tests were listed in table 3.4. RNAi lines affecting these genes exhibit the normal bimodal behavioural pattern in LD but show abnormal behaviour during temperature cycles. This suggests that these four genes participate in temperature synchronization, which is consistent with the role of Nocte in temperature entrainment.

3.3.2.1 *CG9297*

The protein encoded by *CG9297* is predicted located in the cytoplasm (Table 3.4), and so is the Nocte, indicating the interaction between these two proteins may be real. Functionally, *CG9297* is predicted to encode a calcium ion transport protein (Table 3.4). The homologue of *CG9297* in mouse (*Mus musculus*) is Sarcalumenin (SAR), a sarcoplasmic reticulum

(SR) luminal glycoprotein, which is highly abundant in longitudinal SR. A study using the mouse model showed that SAR is responsible for Ca^{2+} cycling in skeletal and cardiac muscles through the down-regulation of the Ca^{2+}-cycling related SR Ca^{2+}ATPase type 2a (SERCA2a) (Jiao et al., 2010). Although this gene has not been studied in *Drosophila melanogaster*, several studies have demonstrated that calcium plays a crucial role in modulating circadian clocks output through manipulating neuronal activity in the central clock neurons, especially in s-LNvs (Jepson et al., 2012; Harrisingh et al., 2007; Harrisingh and Nitabach, 2008). Strikingly, a recent paper (Ng et al., 2012) showed that expression of *Drosophila* SERCA (CaP60A) in glial cells is required for the maintenance of behavioural rhythmicity in DD. Will the protein encoded by *CG9297* also be involved in *Drosophila* circadian clocks? It will be a very interesting question to address, although it remains to be investigated if *CG9297* has a similar calcium binding and transport function in *Drosophila*.

3.3.2.2 *Mcm3*

MCM3 belongs to the minichromosome maintenance (MCM) protein family, which forms the core components for DNA helices complexes (Forsburg, 2004, Table 3.4). Although they were first identified in yeast,

all six family proteins (MCM2-7) were later shown to be conserved in all eukaryotes and to be central players for the initiation of DNA replication. However, the relationship between DNA replication and temperature entrainment is not clear. All MCM proteins including Mcm3 belong to a family of AAA^+ proteins (ATPase Associated with various cellular Activities) and carry well-conserved sequence elements for ATP binding, which may indicate that *Mcm3* has a novel function as an ATPase in temperature entrainment. In addition, MCM3 is a DNA binding protein, located in the nucleus, while Nocte is in the cytoplasm, whether Nocte can translocate into nucleus and interact with Mcm3 is still an open question.

3.3.2.3 *CG1440*

Another gene *CG1440* is predicted to encode a cysteine peptidase (Table 3.4). The protein encoded by *CG1440* is also located in the cytoplasm, the same as Nocte. The homologue of *CG1440* in humans is *bleomycin hydrolase*, a neural cysteine protease genetically linked with an increased risk for Alzheimer disease (Smach et al., 2010). It is believed that *bleomycin hydrolase* can cleavage amyloid precursor protein (APP) and induce the release of its proteolytic fragment, beta amyloid (Aβ) (Lefterov et al., 2000).So far there is no evidence shown that *bleomycin*

hydrolase is involved in the circadian clock. But there are links between Alzheimer to circadian clocks (Cermakian et al., 2011). However, based on its predicted peptidase properties, *Drosophila bleomycin hydrolase* could also be involved in the hydrolysis of clock proteins which is the downstream step of ubiquitination.

3.3.3 Is IR25a a real partner interacting with Nocte in temperature entrainment?

The last promising candidate I present here makes me very excited. *CG15627* encodes IR25a, a novel chemosensory receptor in *Drosophila* that belongs to a recently isolated super family of variant ionotropic glutamate receptors (Benton et al., 2009).The receptor property of IR25a made me imagine the possibility of IR25a functioning as a putative thermo receptor for temperature entrainment in *Drosophila*. To prove this hypothesis, the following questions needed to be addressed in my further studies.

1. Does IR25a directly bind to Nocte *in vivo*? Although we isolated IR25athrough protein affinity purification, the interaction could be an experimental contamination. to rule this out, the interaction between Nocte and IR25a needed to be confirmed by independent co-IP

experiments using tagged Nocte and wild type IR25a.

2. Are IR25a and Nocte co-expressed in the same cells? For a real interaction to occur in nature, the two proteins have to be expressed in the same cells or directly neighbouring. In addition to the chordotonal organs in the antenna (also known as Johnston's Organ), leg and wings, Nocte is also highly expressed in the 3rd antennal segment and arista (Sehadova et al., 2009), where IR25a is also reported to be expressed (Benton et al., 2009). Interestingly, the arista and sacculus (a chamber like structure in the 3rd antennal segment) where IR25a and Nocte highly expressed (Benton et al., 2009) were recently identified to also express the thermosensory receptor *brv,* which belongs to the TRP-channel families (Gallio et al, 2011). Of course the most interesting question is if IR25a is also expressed in chordotonal organs, which have been implicated in temperature synchronization (Sehadova et al., 2009).

3. Is IR25a required for temperature entrainment? Although I demonstrate in this chapter that down regulation of IR25a in chordotonal organs (but not in clock-cells) disrupt temperature entrainment at the behavioural level with two independent RNAi lines, it is not clear that the expression of IR*25a*is indeed decreased in the RNAi lines. Even in case the RNAi lines work, due to off-target effects often

observed in behavioural tests with RNAi, independent IR25a mutant alleles should be analysed. And it's also need to be repeated by using other related mutants. In addition, to further validate the genetic interaction between *nocte* and *IR25a*, double mutants of *nocte* and *IR25a* need to be generated and tested.

4. Does IR25a function alone or with another IR partners as a functional thermo receptor complex in this uncanonical temperature sensation organ (Ch organ)? It has been shown that ectopic olfactory sensitivity can be induced by misexpression of IR25a, IR76a and IR76b (Abuin et al., 2011), suggesting that IRs themselves are sufficient to encode chemosensory receptors. Similar experiments also need to be performed to investigate if IR25a encodes a thermo receptor.

Last but not least, except for the four genes mentioned above which are required for temperature synchronization, several other genes (*pkn*, *tweek* and *CG17097*) were also isolated in my pull-down experiments, but exhibited normal activity behaviour during temperature cycles (Table 3.4). This indicates that the Nocte protein may have multiple important functions besides temperature synchronization. For example, Nocte may be required for development by interacting with these components, which is in agreement with the data of the adult lethality phenotype

observed after downregulation or overexpression of Nocte under the control of *nocte-gal4* (Gentile et al, unpublished; also this study).

Gene	Gene Function	Protein location	Protein categories	RNAi lines	Beh. in LD	Beh. in TC Driven by F-gal4	Beh. in TC Driven by tim-gal4:27
IR 25a	ionotropic receptor	Membrane	Ion channel	2	+	-	+
CG9297	Calcium ion binding and transport	cytoplasm	ion transporter	2	+	-	n.d.
CG1440	proteolysis	cytoplasm	enzyme	2	+	-	+
Mcm3	DNA replication ATPase	nuclear	Protein kinase	1	+	-	+
Pkn	C2 calcium-dependent membrane targeting	membrane	Protein kinase	1	+	+	+
tweek	synaptic vesicle recycling	membrane	pre-synaptic protein	1	-	+	+
CG17097	lipid metabolic	cytoplasm	Lipase	2	n.d.	+	+

Table 3.4. Validation of the potential interactors using RNAi lines via behavioral analysis.

List of 8 candidate genes which have the highest confidence scores. Gene names, gene functions, the location of the gene productions, protein category and already analyzed RNAi lines are indicated. The last three lanes indicate what we already tested the respective RNAi lines for its involvement in temperature synchronization using behavioural (Beh)assays either in LD 12hr:12hr cycles with constant 25℃ or in 12hr:12hr (25:20℃)temperature cycles under the control of F-gal4(33-5) or *tim-gal4 27*. (+:normal, -:abnormal, n.d.: not determined. Either because there was no RNAi lines available or the progeny of indicated crosses could not survive until adulthood.)

3.4 Summary of Main Results

3.4.1 Generation and validation of the *nocte* and *nocte*^{1} tagged transgenic flies.

3.4.2 Eight promising candidates have been isolated using affinity purification combined with mass spectrometry.

3.4.3 Four candidates (*IR25a*, *CG92927*, *CG1440* and *Mcm3*) show temperature entrainment defects after downregulation in Ch organs.

Chapter 4
IR25a, an ionotropic receptor, is required for synchronization of circadian clocks to temperature cycles

4.1 Introduction

Circadian clocks are internal daily time keeping systems that allow organisms to synchronize to the natural day/night and temperature fluctuations. Compared with the knowledge about light entrainment, there is relatively little known about temperature synchronization, both with respect to genes and the neuronal circuits involved.

In the previous chapter, I reported a protein interactome study of isolating novel proteins interacting with Nocte, a chordotonal organ enriched protein required for normal temperature entrainment in *Drosophila* (Glaser and Stanewsky, 2005; Sehadova et al, 2009). In that study, I have successfully isolated four candidates potentially involved in Nocte-mediated temperature entrainment inputs. In this chapter, I will systematically investigate the function of one candidate, *IR25a*.*IR25a* encodes a member of the IR receptor family recently shown to function as chemosensory receptor(Benton et al., 2009). For more background

about IR25a see chapter1. Combining biochemistry, genetics and behavioural studies, here I report that IR25a plays a crucial role in temperature entrainment.

4.2 Results

4.2.1 IR25a physically interacts with Nocte *in vivo*.

First of all, to confirm the interaction between IR25a and Nocte, I carried out the co-IP experiments with ectopic co-expression of IR25a and Nocte in fly heads. *UAS-IR25a/UAS-IR25a; tim-gal4:67* flies were crossed either with *UAS-FSNH*(Flag tagged Nocte), or with *UAS-GFP* (which served as negative control), 500ul fly heads of the offspring were harvested in parallel and homogenized on ice. Protein lysates of the indicated genotypes flies were immnuo-precipitated by FLAG antibody and detected with IR25a (Benton et al., 2009) and FLAG antibodies (Figure 4.1 A and B), A protein with the correct size of 100 KD of IR25a was visualized in both FSNH and GFP samples in the input blot but only can be detected in the FSNH sample in the IP blot, suggesting that IR25a physically interacts with Nocte *in vivo*. To investigate which domain in Nocte is required for the interaction between IR25a and Nocte, FSN^{1} (FLAG tagged $Nocte^{1}$,which lacks 600 amino acids at the C-terminus of

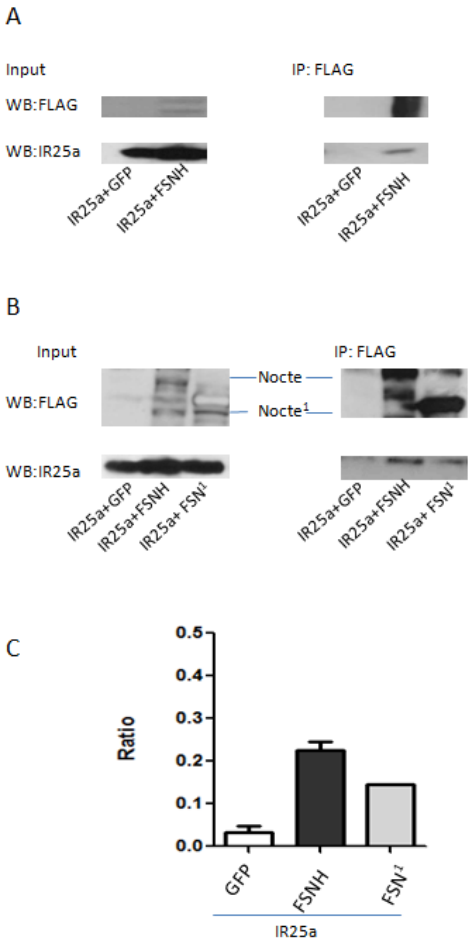

Figure.4.1 IR25a physically interacts with Nocte *in vivo*.
(A) In vivo Co-IP experiments using protein extracts from fly heads. Head lysates were immunoprecipitated using anti-Flag antibody. The immunoprecipitates were examined by Western blotting using anti-FLAG and anti-IR25a antibody. Input represents 30% of cell lysates used in the Co-IP experiment. The genotypes of the flies used here are: GFP+IR25a: *UAS GFP/UASIR25a;tim67/+*. FSNH+IR25a: *UAS FSNH/UAS IR25a;tim67/+*.
(B) The *nocte*^{1}mutation *does* not disrupts the interaction between Nocte and IR25a. Same flies and antibodies as used in (A),except a new genotype of flies was employed. IR25a+FSN^{1}: *UAS FSN*^{1}*/UAS-IR25a;tim67/+*.
(C)Quantification of the protein bands detected by IR25a in (A) and (B). Ratio=IR25a $Pr._{IP}$/IR25a$Pr._{Input}$.

Nocte) generated in chapter 3 was used to perform Co-IP experiment with IR25a. The same experiment was repeated with FSN^{1} , similar to the case of FSNH, an IR25a band can be detected after immunoprecipitation (Figure 4.1 B), although the band appears less abundant compared with wild type Nocte pull-down (Figure 4.1 C). So I conclude that IR25a physically interacts with Nocte and that the C-terminal 600 amino acids of Nocte are not required for the interaction.

4.2.2 IR25a is expressed in subsets of chordotonal organs.

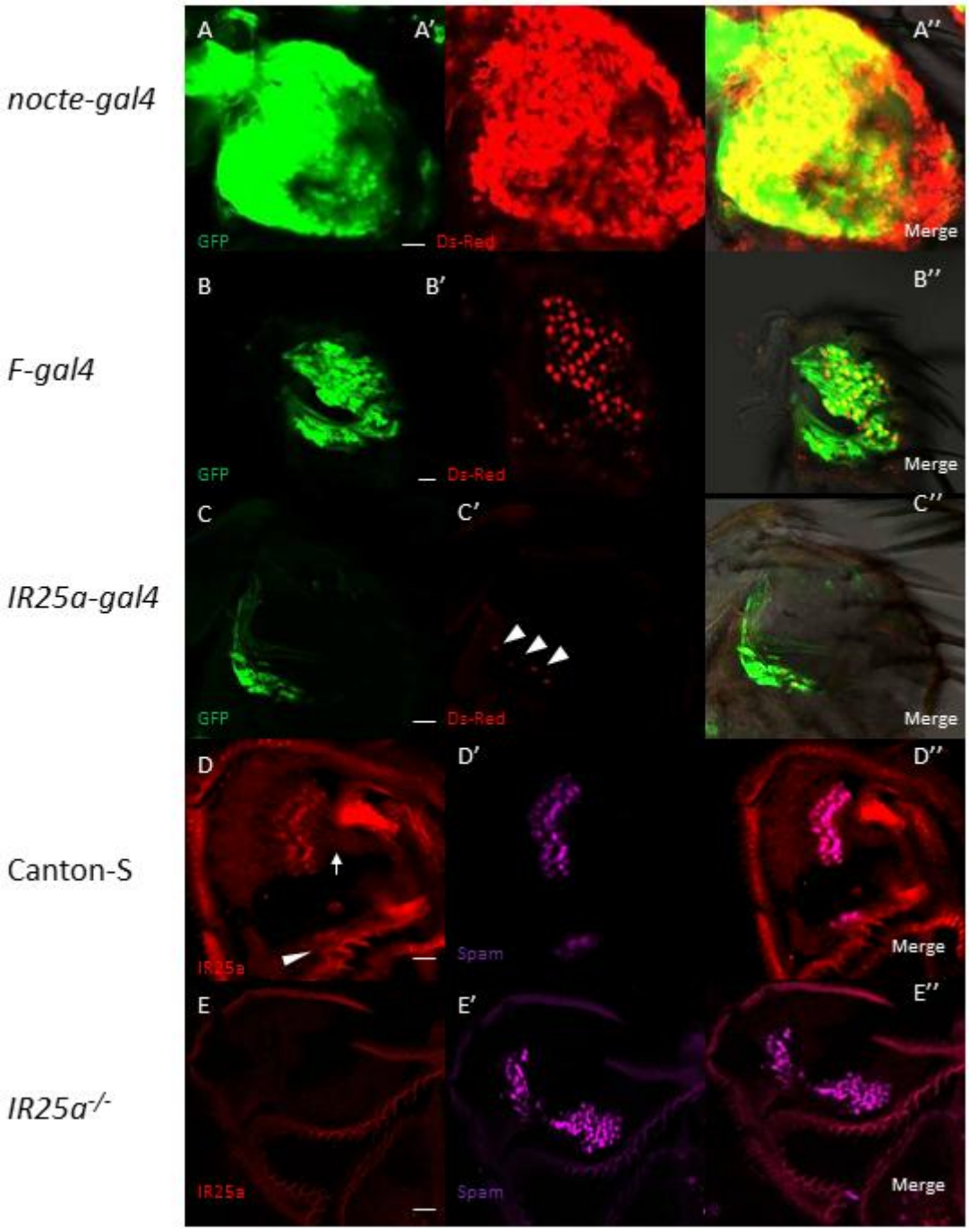

Figure 4.2 The expression pattern of IR25a in Johnston's organs.

(A-C'') Expression of mCD8:GFP (Green) and Ds-Red (Red) under the control of *nocte-gal4* (A-A''), *F-gal4* (B-B'') and *IR25a-gal4* (C-C'') in Johnston's organ. Arrow heads in C' indicate the nucleus visualized by Ds-red. Detailed genotypes of the flies in each figure are: nocte-gal4:*UAS-mCD8:GFP/nocte-gal4;UAS-Ds-Red/+.* F-gal4: *UAS-mCD8:GFP/+;UAS-Ds-Red/F-gal4 (33-5).* IR25a-gal4: *UAS-mCD8:GFP/IR25a-gal4;UAS-Ds-Red/+.*

(D-E'') Immunostainings on antennal sections from wild-type (Canton-S, D-D''), $IR25a^{-/-}$ (allele $IR25a^{2}/IR25a^{2}$, used for all experiments in this chapter, E-E'') flies with IR25a (red),and Spam (also known as 21A6,magenta) antibodies. Arrow heads indicate the signals which were also detected using IR25a-gal4 (C-C''). Scale bar=20um. Arrow indicate cilium recognized by Anti-IR25a antibody.

Although Nocte is broadly expressed in many tissues including the tissues where IR25a is expressed (Sehadova et al, 2009), it is believed that Nocte located in chordotonal organs is important for temperature entrainment. In order to determine if *IR25a* is also expressed in chordotonal organ, I investigated the expression pattern of *IR25a* in chordotonal organs using a cell membrane (mCD8: GFP) and nuclar marker (Ds-Red) under control of *IR25a* promoter gal4 line (Abuin et al., 2011). I first investigated the expression pattern of IR25a in Johnston's organ, the most prominent chordotonal organ in the fly. As shown in Figure 4.2, both GFP and Ds-Red signals controlled by *IR25a-gal4* (C-C'') are visible in the subsets of Johnston's organ, although fewer cells are labelled by this driver and the signals are weaker compared with the signals obtained by *F-gal4* (B-B'') or *nocte-gal4* (A-A''). This indicates that either *IR25a* is only expressed in some areas of Johnston's organ or that the *IR25-gal4* line is a weaker driver. To determine if the expression pattern generated by *IR25a-gal4* represents the expression pattern of the endogenous IR25a protein, we performed immunostaining on antennal sections using IR25a (Benton et al., 2009) and 21A6 (anti-spam) antibodies, a chordotonal organ marker expressed in the extracellular space surrounding the connecting cilium (Chung et al., 2001). In Canton S flies, I observed the strong signals of IR25a overlapping with 21A6 and medium expression level in dendritic cilia(Figure 4.2 D-D''). To test if the

signals are specific, the same experiment was performed in *IR25a* null mutant (*IR25a*$^{-/-}$) flies (Figure 4.2 E-E''), and I observed strong fluorescent signals with 21A6 (Figure 4.2 E') but not with IR25a antibodies, suggesting that the signals I observed in wild type flies are real and also that *IR25a*$^{-/-}$ does not affect the anatomic structure of Johnston's organ. Although, I did notice that endogenous IR25a is broadly expressed in almost all of the cilium compared with shallow signals from *IR25a-gal4*, I did not observe any cells labelled from *IR25a-gal4*which did not express IR25a protein, which indicates that *IR25a-gal4*is a useful marker to label IR25a positive cells. Based on the observations above, I conclude that IR25a is expressed in Johnston's organ.

I next checked if IR25a is also expressed in femur chordotonal organs like Nocte. The legs from the same genotypes of flies mentioned above were dissected and the fluorescent signals from GFP and RFP driven by *IR25a-gal4* were observed (Figure 4.3 C-C'').Like observed for Johnston's organ (Figure 4.2), signals from *IR25a-gal4* are weaker and less cells were labelled compared with the signals from *F-gal4* and *nocte-gal4* (Figure 4.3 A-B''), which may be caused by the weaker *IR25a-gal4*. To examine the subcellular location of IR25a, we tried to perform the immunostainings on leg sections with IR25a antibodies. Unfortunately, we failed to observe any positive signals with either IR25a or 21A6

antibodies in Canton S flies. Therefore a different strategy using IR25a fused with RFP under the control of *IR25a-gal4* was applied. signals in the membranes of the sensory neurons as well as cilium were visualized (Figure 4.3 D') but not in the dendritic cap which was marked by NOMPA-GFP (Chung et al., 2001), suggesting that as in Johnston's organ, IR25a is located in the cilium as well as in sensory neurons of the femur chordotonal organs.

In order to check if IR25a is expressed in the central nervous system, an IR25a immunostaining of brains from Canton S flies were performed. Interestingly, there are 4 neurons in the dorsal and 1 neuron in the lateral part of the brain labelled withanti-IR25a (Figure 4.4 B', C'), the membrane distribution of IR25a antibody suggest the signal is real, but stainings in the *IR25a* null mutant flies have not been performed. To examine if these neurons are clock neurons, TIM antibody served as a clock neuronal marker (Figure 4.4 B'', C''). As shown in the Figure 4.4 B'' and C'', the potential IR25a^{+} neurons do not co-express TIM, suggesting that IR25a^{+} neurons are located close to clock neurons. However, if the *IR25a* signal is specific and whether there is communications betweenIR25a^{+} and clock neurons remain unclear.

I also checked the projection pattern of IR25a neurons in the brain using

membrane bound GFP driven by *IR25a-gal4*. Although IR25a is not expressed in the antennal lobe, the olfactory projection centre (Benton et al., 2009), IR25a neuronal projections are formed in the antennal lobe (Figure 4.4 E) as well as to SOG (subesophageal ganglion), a centre for taste in *Drosophila*. This is not surprising as IR25a functions as an olfactory receptor (Benton et al., 2009; Abuin et al., 2011) and a potential taste receptor (Croset et al., 2011).

Figure 4.3 The expression pattern of *IR25a* in femur chordotonal organs. (See next page)

(A-C'') Expression of mCD8:GFP (Green) and Ds-Red (Red) under the control of *nocte-gal4* (A-A''), *F-gal4* (B-B'') and *IR25a-gal4* (C-C'') in Johnston's organ. The arrow head in C' indicates nuclei visualized by Ds-Red. Genotypes of the flies in each figure are the same as in figure 4.2 (A-C'').
(D-D'') Expression of *IR25a-mRFP* (Red) under the control of the *IR25a-gal4* together with the expression of a NOMPA-GFP fusion protein (Green) under control of the endogenous *nompA* promoter. Genotype of the fly in (D-D'') is: *IR25a-gal4/IR25a-gal4;UAS-IR25a-mRFP/NOMPA-GFP*. Scale bar in A-D'' =50um.
(E) Cartoon showing the structure of chordotonal organ (ChO) neurons with sensory cilia and the selected gene expression patterns.
(F) Quantification of cell numbers in ChO neurons visualized by Ds-Red driven by different gal4 lines. One way ANOVA followed by student t test was used for statistical analysis ＃＃indicates $p<0.01$, ns: not significant.
(G-I) Comparison of the relative mRNA expression of *IR25a* and *nocte* in the femur of wild type (Canton S) and *IR25a* null mutants. Total RNA was isolated from femur (G) of the flies with the indicated genotypes. RT-PCR reactions were performed and *rp49* (H) served as a loading control. Relative gene expression was measured by *Imagine J* and normalized using *rp49,* and plotted in I. Statistical analysis is the same as in F. ＃indicates $p<0.05$, ns: not significant.

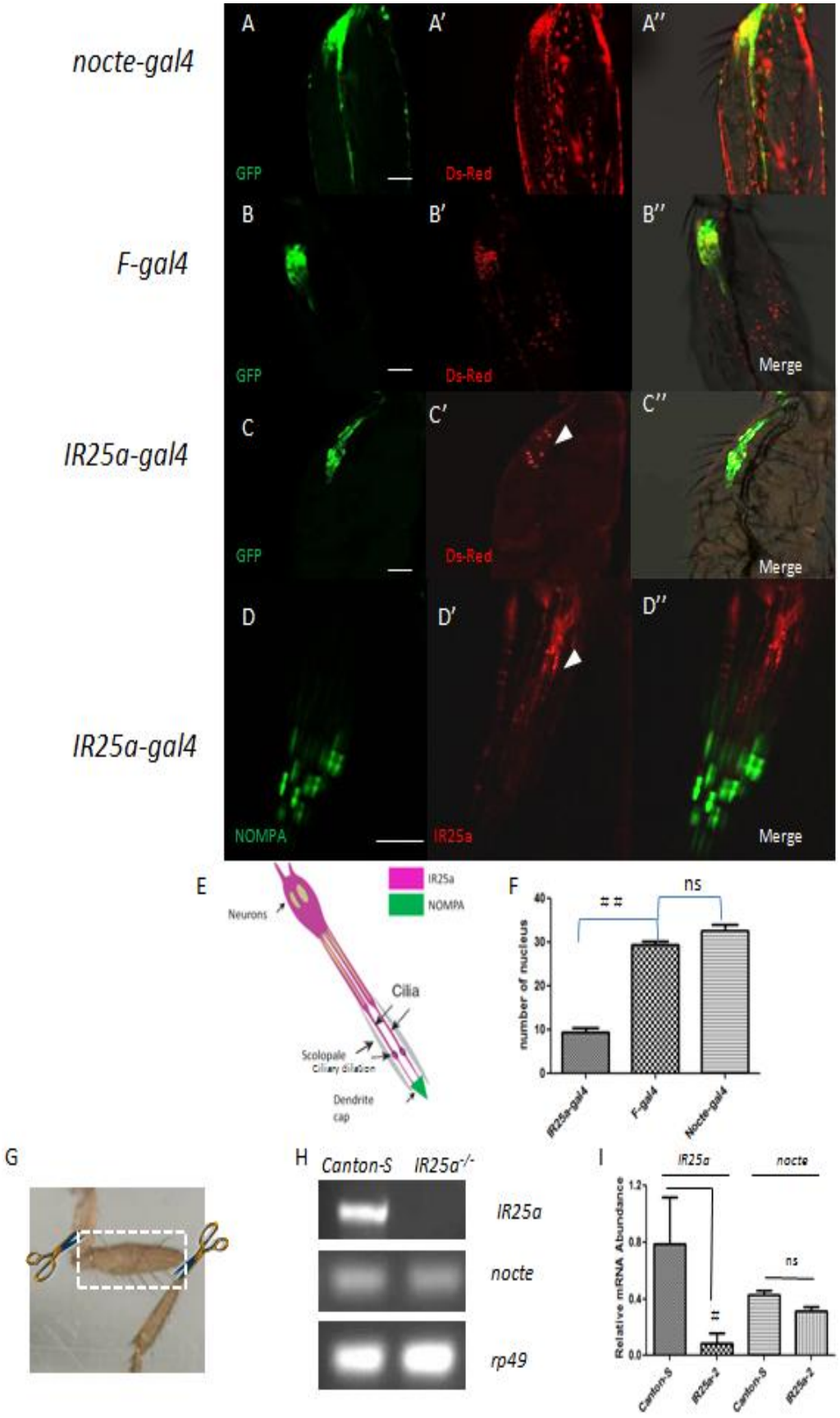
nocte-gal4
A
A'
A''
GFP
Ds-Red
F-gal4
B
B'
B''
Merge
IR25a-gal4
C
C'
C''
IR25a-gal4
D
D'
D''
NOMPA
IR25a
E
IR25a
NOMPA
Neurons
Cilia
Scolopale
Ciliary dilation
Dendrite
cap
F
ns
number of nucleus
IR25a-gal4
F-gal4
Nocte-gal4
G
H
Canton-S
IR25a-/-
IR25a
nocte
rp49
I
IR25a
nocte
Relative mRNA Abundance
ns
Canton-S
IR25a-2

Interestingly, IR25a^{+} neurons also project into the subzone (C and E) of AMMC (antennal mechanosensory and motor centre, Figure4.4, F and F'), where the peripheral neurons from chordotonal organs project to, which is also consistent with IR25a peripheral expression in these sensory structure. Strikingly, IR25a also seems to project to one of the DN2 (dorsal clock neuron 2, Figure 4.4 G-J). Lack of IR25a antibody signal in the DN2 cell suggests a projection but not the DN2 cell that *IR25a-gal4* indeed label's (Figure 4.4 I).This is in agreement that IR25a is not expressed in any of the central clock neurons, in particular the DN2, although we cannot rule out that *IR25a-gal4* ectopically labels this DN2 cell. If not, the result is a strongly evidence indicates that IR25a may be involved in modulating the function of circadian clock neurons.

Based on the observations of the IR25a expression pattern in both the peripheral and central nervous system, I conclude that IR25a is expressed in peripheral chordotonal organs but not in the central clock neurons. Peripheral IR25a^{+} neurons may directly project to DN2, further experiments with post-synaptic markers need to be carried out to confirm this.

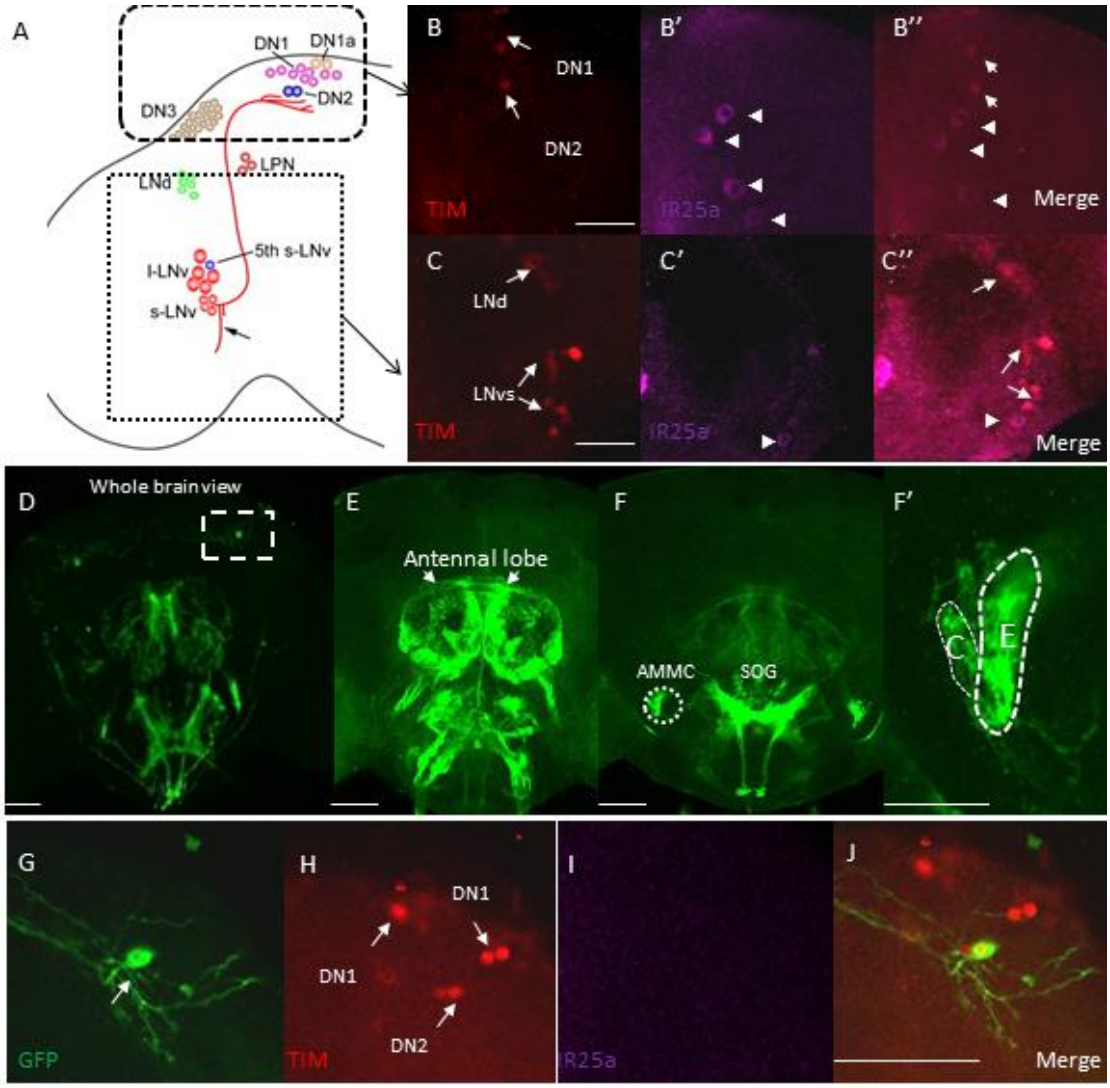

Figure 4.4 Expression and projection patterns of IR25a neurons in the CNS

(A) Cartoon showing the distribution and projections of clock neurons in a hemisphere of a fly brain (Nassel and Winther, 2010).

(B-C'') Immunostainings of brains from wild-type (Canton-S) flies with TIM (red) and IR25a (magenta) antibodies. Wild type flies were entrained at LD for 5 days and fixed at ZT22. Clock neurons and IR25a positive cells are indicated with white arrows and white arrow heads, respectively.

(D-F') The projection pattern of *IR25a-gal4* neurons in the brain visualized by mCD8:GFP (Green). (F') is a larger magnification of the dotted circle in F.

(G-J) The *UAS-mCD8:GFP/y; IR25a-gal4* flies were entrained and fixed as Canton-S in (B-C'') and co-stained with TIM (red) and IR25a (magenta) antibodies. Note that there is no IR25a staining signal in the brain. Indicating the GFP signal in G is the projection from peripheral tissue. (G) is a larger magnification of the dotted square in D. Scale bar=20um

4.2.3 *IR25a* is not necessary for light entrainment

In order to investigate the function of *IR25a* in temperature entrainment, $IR25a^{2}$null mutant (*refered to* as $IR25a^{-/-}$ in this thesis, Benton et al., 2009) was analyzed. First, I examined if $IR25a^{-/-}$ disrupts light entrainment and central clock function. Canton S (which served as a positive control) as well as $IR25a^{-/-}$ flies were initially exposed to a 12h: 12h light: dark (LD) cycle at constant 25°C for 5 days followed by 6 days in constant darkness (DD).Like Canton-S, $IR25a^{-/-}$shows robust bimodal activity patterns (Figure 4.5 A-B, D-E) in LD and strong behavioural rhythms pattern in DD (Figure 4.5 A-B). In addition, $IR25a^{-/-}$ has a similar rhythmic strength and free running period compared to Canton S in DD after light entrainment (Table 4.1). I also tested the ability of re-synchronization to light of $IR25a^{-/-}$. $IR25a^{-/-}$ flies were initially exposed to constant light (LL) for 2 days to abolish the previous rhythm, followed by two LD cycles at 25°C, each of which is 6 hours delayed compared to previous one (Figure 4.5 C), Similar to Canton-S flies (Stanewsky et al., 1998), $IR25a^{-/-}$ can quickly re-synchronized to both LD cycles with a bimodal activity pattern during each LD cycle. These results suggest that $IR25a^{-/-}$ mutant has a normal endogenous core clock system, and that IR25a is not required for light entrainment at the behavioural level.

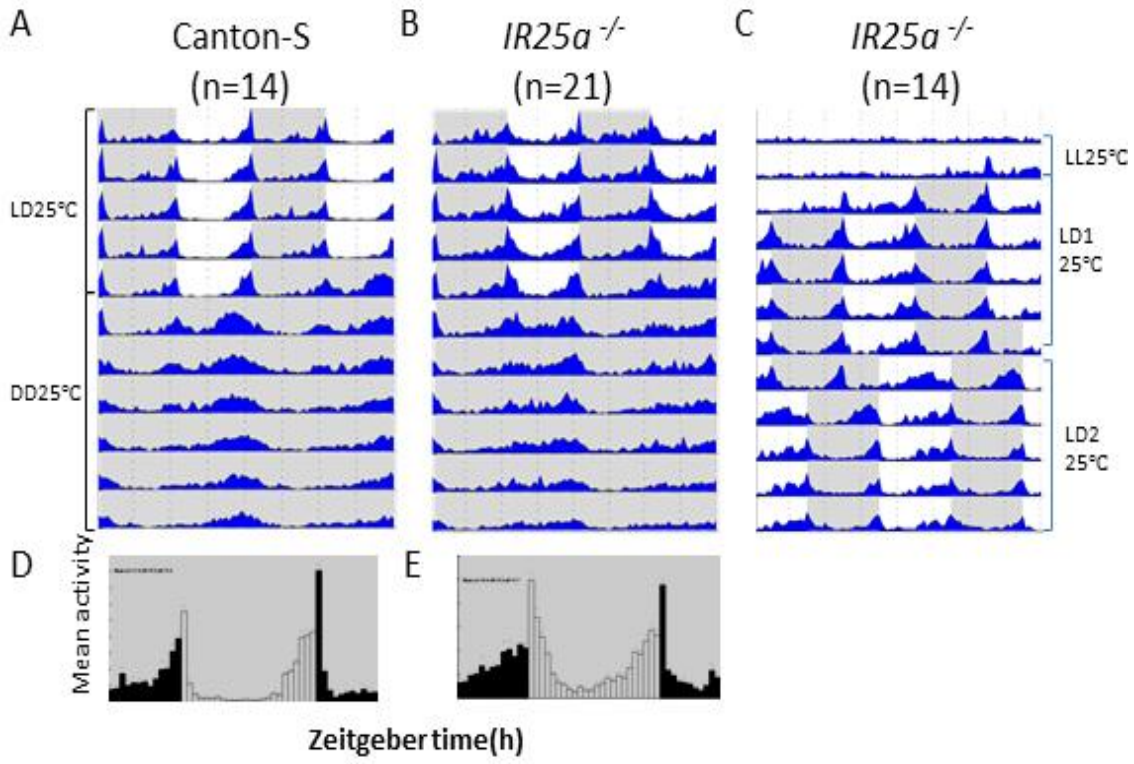

Figure 4.5 IR25a is not required for synchronization of locomotor activity to light: dark cycles and rhythmicity under constant conditions.

(A-B) Canton S (A) and *IR25a* $^{-/-}$ (B)flies were initially exposed to a 12h: 12h LD for 5 days and then released to DD for 6 days. Double-plotted average actograms on the top depict behavioural activity throughout the experiment. Conditions are also indicated to the left of the actograms. The genotypes are indicated above each plot. Number of individuals tested is indicated in parentheses.

(C) Actograms of *IR25a*$^{-/-}$ mutant flies exposed to LL for 2 days followed by two LD cycles, each of which was delayed by 6 hours compared to the previous regime.

(D-E) Daily averages (histograms) of the 5 days in LD in (A) and (B) for Canton S (D) and *IR25a*$^{-/-}$ (E) flies.

To investigate if *IR25a* is required for synchronization of peripheral clocks to light, Western blot analysis of TIM and PER with fly head protein extracts was performed using Canton S and *IR25a*$^{-/-}$ flies entrained in LD cycles. Both TIM and PER exhibit similar oscillations in Canton S and *IR25a*$^{-/-}$ flies, whereby TIM and PER gradually accumulate and become phosphorylated during the night and decrease during day time. These

results suggest that *IR25a* is not required for peripheral clock synchronization to light.

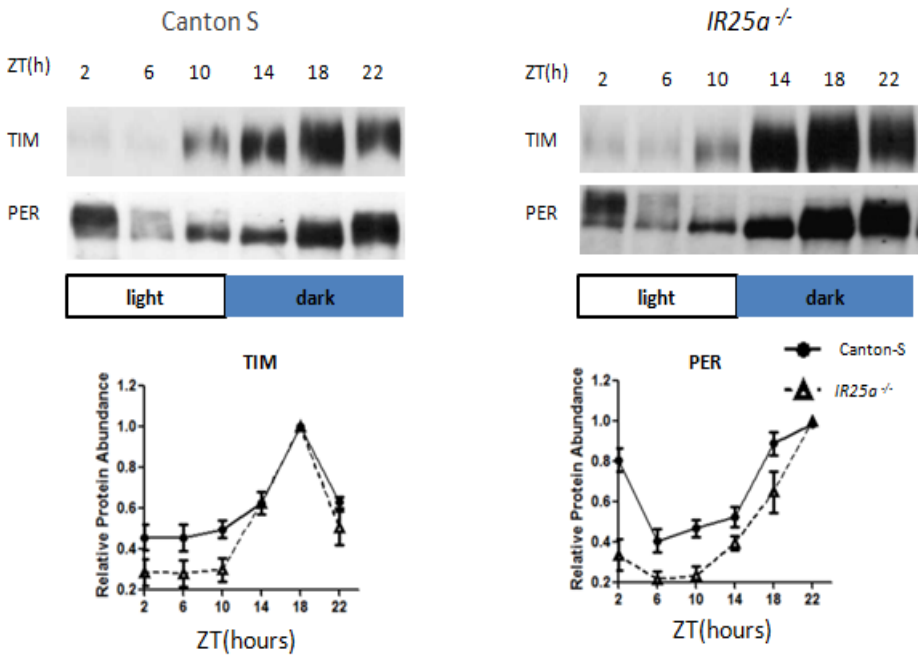

Figure 4.6 IR25a is not required for synchronization of peripheral clocks to light: dark cycles.

Anti-TIM (upper panel) and anti-PER (lower panel) western blots using head extracts from Canton S and *IR25a*$^{-/-}$ flies collected at the time points (ZTs) indicated on the 5th day of LD. Quantifications show averages of TIM and PER intensities from three independent experiments. Error bars indicate SEM.

Finally, I investigated if *IR25a* is required for synchronization of central clocks to light. In order to check if IR25a mutants affect the normal development of clock neurons, brains from Canton S and *IR25a*$^{-/-}$ were dissected and immunostained with PDF antibody (Figure 4.7 A and B). No obvious anatomical defects of either LNv neurons or their projection to DNs were observed in the brains of *IR25a*$^{-/-}$ flies. Next, I compared the

oscillation of TIM in the clock neurons between Canton S and *IR25a*$^{-/-}$.

Brains of the indicated genotypes were fixed at ZT4 and ZT22 on the 5th

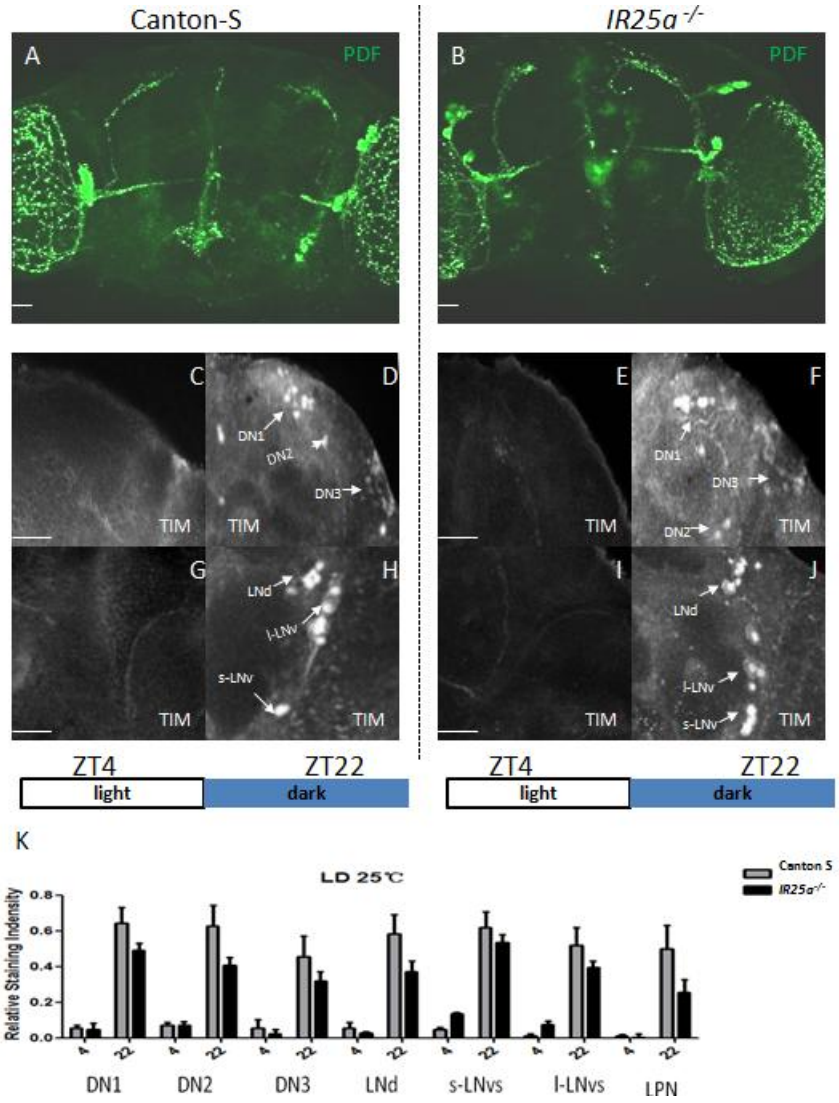

Figure 4.7 *IR25a* is not required for synchronization of central clock neurons to light: dark cycles.

(A-B) The anatomical structure of LNvs appears normal in *IR25a*$^{-/-}$ (B) and Canton S flies (A).

(C-J) Anti-TIM immunostainings of brains from Canton S (C, D, G, H) and *IR25a*$^{-/-}$ flies (E, F, I, J) at the indicated time points on the 5th day of LD.

(K) Quantifications of TIM levels in all clock neurons of Canton S and *IR25a*$^{-/-}$ flies in LD. Error bars indicate SEM. Scale bar= 20um

day of LD at 25°C, stained with TIM antibody, and examined under the

confocal microscope (Figure 4.7 C-J). Again, no significant differences were observed between wild type and mutant brains, which are also supported by the quantification of the staining signals (Figure 4.7 K).As a result, I conclude that *IR25a* is not required for synchronization of central clocks to light. These results, along with the behavioural studies and western blotting results, suggest that IR25a is not required for light entrainment.

4.2.4 IR25a is required for temperature entrainment at the behavioural level

It has been shown that daily temperature fluctuations with amplitude of only 2-3°C in either constant darkness (DD, Wheeler et al., 1993) or light (LL, Yoshii et al., 2005; this study) can robustly synchronize behavioural rhythms in *Drosophila*. A pilot study indicated that *IR25a*$^{-/-}$can synchronize to TC with a 10 °C interval (12h: 12h, 25°C:16°C, data not shown), so I tried to investigate if a narrow temperature interval will induce phenotype of temperature entrainment defect. I first tested if a temperature cycle with 2°C difference is sufficient to synchronize circadian clocks in wild type flies to temperature cycles. Canton S flies were initially exposed to LL at constant 25°C for 2-3 days, followed by two TCs of 12h: 12h 25°C:27°C, each of which was 6 hours delay

compared to the previous one (Figure 4.8 A-B). To make sure the incubator used for the behavioural tests reliably controls the environment condition, a measuring device was also placed in the incubator along with the behavioural monitors to record real-time environmental data during the entire experiment(Figure 4.8 D-F). As expected, Canton S flies quickly re-entrained to TC1 and exhibited a rhythmic behavioural pattern with a pronounced activity peak in the second half of the warm phase (Figure 4.8 A). More importantly, this activity peak can be shifted after exposure of the flies to TC2 which is 6-hour delay compared to TC1. To confirm that the activity rhythm I observed is modulated by the endogenous clock, per^{01} flies served as a negative control. Unlike Canton S flies, no anticipating activity peaks before the onset of cryophase could be observed in per^{01} flies, suggesting that the behavioural rhythm I observed in wild type flies is indeed controlled by clocks, and that a temperature cycle with 2°C temperature difference is sufficient for synchronization.

Next I started to investigate the behavioural pattern of IR25a mutants under temperature. $IR25a^{-/-}$ as well as heterozygous positive control $IR25a^{-/+}$ were exposed to the same conditions as described above (Figure 4.9 A). Unlike either Canton S or IR25a-/+ flies, $IR25a^{-/-}$ were constantly active during the warm and cool phase without showing

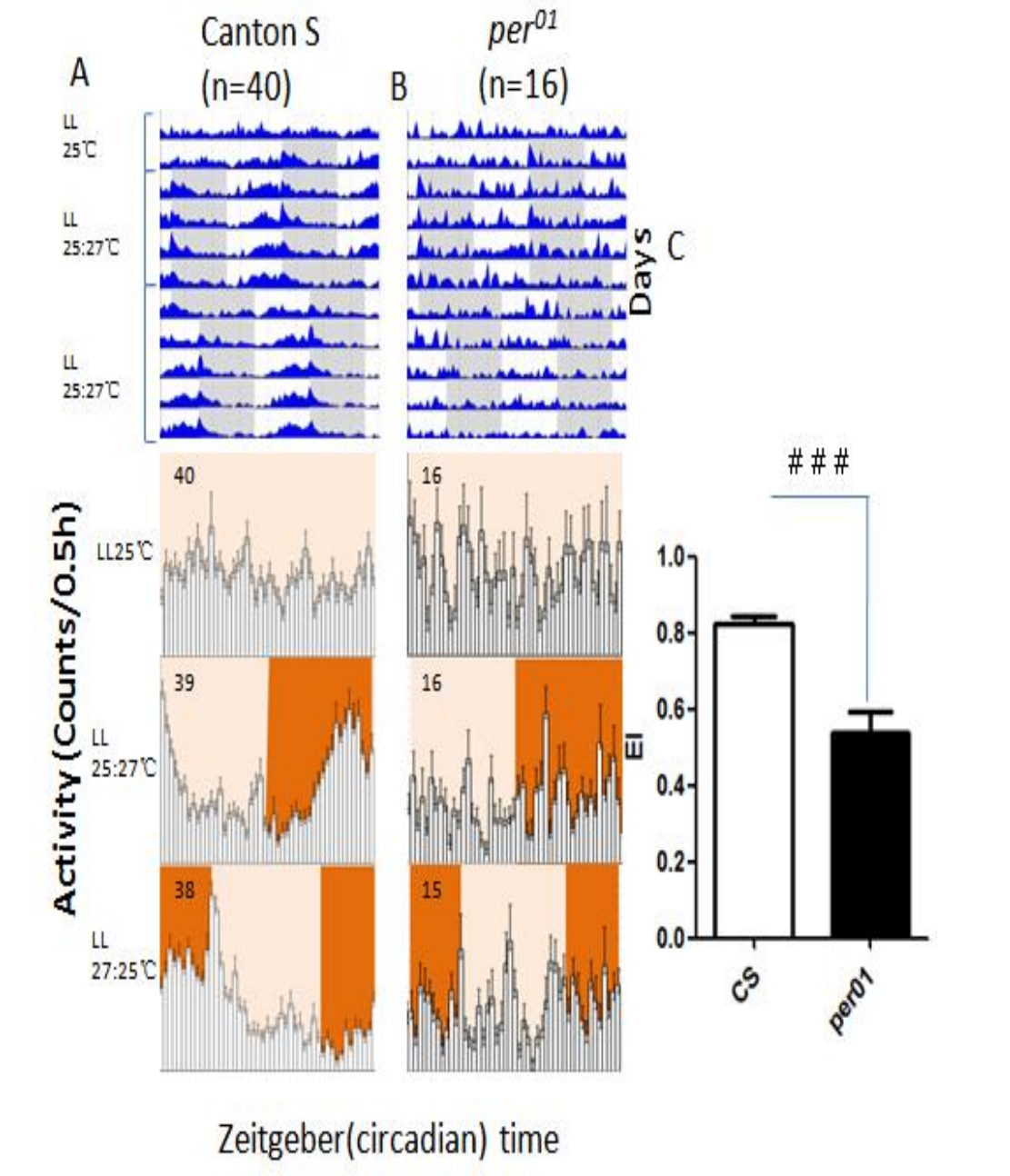
A
Canton S
(n=40)
B
per01
(n=16)
LL
25℃
LL
25:27℃
LL
25:27℃
Days
C
Activity (Counts/0.5h)
LL25℃
LL
25:27℃
LL
27:25℃
40
16
39
16
38
15
###
EI
1.0
0.8
0.6
0.4
0.2
0.0
CS
per01
Zeitgeber(circadian) time

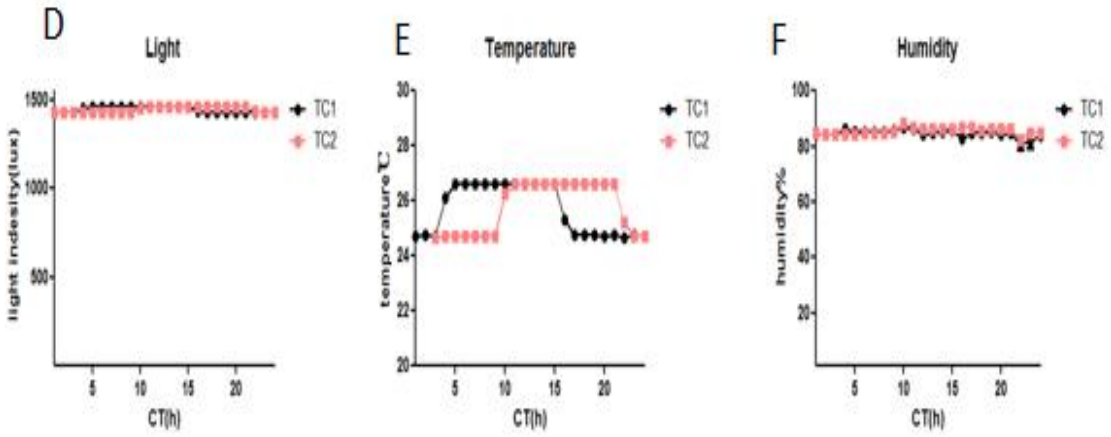
D
Light
light indesity(lux)
1500
1000
500
TC1
TC2
5
10
15
20
CT(h)
E
Temperature
temperature℃
30
28
26
24
22
20
TC1
TC2
5
10
15
20
CT(h)
F
Humidity
humidity%
100
80
60
40
20
TC1
TC2
5
10
15
20
CT(h)

Figure 4.8 Locomotor activity of Canton-S and *per*^{01}flies in temperature cycles and constant light (12h: 12h 27°C: 25°C, LL).

(A-B) Locomotive behaviour of male flies of the indicated genotypes in LL and constant temperature, followed by two 27°C: 25°C TCs in LL. TC2 was delayed by 6 hours compared to TC1. The actograms on the top describe the behavioural activity throughout the experiments. Histograms depict daily average activity of the last two days of each regime. White bars (histograms) or areas (actograms) indicate light and dark periods respectively. Pink areas indicate cool periods, and orange areas indicate warm periods. The number of animals analyzed is indicated in each histogram (combining several independent experiments).

(C) Plotting of the EI (entrainment index) with error bars indicating SEM. Statistical significance was assessed by one-way ANOVA followed by post hoc analysis (see details in chapter 2) ### indicates $p<0.0001$.

(D-F) Daily average of light intensity (D), temperature (E) and humidity (F) conditions recorded by an environmental monitor throughout the experiment.

discerned activity peaks during either cold or warm phase. The behavioural defect in temperature entrainment of *IR25a*$^{-/-}$ was reproducible using transheterozygous *IR25a*$^{-/Df(IR)}$ flies (the deficiency covering the entire *IR25a* gene region) and can be rescued by restoring wild type *IR25a* exposed under the control of the endogenous *IR25a* promoter (*BAC,IR25a*$^{-/-}$referred to as *IR25a*$^{-/-}$ *+rescue* in this chapter) (Figure 4.9).

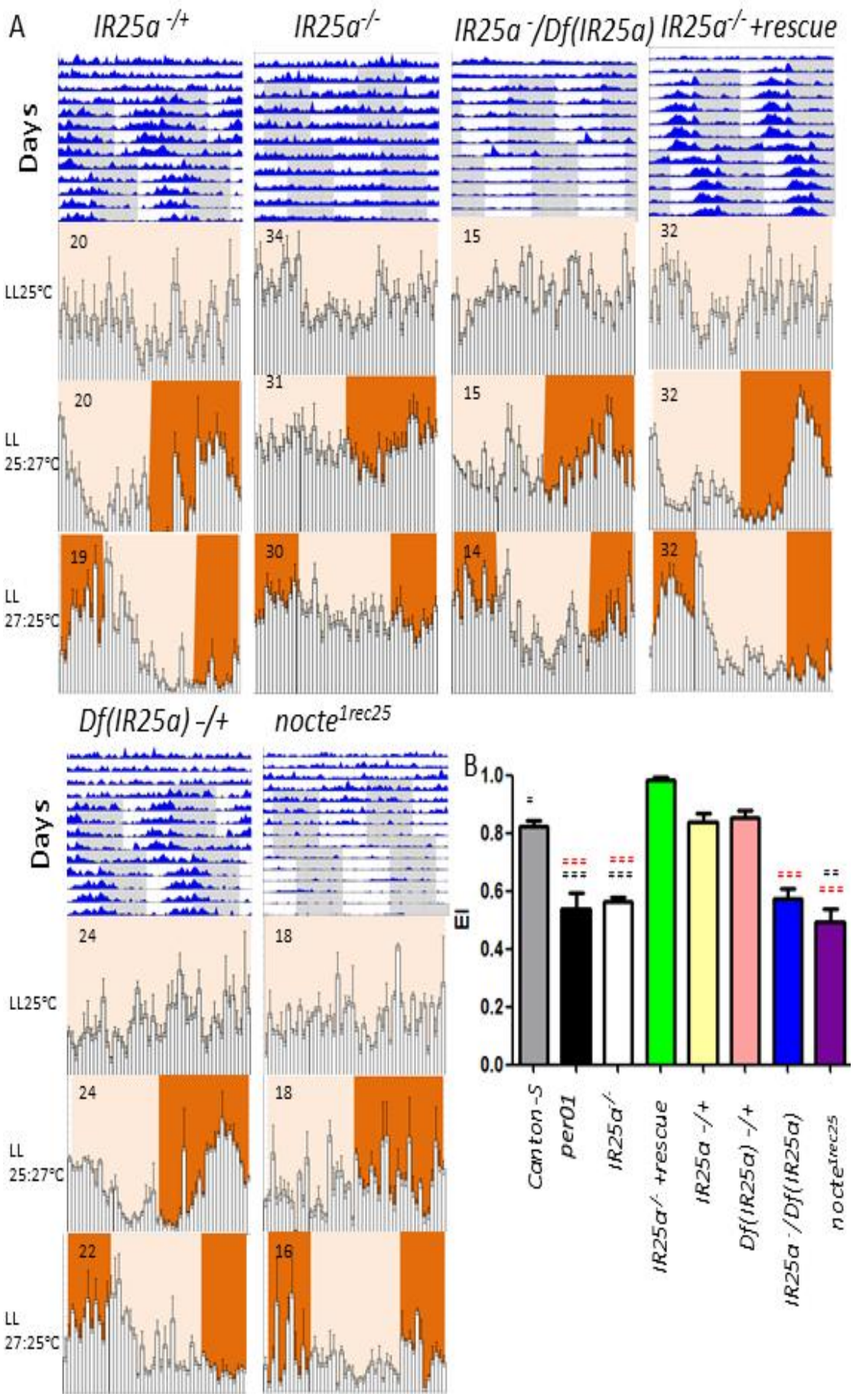
A
IR25a -/+
IR25a-/-
IR25a -/Df(IR25a)
IR25a-/- +rescue
Days
LL25°C
LL 25:27°C
LL 27:25°C
20
34
15
32
20
31
15
32
19
30
14
32
Df(IR25a) -/+
nocte1rec25
24
18
24
18
22
16
B
EI
1.0
0.8
0.6
0.4
0.2
0.0
Canton-S
per01
IR25a-/-
IR25a-/- +rescue
IR25a -/+
Df(IR25a) -/+
IR25a -/Df(IR25a)
nocte1rec25

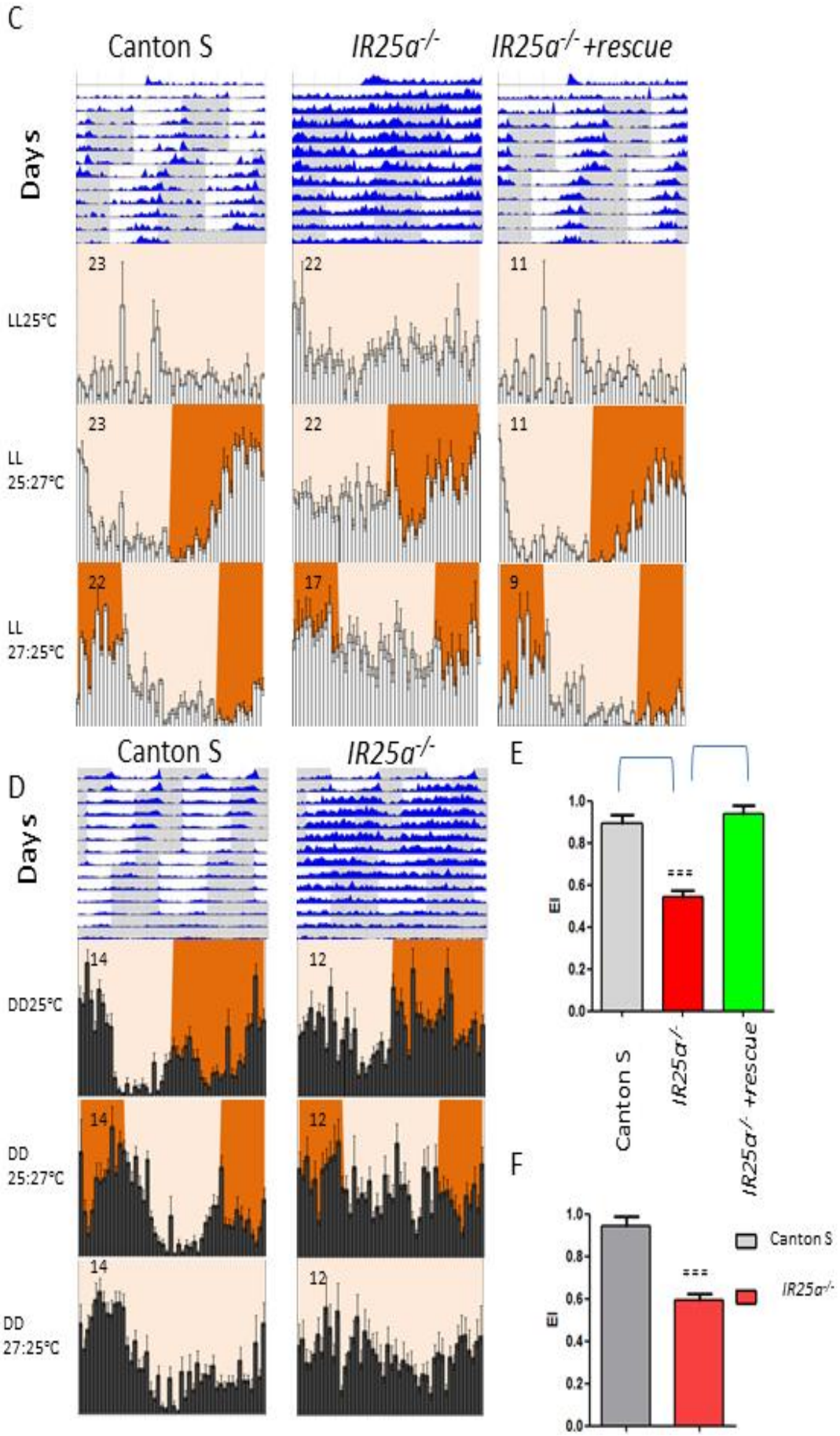
C
Canton S
IR25a-/-
IR25a-/-+rescue
Days
LL25°C
LL 25:27°C
LL 27:25°C
23
22
11
23
22
11
22
17
9
D
Canton S
IR25a-/-
Days
DD25°C
DD 25:27°C
DD 27:25°C
14
12
14
12
14
12
E
EI
1.0
0.8
0.6
0.4
0.2
0.0
***
Canton S
IR25a-/-
IR25a-/- +rescue
F
EI
1.0
0.8
0.6
0.4
0.2
0.0
***
Canton S
IR25a-/-

Figure 4.9 *IR25a* is required for temperature entrainment at the behavioural level.

(A) Flies of the indicated genotypes were exposed to the same condition used in Figure 4.8 (A-B). Actograms and histograms as described in Figure 4.8. Genotypes: *IR25a$^{-/+}$:IR25a^{2}/$^{+}$* (+ is derived from Canton S). *IR25a$^{-/-}$:IR25a^{2}/IR25a^{2}*. *IR25a $^{-}$/Df(IR25a): IR25a^{2}/Df(IR25a). Df(IR25a) /+*: *Df(IR25a)/+*(+ is derived from Canton S). *IR25a$^{-/-}$ +rescue: BAC, IR25a^{2}/BAC, IR25a^{2}.* See table 2.4 for more genotype details.

(B) Quantification of behaviour as described in Figure 4.8 C. ＃＃＃p<0.001, ＃＃p<0.01, ＃p<0.05, ns: not significant. Black and red ＃'s indicates significant differences compared to Canton S and rescue flies, respectively.

The indicated genotypes of flies were initially exposed to LL (C) or LD (D) followed by two TCs (12h: 12h 27℃: 25℃) in LL (C) or DD (D). TC1 in D was advanced by 6 hours compared to LD, and TC2 in both (C) and (D) was advanced by 6 hours compared to TC1. Actograms and histograms are as described in Figure 4.8.
(E-F) Quantification of behaviour (E for C, F for D) as described in Figure 4.8 C. ＃＃＃p<0.001.Sample numbers is histograms are shown on the top left in every histograms. Numbers of the samples tested of every genotypes in actograms are the same as in the first histograms.

To check if different shifts (advances or delays) of temperature cycles change the behavioural pattern of Canton S and *IR25a$^{-/-}$*, I performed similar experiments using the same temperature interval but with 6 hour advance (meaning that TC2 is 6 hours advanced compared to TC1) (Figure 4.9 C,E).Canton S flies synchronized their behaviour to this regime with a similar behavioural pattern observed in delay experiments (Figure 4.8 A), whereas *IR25a$^{-/-}$* again showed no signs of entrainment (Figure. 4.9 C, E). Moreover, to investigate if the temperature entrainment defect induced by *IR25a$^{-/-}$* was light-dependent, I repeated the same experiment in DD. Again, *IR25a$^{-/-}$* shows a clear temperature

entrainment defect without showing discerned activity peaks during TCs (Figure 4.9 D, F). The behavioural analysis indicates that *IR25a* is required for temperature entrainment, at least in the 25°C-27°C range.

To test if any other members from IRs are also involved in temperature entrainment, the null mutant of the other co-receptor *IR8a*, $IR8a^{1}$ (Abuin et al., 2010) was used to perform the behavioural test with the same temperature range (25°C:27°C), however, I didn't find any temperature entrainment defect in $IR8a^{1}$ (Figure 4.10). Further behavioural test using a different temperature range (25°C:29°C, data not shown) was also performed but no temperature entrainment defect phenotype was observed. So far, IR25a is the only receptor form IR family that required for temperature entrainment.

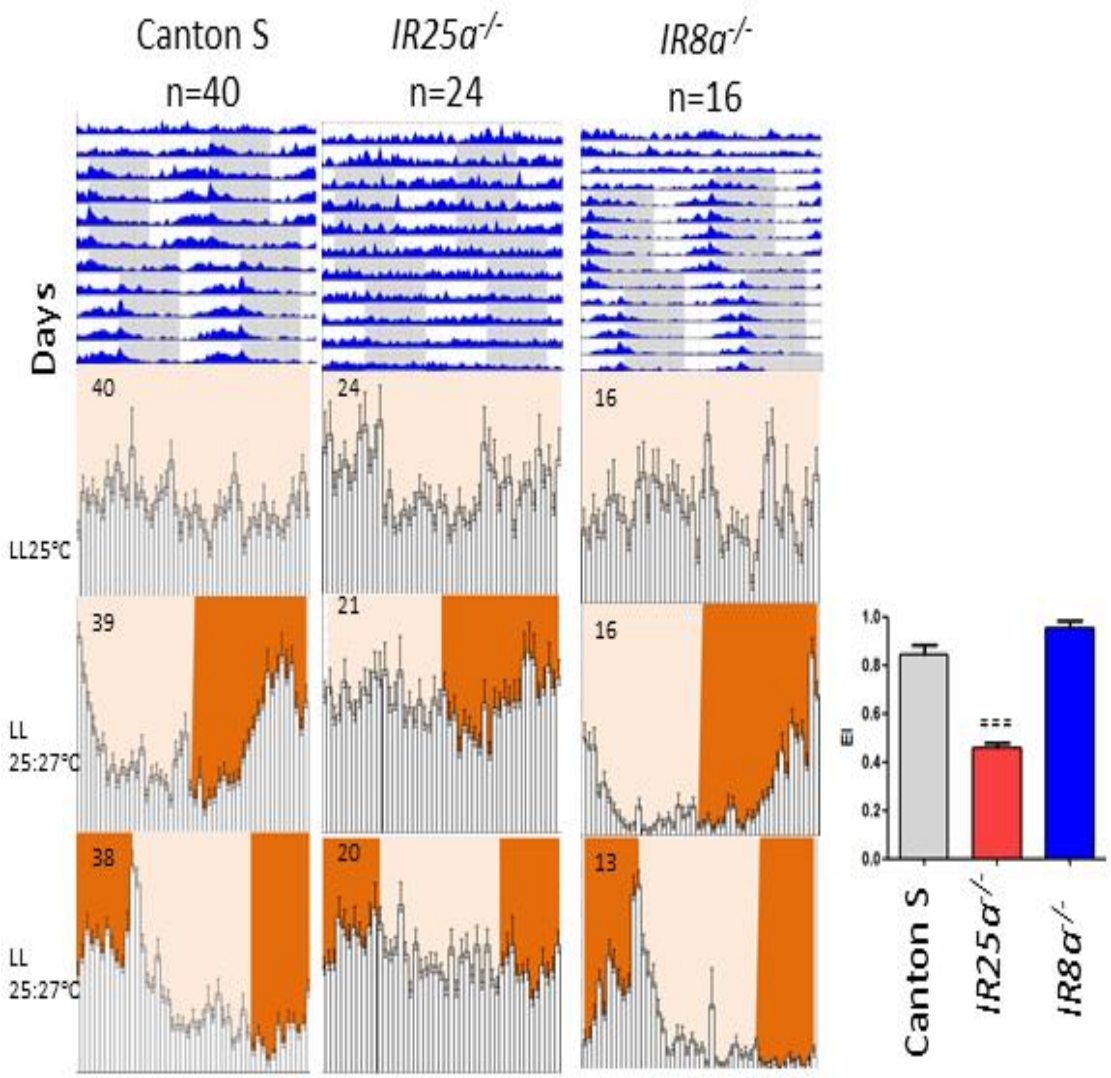

Figure 4.10 *IR8a* is not required for synchronization of clocks to temperature cycles (12h: 12h 27℃: 25℃, LL).

The *IR8a*^{1} flies were exposed to temperature cycle as in Figure 4. 8. Actograms and histograms as described in Figure 4.8, the results for Canton S and *IR25a*$^{-/-}$ were taken from Figure 4.8 (A) and Figure 4.9. Quantification of behaviour was performed as described in chapter 2. ＃＃＃indicate p<0.0001, ns: not significant.

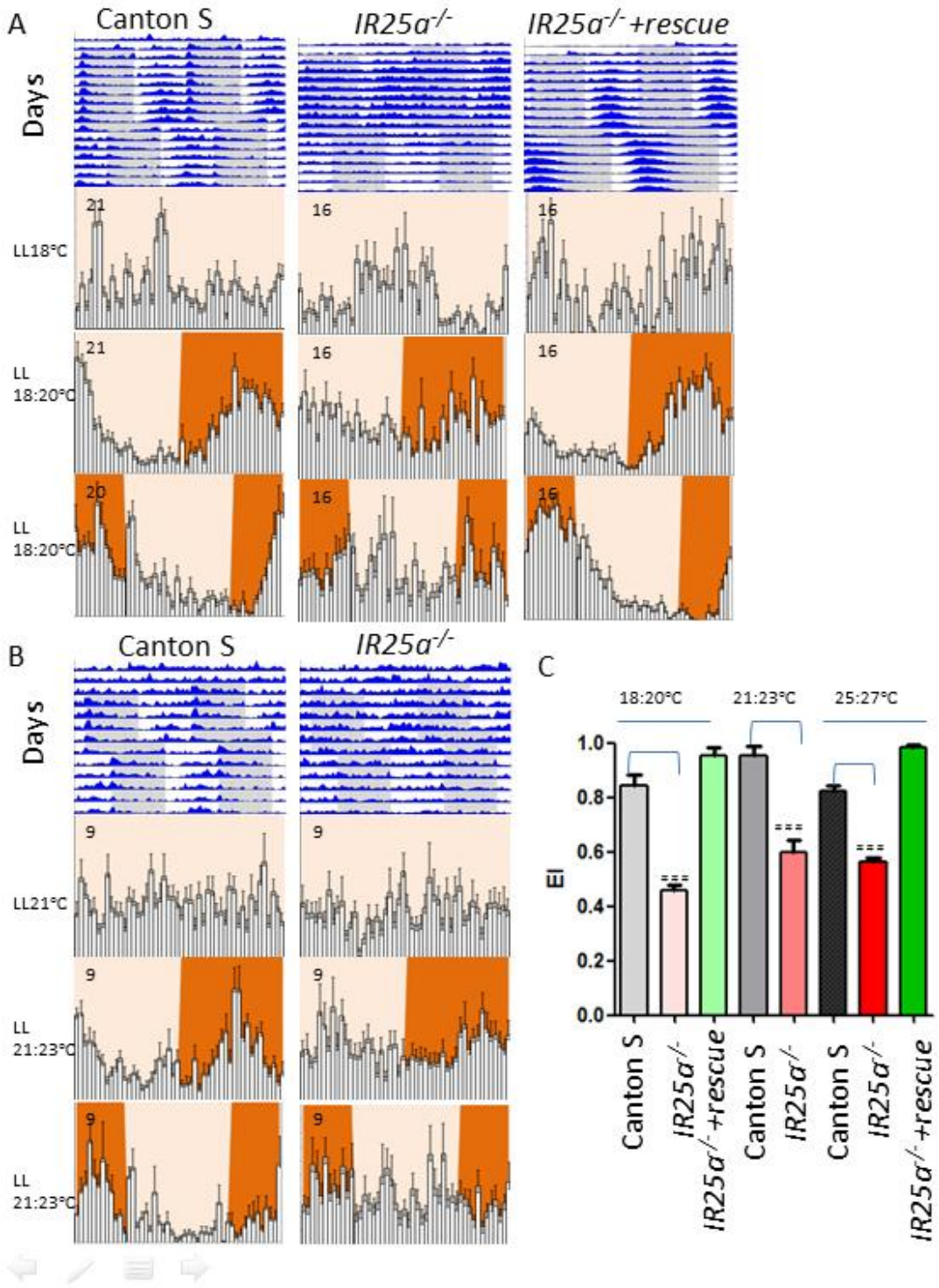

Figure 4.11 Mapping the temperature ranges requiring *IR25a* function.
Flies of the indicated genotypes were exposed to the same TC shifts as in Figure 4.8 (A-B) but with different absolute temperatures: 18°C: 20°C (A) and 21°C: 23°C (B).Quantification of behaviour in (C) as described in Figure 4.8 (C). The result of flies in 25: 27°C was taken from Figure 4.9 (B). ### $p<0.001$. Numbers tested for every genotype were shown in every histograms.

Temperature entrainment in *Drosophila* can be achieved with TCs covering their whole physiological temperature range (15°C–30°C), and it has been shown that different genes are only involved in temperature entrainment at certain temperature ranges. For example, the TRP channel encoded by the *pyrexia (pyx)* gene is required for synchronization to low temperature cycles(16°C: 20°C) but is not involved in synchronization to higher temperature intervals (20°C:25°C and 25°C: 29°C)(Wolfgang et al., 2013). To investigate if *IR25a* also has a defined 'working range' for temperature entrainment, I performed TCs experiments with two additional temperature intervals (18°C: 20°C and 21°C: 23°C). Interestingly, $IR25a^{-/-}$ cannot be synchronized (18°C: 20°C and 25°C: 27°C) or weakly synchronized (21°C: 23°C) by the various TCs (Figure 4.11), which suggests that IR25a is involved in synchronizing clocks to a broad temperature range.

4.2.5 Antennal expression of *IR25a* is not required for temperature entrainment at the behavioural level.

A previous study revealed that IR25a is enriched in the 3rd antennal segment (Benton et al., 2009; Sayeed and Benzer, 1996) revealed that an unknown receptor for temperature preference behaviour is located in this part of the antenna. In this study, I showed that IR25a is

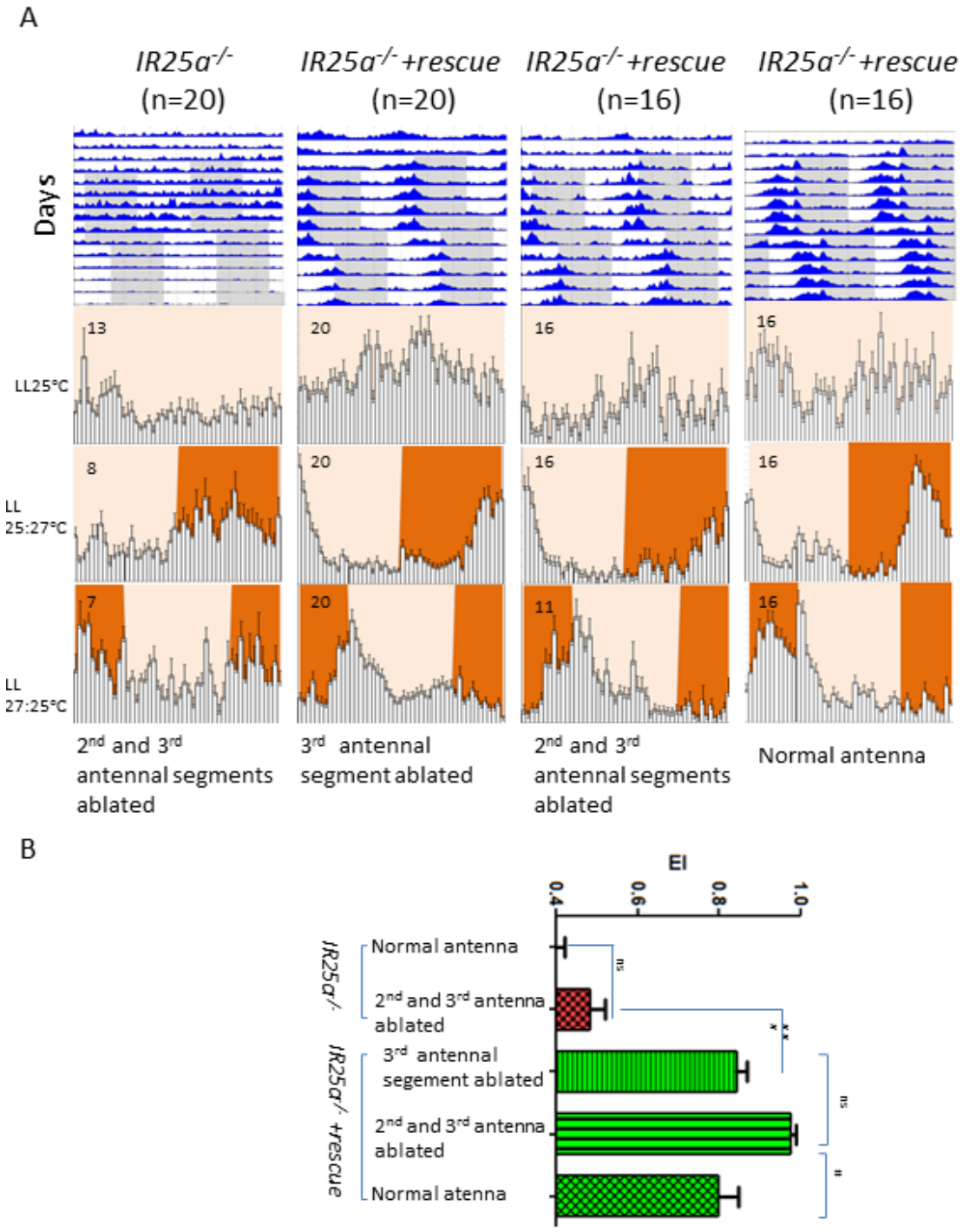

Figure 4.12 Antennal IR25a is not necessary for locomotor activity rhythms to temperature cycles.

(A) *IR25a*$^{-/-}$ and *IR25a*$^{-/-}$ *+rescue* flies with the indicated treatments were exposed to the same condition used in Figure 4.8 (A-B). Actograms and histograms as described before. (B) Quantification of behaviour as described in Figure 4.8 (C). The result of *IR25a*$^{-/-}$ with normal antenna was taken from Figure 4.11 (B). ＃＃＃p<0.001, ＃＃p<0.01, ＃p<0.05, ns: not significant.

also expressed in Johnston's organ (Figure 4.2), a highly specialized organ mediating hearing and mechanosensory as well as temperature preference (Tang et al., 2013), located in the 2nd antennal segment. Moreover, a recent study showed that 4 neurons in arista of the 3rd antennal segment house thermoreceptors encoded by the *brivido* (*brv* for 'cold' sensation) (Gallio et al., 2011). Interestingly, *IR25a* is also expressed in arista (Benton et al., 2009). However, pioneer studies in our lab suggest that the antennae are not required for temperature synchronization under a TC of 25°C: 16°C (Glaser and Stanewsky, 2005; Sehadova et al, 2009). I wanted to ask if IR25a in antennae required for temperature entrainment to relative shallow TC. *IR25a*$^{-/-}$rescue flies with ablated 3rd antennal segments or both 2nd and3rd antennal segments ablated were tested in TCs (Figure 4.12). Behaviour of the manipulated flies was very similar to that of the flies with normal antennae, demonstrating that the antennae are not necessary for temperature entrainment. I also checked the behaviour of ablated *IR25a*$^{-/-}$ flies with ablated 2nd and 3rd antennal segments, and also fail to observe any difference compared to intact *IR25a* mutants (Figure 4.12 B). Together the data demonstrate that the thermoreceptors present in antenna are not required for temperature entrainment to 25°C: 27°C TC, but we cannot rule out that they may still contribute to it.

4.2.6 *IR25a* is required for synchronization of peripheral clocks to temperature cycles

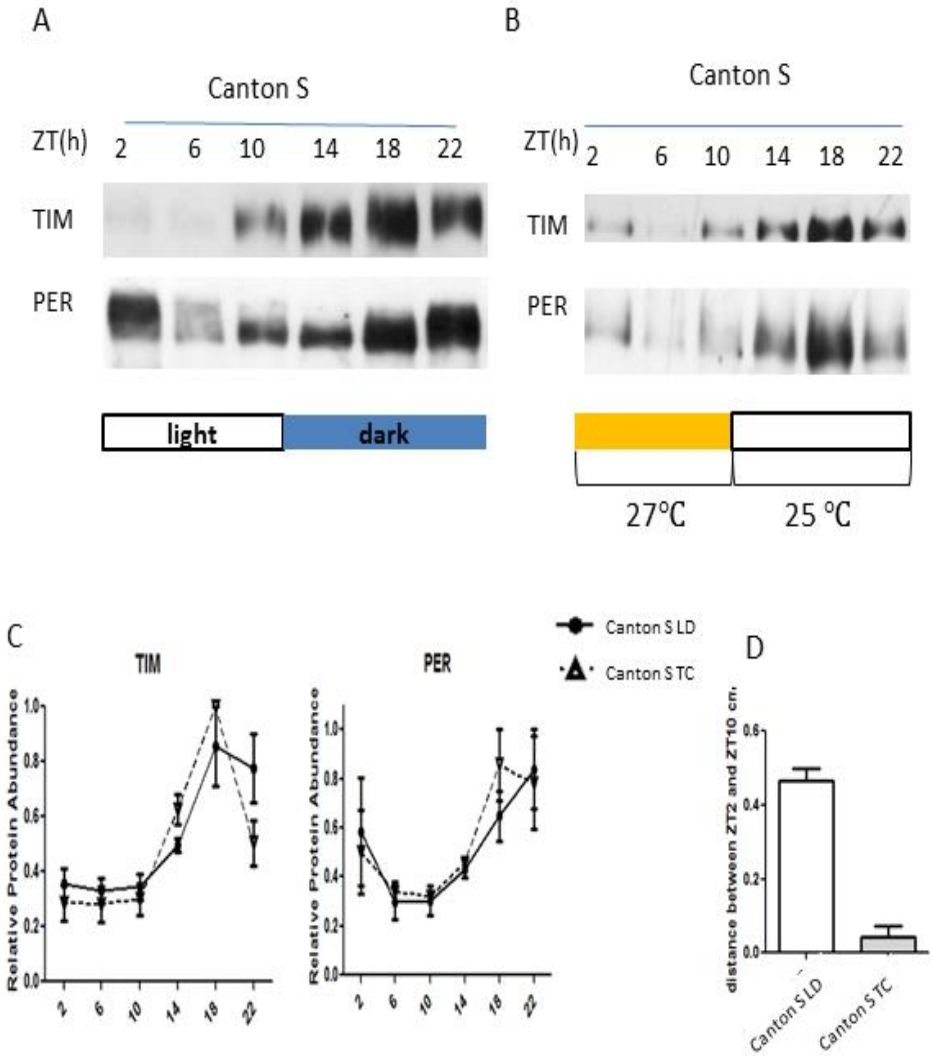

Figure 4.13 Comparison of TIM and PER protein levels of Canton S flies under LD and temperature cycles (12h: 12h 27°C: 25°C, LL).

(A-B) Anti-TIM (upper panel) and anti-PER (lower panel) western blots using head extracts from Canton S flies collected at the indicated time points (ZTs) in different conditions. For LD experiments, flies were collected on the 5th day, whilst for TC experiment, flies were collected on the 14th day of exposure to the respective Zeitgeber cycle.

(C) Quantification of TIM and PER averages intensities from three independent experiments.

(D) PER Protein distance between ZT2 and ZT10 in LD and TC measured in [cm].

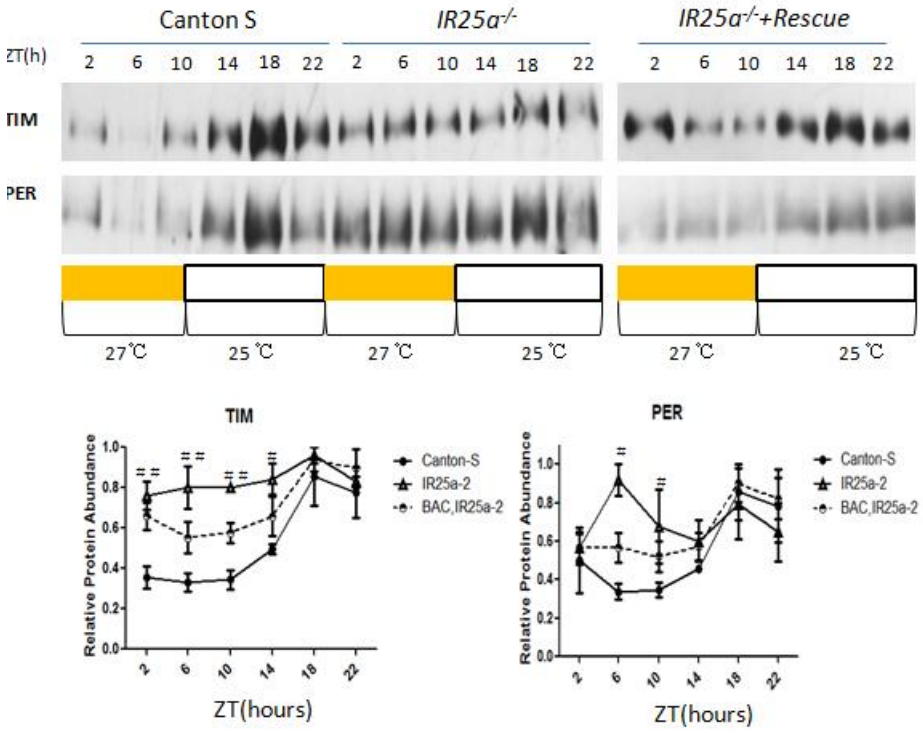

Figure 4.14 *IR25a* is required for peripheral clocks synchronized to temperature cycles.

TIM (upper panel) and PER (lower panel) western blots analysis using head extracts from Canton-S, *IR25a*$^{-/-}$ and rescue flies collected at the indicated time points (ZTs) during the 14th day of TC (27°C: 25°C, LL). Quantification (bottom) of TIM and PER intensities from three independent experiments. Statistical analysis was performed as detailed in chapter 2.

To investigate if *IR25a* is required for synchronization of peripheral clocks to temperature cycles of 12h: 12h 25°C:27°C, Western blotting analysis of TIM and PER with fly head protein extracts under temperature cycles were performed. In Canton S flies, both TIM and PER in TC exhibit similar oscillations as in LD: TIM and PER gradually accumulate during the cool phase (dark phase in LD) and gradually decrease during the warm phase (the light phase in LD) (Figure 4.13). Intriguingly, phosphorylation especially of PER is drastically reduced during TC (Figure 4.13 B),which

can be quantified by measuring migrated distance between the PER band at ZT2 and ZT10 (Figure4.13 D), suggesting that modification by phosphorylation of core clock proteins may not be as important for temperature entrainment compared to light. Overall, both TIM and PER robustly oscillate in Canton S head extracts under temperature cycles.

Next, I determined the effect of *IR25a* on TIM and PER cycling during TC. Both TIM and PER do not oscillate in *IR25a*$^{-/-}$ flies but oscillations can be restored in genomic rescue flies (Figure 4.14). Therefore, I conclude that *IR25a* is required for synchronization of peripheral clocks to temperature cycles.

4.2.7 IR25a is required for synchronization of central clocks to temperature cycles

To investigate whether IR25a is also required for synchronization of central clocks to temperature cycles, immunostainings of brains of Canton S and *IR25a*$^{-/-}$ flies with TIM antibodies were performed. In Canton S flies, robust oscillations of TIM in all known clock neurons (except LPN, which were not visible under this condition) were observed. In all clock neurons, TIM signals gradually increase from ZT2 up to the peak value at ZT 16 and thereafter drop again to medium levels at ZT22

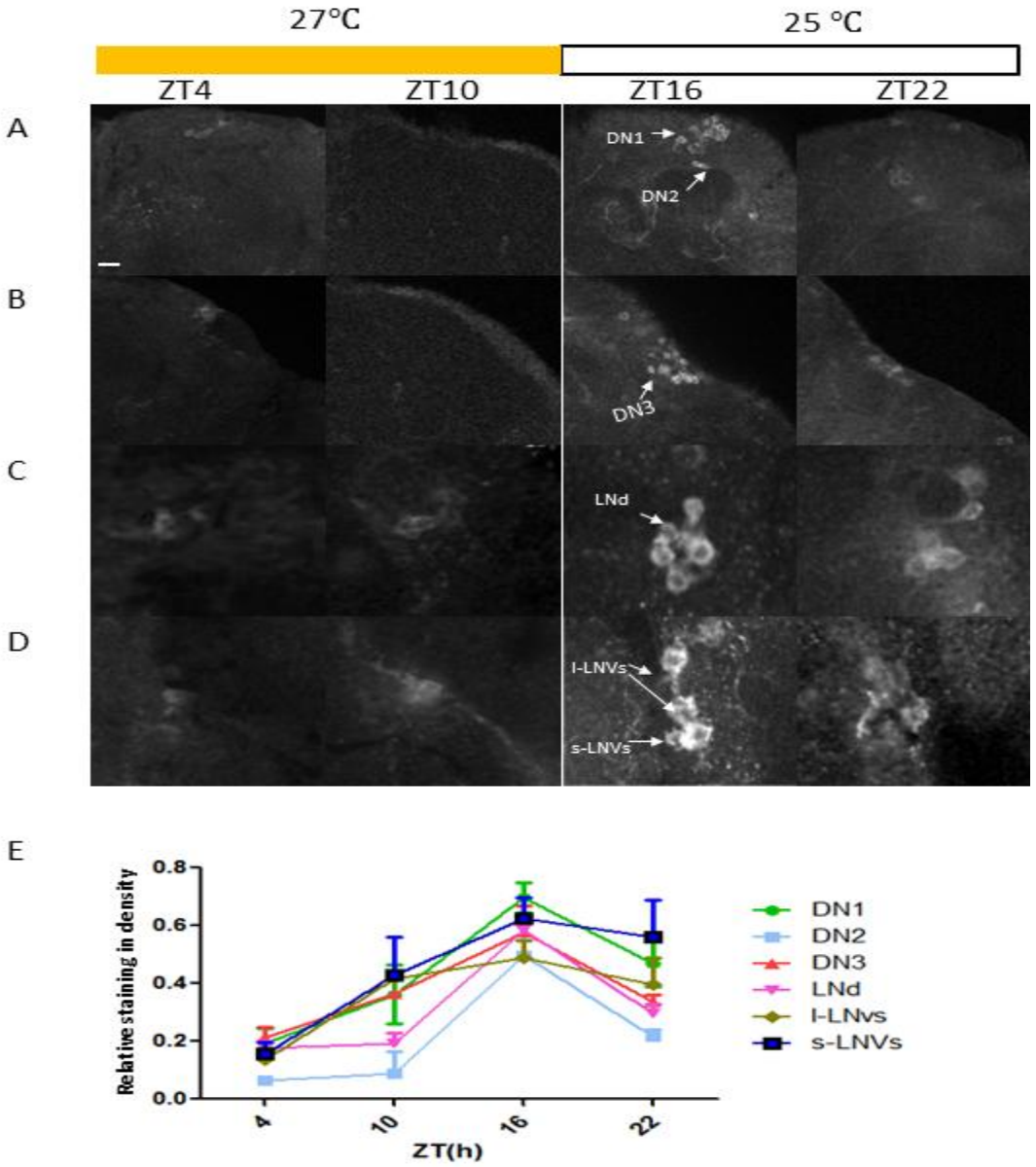

Figure 4.15 Oscillation of TIM in clock neurons of Canton S flies exposed to temperature cycles (12h: 12h 27°C: 25°C, LL).

(A-D) Anti-TIM immunostainings of Canton S brains at the indicated time points during the 7th day of the. Scale bar= 10um.

(E) Quantifications of TIM levels in all clock neurons. Error bars indicate SEM.

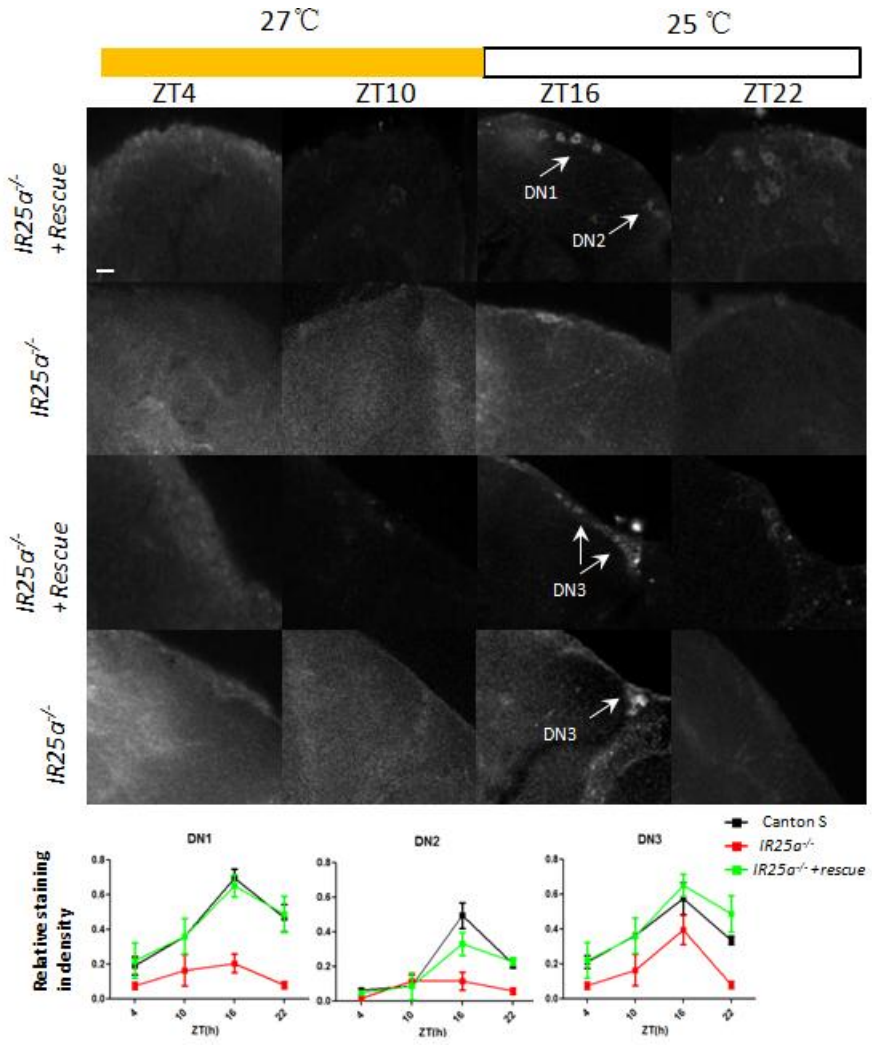

Figure 4.16 Oscillation of TIM in dorsal clock neurons of *IR25a*$^{-/-}$ and rescue flies exposed to temperature cycles (12h: 12h 27°C： 25°C, LL).

A: Immunostainings on brains of the flies of indicated genotype at the indicated time points during the 7th day of TC with TIM antibody.Scale bar= 10um

B:Quantifications of TIM levels in dorsal clock neurons of the flies with indicated genotypes in TC. Error bars indicate SEM.

(Figure 4.15), which is similar to the observations for Canton S flies under TCs with large absolute temperature intervals (Gentile et al., 2013). Overall, the signals in brains of Canton S under TC are much weaker than the signals obtained under LD conditions, which may suggest that light is a much stronger zeitgeber than temperature. Interestingly, all signals I

observed were restricted to the cytoplasm (Figure 4.15). The mechanisms underlying this remain unclear, but may be linked to the observation that TIM and PER are hypo-phosphorylated in peripheral clocks during TC (Figure 4.13).

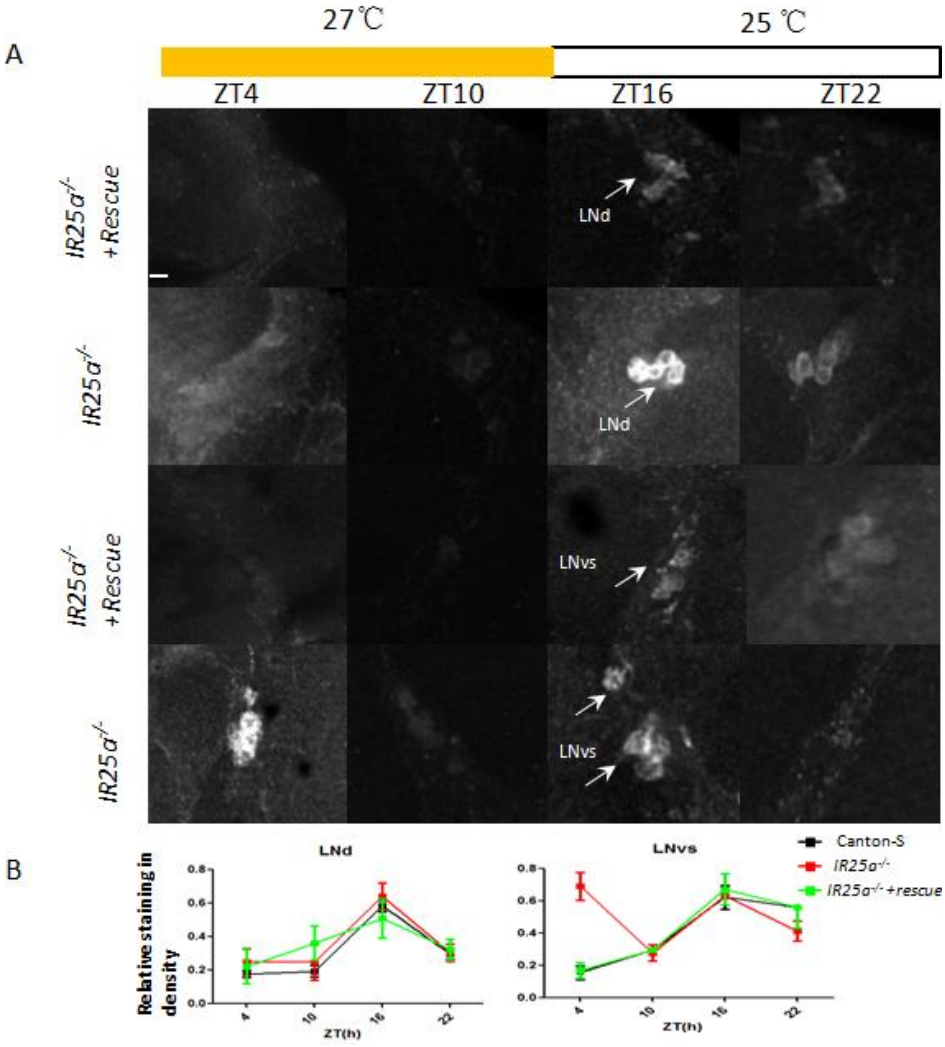

Figure 4.17 Oscillation of TIM in lateral clock neurons of *IR25a*$^{-/-}$ and rescue flies exposed to temperature cycles (12h: 12h 27°C： 25°C, LL).

A:Anti-TIM immunostainings of brains from flies of the indicated genotypes and Zeitgeber Time performed on the 7thday of TC. Scale bar= 10um

B:Quantifications of TIM levels in Lateral Neurons. Error bars indicate SEM.

Next, I carried out the same experiment with *IR25a*$^{-/-}$ mutants. Surprisingly, the LNd neurons in *IR25a*$^{-/-}$ mutants exhibit robust oscillation of TIM as in Canton S (Figure 4.17). However, other groups of clock neurons behave different pattern compared to Canton S: TIM levels in both DN1 and DN2 neurons are constitutively low throughout the experiment (Figure 4.16). In contrast, TIM in LNvs is abnormally high in *IR25a*$^{-/-}$ at ZT4 (Figure 4.17). Although *IR25a*$^{-/-}$ has less effect on the DN3, less DN3 cells were observed at ZT16 compared with Canton S. These defects can be restored by IR25a genomic rescue (Figure 4.16 and 4.17), suggesting that the molecular phenotypes in *IR25a*$^{-/-}$ are indeed due to a lack of *IR25a* gene function.

4.2.8 IR25a is not required for temperature compensation.

Like in other organisms, the circadian clock of *Drosophila* is well compensated to non-rhythmic changes in ambient temperature, meaning that at different constant temperatures(i.e. in the absence of TC), the free-running period is very similar (Konopka et al., 1989). All mutants known to affect TC synchronization so far, do not affect temperature compensation (Glaser and Stanewsky et al., 2005; Wolfgang et al., 2013), and I show here that IR25a mutants is also not required for this trait (Figure 4.17 and Table 4.1). My data, along with the previous

data, suggests that the mechanisms underlying temperature inputs of entrainment and compensation are different.

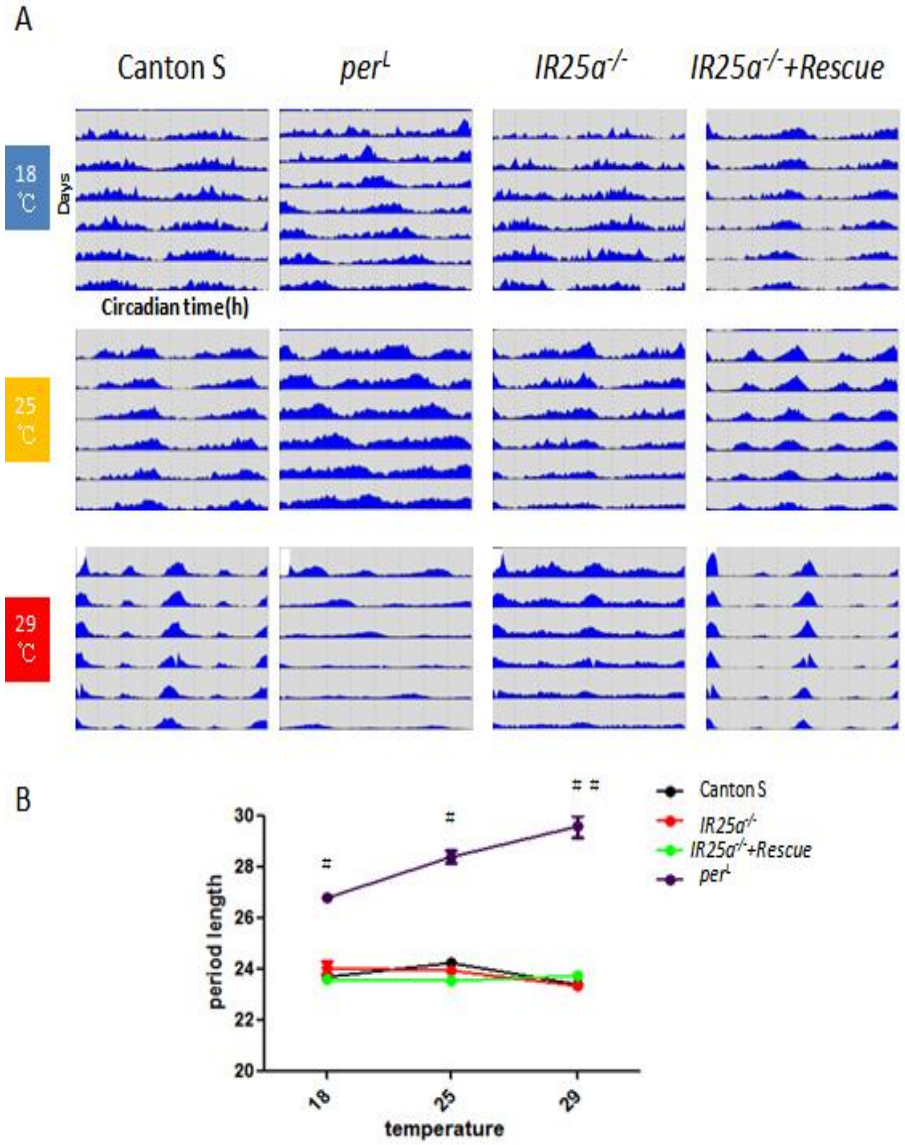

Figure 4.18 IR25a is not required for temperature compensation.

(A) Actograms of male flies of the indicated genotypes at constant temperatures of 18°C, 25°C and 29°C in DD after initial LD entrainment at the same temperature.

(B) Free running period analysis of the indicated genotypes. All genotypes except *per*^{L} show robust temperature compensation. Error bars indicate SEM, # p<0.05, # # p<0.01. Numbers of indicated genotypes were shown in Table 4.1.

Table 4.1 Locomotor activity rhythms in DD at three different temperatures

Genotype	℃	n	%Rhythmic	Period(hr) ± SEM
Canton S	18	32	84	23.7 ± 0.2
IR25a²	18	32	75	24.1 ± 0.3
BAC, *IR25a²*	18	28	60	23.6 ± 0.1
per^L	18	22	82	26.8 ± 0.1
Canton-S	25	45	96	24.2 ± 0.1
IR25a²	25	44	75	24.0 ± 0.1
BAC, *IR25a²*	25	30	97	23.6 ± 0.1
per^L	25	26	38	28.4 ± 0.2
Canton S	29	60	100	23.4 ± 0.1
IR25a²	29	39	77	23.4 ± 0.1
BAC, *IR25a²*	29	27	100	23.8 ± 0.1
per^L	29	54	52	29.6 ± 0.4

4.2.9 Silencing neural activity of IR25a-expressing neurons severely affects temperature entrainment

Postsynaptically located iGluRs modulate neuronal activities in *Drosophila* (Xia et al., 2005).As IRs are closely related to iGluRs, I investigated if IR25a function in temperature entrainment by modulating the neural activity of the chordotonal organ. To answer this question, *kir2.1*, a mammalian inward rectifier K^+ channel (Baines et al., 2001) was employed to silence the neural activity in *IR25a*$^+$ neurons. As expected, flies with silenced *IR25a*$^+$ neurons have a clear temperature entrainment defect (Figure 4.19 1st panel) compared to control flies (Figure 4.19 2nd

and 3rd panel). I repeated the experiment with *F-gal4 33-5*. However, adult flies expressing *kir2.1* controlled by *F-gal4* do not survive long enough to perform behavioral tests. Although *F-gal4* shows a very restricted expression pattern (Sehadova et al, 2009; Kim et al., 2003), it may be expressed in some unidentified cells which are important for the survival of the flies.

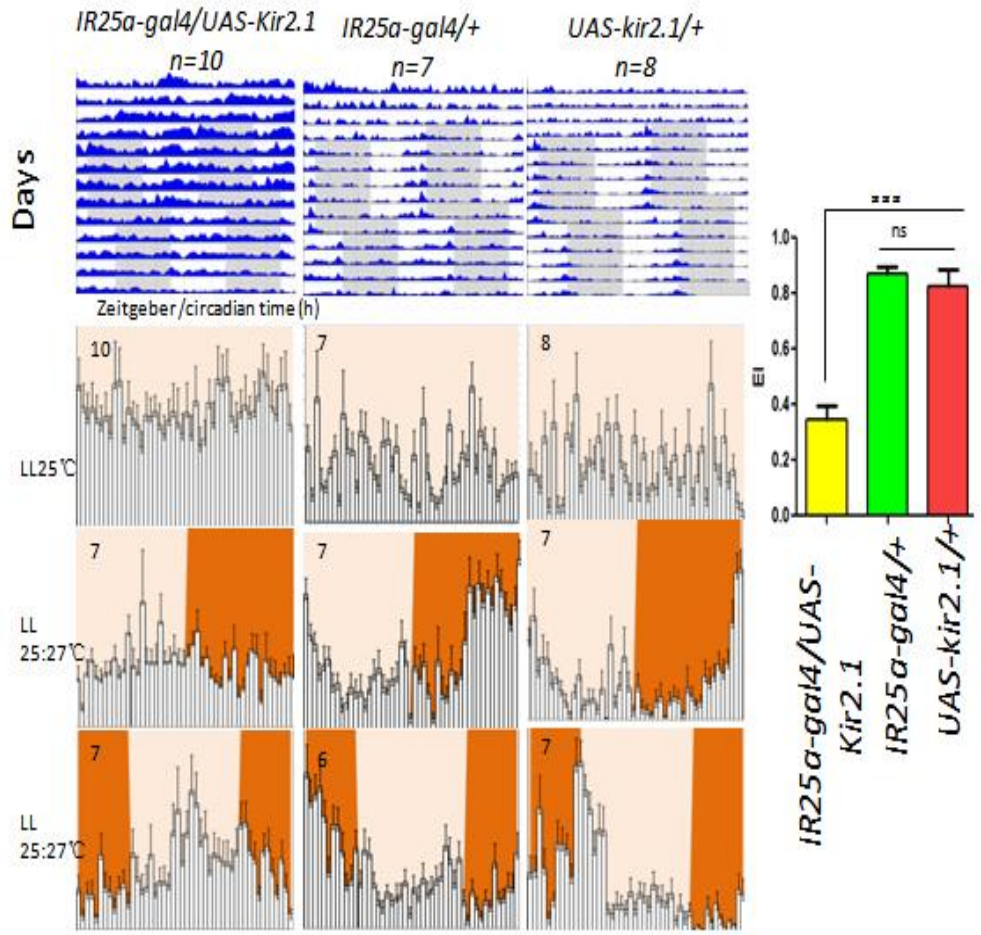

Figure 4.19 Silencing neural activity in *IR25a*$^{+}$ neurons severely affects temperature entrainment.

The *IR25a-gal4/UAS-kir2.1* flies as well as control flies were exposed to temperature cycles as in Figure 4. 8. Actograms and histograms as described in Figure 4.9. Quantification of behaviour was performed as described before in Figure4.9 $p<0.0001$; ns: not significant.

4.2.10 Behavioural temperature entrainment defects caused by *IR25a* mutants can be partially rescued by larger temperature intervals.

Finally, I wanted to ask if *IR25a* is also required for synchronizing clocks to larger temperature intervals. To answer this question, Canton S and *IR25a*$^{-/-}$ flies were exposed to TC of 29°C: 25°C. Unexpectly, at least in the first TC, *IR25a*$^{-/-}$ shows a robust entrained activity peak similar to Canton S flies (Figure 4.20 A), although *IR25a*$^{-/-}$ fail to re-synchronize to TC2. The behavioural results I observed strongly suggest that there is another IR25a independent pathway mediating temperature entrainment. Indeed, preliminary immunostaining data also showed partial rescue of TIM cycling in DNs under this condition (data not shown), which is in good agreement with the behavioural data. This data, along with the temperature range mapping results (Figure 4.12), suggests IR25a may function as a temperature amplitude detector other than an absolute temperature sensor. However, this pathway seems not to contribute to peripheral clocks synchronization during TC of 29°C: 25°C, as *IR25a*$^{-/-}$still abolishes TIM and PER cycling in peripheral clocks (Figure 4.20 B).

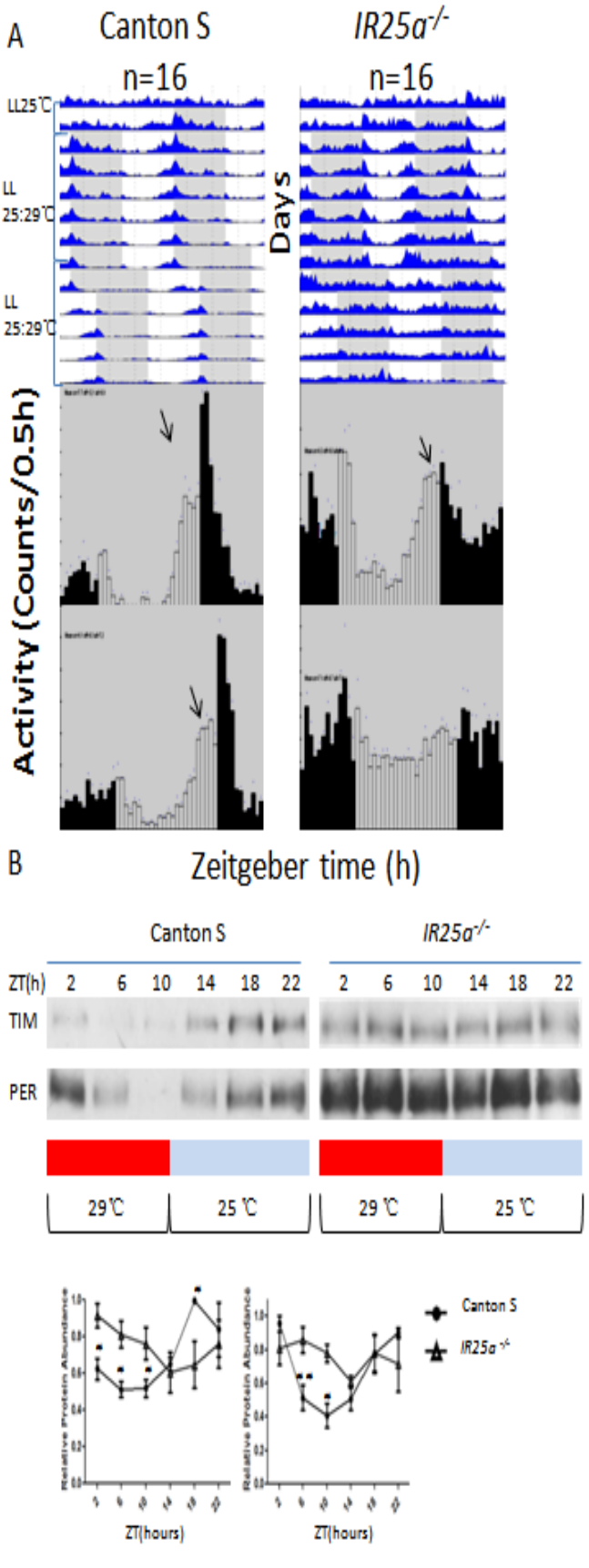

Figure 4.20 IR25a$^{-/-}$ Temperature entrainment defects are partially rescued by larger temperature intervals at the behavioural level.

(A) 16 Canton S and *IR25a*$^{-/-}$ male flies were initially exposed to LL for two days and then transferred to two TCs of 29℃: 25℃, each of which was delayed by 6 hours compared to the previous regime. Actograms on top show activity during the entire experiment, histograms below show average activity in the last two days of each TC. Arrows in each histograms indicate anticipatory behavioural activity.
(B) Anti-TIM (upper panel) and anti-PER (lower panel) western blot analysis using head extracts from Canton S and *IR25a*$^{-/-}$ flies collected at the indicated time points (ZTs) during the 14th day of TC (29℃: 25℃, LL). Quantification of TIM and PER intensities from three independent experiments.

4.3 Discussion

4.3.1 Comparison between light and temperature entrainment at the molecular level.

Both light and temperature are predominant zeitgebers in nature used by organisms to synchronize their endogenous clocks. It has been shown that TC's with an amplitude of only 2-3°C in either constant darkness (DD, Wheeler et al., 1993) or light (LL, Yoshii et al., 2005) can robustly synchronize behavioural rhythms in *Drosophila*. Here I show that temperature cycles with 2°C (25°C: 27°C) amplitude are sufficient to synchronize behavioural rhythms. Moreover, I showed that also at the molecular level both central and peripheral clocks can be robustly synchronized to this shallow temperature interval. Interestingly, in addition to the well described differences of behavioural pattern during

TC and LD, respectively (Yoshii et al., 2005, Glaser and Stanewsky et al., 2005), I also observed differences between light and temperature entrainment at the molecular level. First of all, the striking gel-mobility changes observed over the course of the day during LD cycles are much reduced in temperature cycles. These mobility changes are caused by phosphorylation (Edery et al, 1994), suggesting that during temperature cycle, PER and TIM are constantly hypophosphorylated. It is possible that this altered phosphorylation pattern is contributing to the largely cytoplasmic localization of PER and TIM (Kim et al., 2007).However, further experiments need to be performed to confirm the relationship betweenphosphorylation and nuclear entry under temperature cycles.

My observation of constant cytoplasmic localization of TIM is different from the previous descriptions of PER signals under TC in either DD (Busza et al., 2007) or LL (Yoshii et al., 2005). Although we have no explanation for this difference, it could be caused by the different temperature ranges (at least 5 degree amplitude TCs in their studies) or the different clock proteins we observed (TIM in our study vs PER in theirs). Nevertheless, if what I observed is real, that suggests only post-translation modification of ubiquitination and glycosylation beyond the transcription feedback loop is sufficient to drive the oscillation of clock proteins, which is also true in human blood cells (O'Neill et al.,

2011).

4.3.2 Putative function of IR25a in temperature entrainment

I showed here IR25a, a chemosensory co-receptor also has crucial role in temperature entrainment. This distinct function of IR25a in temperature entrainment is perhaps mediated by structures, different from its function which is involved in olfactory sensation, as antennal IR25a is not required for temperature entrainment, at least at the behavioural level. Although we are short of direct evidence, it seems that IR25a in non-antennal chordotonal organs is casually linked to sensing temperature changes relevant for entraining insect clocks. Moreover, these data along with the non-requirement of IR25a in temperature compensation, also suggest that the potential function of IR25a in temperature preference is distinct from that in entrainment: IR25a is expressed in arista and JO, both implicated and known to function in temperature preference behaviour. But as mentioned before, we cannot rule out that antennal structures contribute to temperature entrainment and that both behave (entrainment and preference) use similar cellular and molecular substrates. In this respect, it is interesting to note that temperature preference is circadianly regulated (Kaneko et al., 2012).

The investigation of TIM cycling in central clock neurons also suggests that Dorsal Neurons (especially DN1 and DN2) as well as LNvs are more important than LNd for temperature entrainment under the conditions I used. Moreover, it has been reported that Dorsal Neurons are more important for behavioural outputs in higher temperature intervals (29°C: 20°C), whereas lateral neurons are more important for synchronization to cycles with a lower temperature ranges (25°C: 16°C, Gentile et al., 2013), suggesting that the behavioural phenotypes I observed at higher temperature ranges (27°C: 25°C) are caused by the loss of clock protein oscillations in DN1 and DN2. However, it is unclear if the abnormal high expression of TIM at ZT4 also contributes to the entrainment defects of IR25a, and what causes the distinct effects on TIM between DNs and LNvs. In summary, I present evidence for IR25a acting as a novel potential receptorIR25a is required for temperature entrainment at behavioural, molecular and neural levels.

Finally, it has been shown that the entrainment of central clocks involves temperature inputs from peripheral sensory neurons mainly located in chordotonal organs (Sehadova et al, 2009). However, it remains unclear how peripheral neurons signal to the central clock in the brain. The putative projections of R25a neuron provide us with two hypothetical possibilities: (1) temperature information can be perceived in the

chordotonal organs by IR25a and ChO neurons directly or indirectly projected to the AMMC. The AMMC works as a secondary projection center relaying the temperature information to the clock neurons.(2)Temperature signals reach the DN2 via direct projections from the Ch organs (Figure 4.21).

4.3.3 Future work for IR25a

Here I report that IR25a is required for temperature entrainment, however, more studies are necessary to be carried out in order to understand the underlying mechanism. First of all, although the data I presented here along with molecular properties of IR25a suggest that this Ionotropic Receptor may function as a potential thermo receptor in chordotonal organs. There is no direct evidence showing that IR25a is activated or responding to certain ranges of temperature. Olfactory studies have already shown that ectopic expression of IRs in neurons is sufficient to restore the neuronal responses to its specific odour ligand (Abuin et al., 2011; Ai et al., 20113). Similar studies need to be performed for temperature responses.

Although I showed that IR25a directly interacts with Nocte at the molecular level, we still don’t have enough evidence to support that

IR25a also genetically and functionally interacts with Nocte, which would help us to understand the role of Nocte in temperature entrainment. It has been shown that Nocte affects the distribution of the dendritic cap protein NOMPA and/or the structure of scolpale (Sehadova et al, 2009). This defect was not observed in *IR25a*$^{-/-}$(data not shown).It is possible therefore that the spatial distribution of IR25a in the chordotonal cilium of *nocte* mutants is affected.

Finally, it has been reported that IR25a is insufficient to induce odour responses without partnering with at least one other IR (Abuin et al., 2011). Is this also true for IR25a in temperature entrainment? Does IR25a also need another IR or IRs as partners to function as thermo receptor? I will discuss this open question in the next chapter in detail.

4.4 Summary of Main Results

4.4.1 IR25a physically interacts with Nocte in vivo.

4.4.2 IR25a is expressed in subsets of the neurons of chordotonal organs and projected to DN2.

4.4.3 IR25a is not required for light entrainment at the behavioural,

molecular and neuronal levels.

4.4.4 IR25a is required for temperature entrainment at the behavioural, molecular and neuronal levels.

4.4.5 Antennal IR25a is not required for temperature entrainment.

4.4.6 IR25a is not required for temperature compensation.

4.4.7 Silencing neuronal activity of IR25a-expressing neurons severely affects temperature entrainment.

4.4.8 The temperature entrainment defects caused by IR25a mutants can be partially rescued with larger temperature intervals.

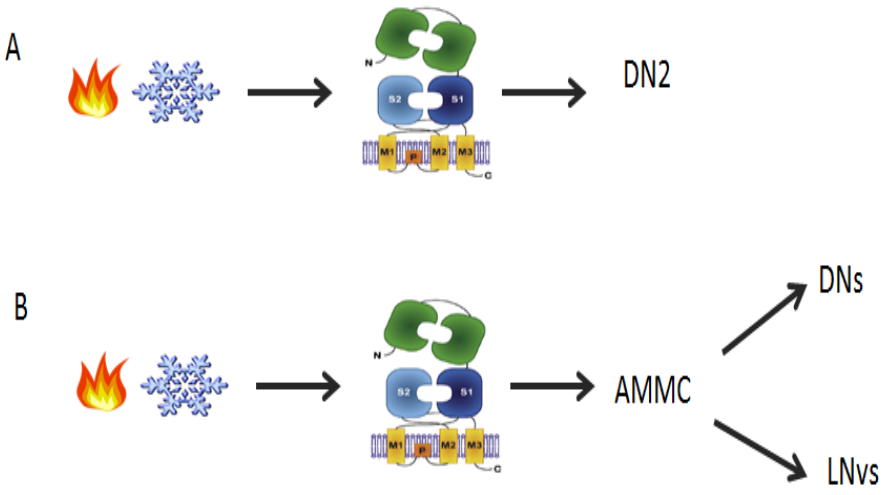

Figure 4. 21 Two potential projections mediated by IR25a

Cycling temperature information can be either transducted to DN2 directly (A) or be preceived by AMMC, and then be projected to Clock

Chapter 5
Is IR56a, a potential IR25a partner involved in temperature entrainment?

5.1 Background

As discussed in chapter1, ion channels like glutamate receptors always function as a complex by assembling different subunits. Various combinations of different iGLURs subunits is the basis of the diverse synapses. It has also been shown that IRs, a homologue of iGluRs, function as complexes, but instead of tetramers, they have two different assembled properties based on the different co-receptors (IR8a or IR25a). Electrophysiological studies in Xenopus oocytes and odor-evoked neuronal responses revealed that expression of IR8a is sufficient to confer responses to phenylacetaldehyde only when co-expressed with the odor specific receptor IR84a (Abuin et al., 2011). Another example demonstrated that for acetic acid detection co-expression of IR8a with a different receptor, sacculus receptor IR64a, is required(Ai et al., 2013).In contrast, for IR25a, reconstitution of the OR22a neuron phenylethylamine-sensing receptor requires the following receptors: the presumed odor-specific IR76a, the broadly expressed IR25a co-receptor,

and IR76b, a receptor which is co-expressed with other IRs in ac1 (antennal cilia), ac2 and ac4(Abuin et al., 2011).Protein sequence alignment also indicated that the ATD in both of the co-receptors (IR8a and IR25a) is relatively conserved with iGluRs (>60% amino acid sequence identity), indicating that the ATD domain may have a similar function as in the iGluRs. Indeed, domain functional analysis in IR8a suggests that ATD in IR8a has an important role in dendrite/cilia targeting and binding to the specific receptors (Abuin et al., 2011). In addition, in a highly divergent homologous ATD domain in arista and sacculus expressed IRs (IR21a, IR40a, IR64a and IR93a), the homology between IRs and iGluRs remained low (<34% amino acid sequence identity), suggesting that the ATD in these IRs has a different molecular function compared to iGluRs.

In the previous chapter, I have shown that IR25a located in chordotonal organs is required for temperature entrainment at both behavioural and molecular levels. To further understand the molecular mechanisms underlying temperature entrainment mediated by IR25a, I conducted experiments to address the possibility that other IRs may be involved in this process as heterodimeric partners with IR25a similar to what has been found in the olfactory system.

5.2 Results

5.2.1 IR76a and IR76b are not required for temperature synchronization.

In the last chapter, I showed that co-receptor IR (IR8a) is not involved in temperature entrainment, suggesting that temperature entrainment may only be mediated by certain IRs, especially the group of IRs using IR25a as their co-receptor. Therefore, the first question I asked was whether IR76a and IR76b, the two IRs that function as complexes with IR25a in odour sensation, are also involved in temperature entrainment. To answer this question, I first investigated if the function of both IR76a and IR76b are necessary for temperature synchronization. Mutants of *IR76a* and *IR76b* were generated and tested in behavioural experiments. For *IR76a*, two independent deletion lines ($IR76a^{1}$ and$IR76a^{2}$) were generated via *piggyBac* mediated deletion, confirmed by RT-PCR(Figure 5.1 A, Benton et al., unpublished data). For *IR76b*, two independent P-element insertion lines ($IR76b^{01}$ and $IR76b^{05}$, Zhang et al., 2007) served as *IR76b* mutants (Figure 5.1 B), both insertions were confirmed by RT-PCR (Benton et al., unpublished data). To avoid genetic background effects, trans-heterozygous flies with mutants for both genes ($IR76a^{1}/IR76a^{2}$ and $IR76b^{01}/IR76b^{05}$) were generated for behavioural

tests using the same conditions as for *IR25a* mutants (12h: 12h 25°C: 27°C, constant light, LL). The *IR76a* and *IR76b* mutants, as well as Canton S flies (served as the positive control) were initially exposed to LL at 25°C, followed by a temperature cycle of 12h:12h, 25°C: 27°C for 6 days. As shown in Figure. 5.2 A, the positive control (Canton S) exhibits arrhythmic behaviour during LL, indicating that endogenous clock function is abolished as expected. However, once they are exposed to TC, as expected, locomotor activity rhythm was restored, with an organized anticipating activity peak in the second half of the warm phase, as shown in the actograms at the top of each columns (Figure 5.2 A, left top panel). Activity peaks can more easily be recognized in the histogram (Figure 5.2 A, left bottom panel),which shows the average activity of the last 2 days of the TC, which is a unique activity peak in the late part of the warm phase. Strikingly, both *IR76a* and *IR76b* mutants exhibit a similar behavioural pattern as Canton S with clear anticipating activity peaks before the onset of the cryophase (Figure 5.2 A centre and right panels), suggesting that IR76a and *IR76b* do not mediate the temperature synchronization, at least not in the same temperature range as for IR25a. Data shown above indicates that although IR76a and IR76b, function with IR25a together in odor sensation, they are not required for temperature synchronization at the behavioural level.

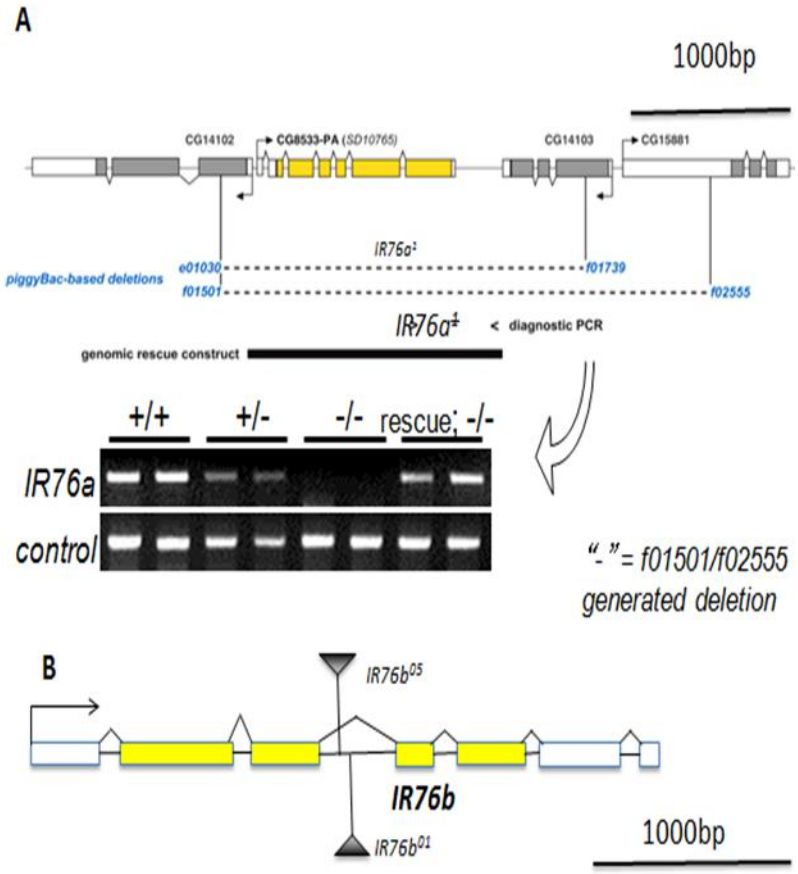

Figure 5.1 Generation of the *IR76a* (*CG8533*) mutants and P-element insertion mutants for *IR76b*.

(A) Characterization of the deletion in the IR76a gene (revised based on Benton et al., unpublished). Top: Schematic representation of the mutants generated by *piggyBac* based deletions in the *Drosophila IR76a* gene. Dotted lines represent the deleted region. Black arrows represent translation starting sites. Yellow and grey bars indicate coding region of the genes whereas open bars represent untranslated regions (UTR). Bottom: RT-PCR analysis of the transcription in the mutant flies. Total RNA was extracted from the fly antenna of wild type flies (Canton S), and flies with a *IR76a* deletion (-/-). PCR reactions for tublin transcripts served as the control.

(B) Gene structure of *IR76b* and the location of the P-element insertion lines indicated by triangles (revised based on information from Flybase (www.flybase.org)).

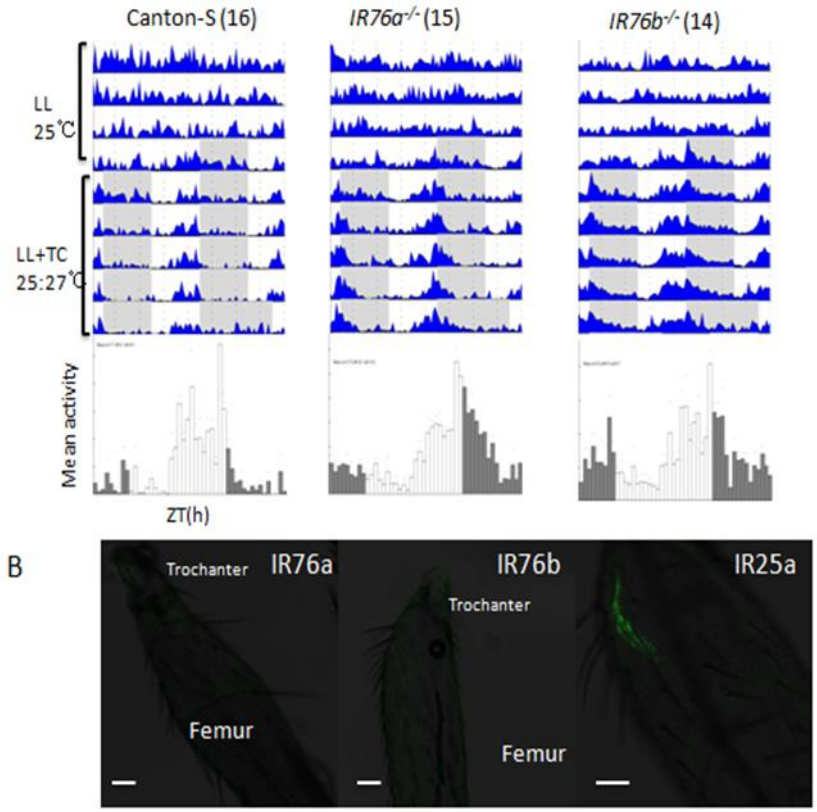

Figure 5.2 IR76a and IR76b are not required for temperature entrainment.

(A)Locomotive activity analysis of *IR76a* and *IR76b* mutants. The plots on top depict actograms. The lower plots depict daily average activity (histograms). Flies of the indicated genotypes were first exposed to LL for three days (LL and 25°C) and then transferred to a 12h: 12h 25°C: 27 °C temperature cycle for another six days. Number of individuals tested is indicated in parentheses. Canton S served as positive control. (B)Genotypes for $IR76a^{-/-}$ and $IR76b^{-/-}$ are $IR76a^{1}/IR76a^{2}$ and $IR76b^{1}/IR76b^{05}$ respectively.

Neither IR76a nor IR76b is expressed in femur chordotonal organs. Expression of *UAS-mCD8:GFP* driven by *IR76a-gal4* (left), *IR76b-gal4* (center) and *IR25a-gal4* (right). Genotypes for (B):Left: *UAS-mCD8:GFP/+;IR76a-gal4/+*. Center: *UAS-mCD8:GFP/+;IR76b-gal4/+.* Right*: UASmCD8:GFP /+;I R76a-gal4/+.* Scale bar=25um

Why IR76a and IR76b are not behaviourally required for temperature entrainment? One possibility is that both genes are not expressed in ChO. As shown in the previous chapter, although IR25a is expressed in Johnston's organs as well as in the 3rd antennal segments, ablations of

these tissues have no effect on the normal role of IR25a in synchronising locomotive activity rhythms to temperature cycles, suggesting that IR25a in the femur chordotonal organs an other tissues play an important role in this process. Thus, to further determine if IR76a and IR76b are expressed in femur chordotonal organs, flies carrying *UAS-mCD8: GFP* were crossed to IR76a and IR76b *gal4* lines (Benton et al., 2009;Silbering et al., 2011)respectively and the offspring carrying both gal4 and UAS elements were dissected and visualized under a florescent microscope (Figure 5.2 B).As predicted, there were no positive signals from either *IR76a-gal4/UAS-GFP* or *IR76b-gal4/UAS-GFP* flies. In contrast, *IR25a-gal4* combined with GFP produced strong signals in subsets of femur chordotonal organ neurons, suggesting that unlike IR25a, IR76a and IR76b do not express in chordotonal organs.

5.2.2 IR56a, a novel ionotropic receptor, expressed in subsets of femur chordotonal organs but not in Johnston's organ.

In the previous chapter, I showed that IR25a plays an important role in temperature entrainment, and I ruled out that IR25a located in 2nd and 3rd antennal segments is not necessary for this process. So any potential partners should be located in the periphery sense organs including ChO. To investigate if there are other IRs interacting with IR25a involved in temperature entrainment, I tried to identify whether other IR's

expressed in chordotonal organ. Genomic analysis has identified 66 *IR* genes (including 9 putative pseudogenes) in the genome of *Drosophila melanogaster* (Benton et al., 2009; Croset et al., 2010). Comprehensive expression analysis of these genes by RT-PCR, fluorescence RNA in situ hybridization and/or using transgenic reporters has shown that 16 of these are expressed in the antenna (Benton et al., 2009; Croset et al., 2010). The remaining 41so-called 'divergent IRs' have diverse expression patterns, and only 22of them are expressed in adult stage (Benton, personal communication). A small-scale screen was performed to reveal their expression pattern using the *UAS-m CD8: GFP* line crossed with various IR-gal4 lines (Table2.5 and Table 5.1). Most of the IRs are expressed in the chemosensory neurons of the tibia and tarsus but not in the antenna, which is similar to the expression pattern of Gr22e (gustatory receptor 22e), therefore suggesting that they work as taste receptors rather than odour receptors. Interestingly, two IRs (IR52c and IR56d) expressed in JO (Table 5.1 and data not shown) but not in the femur chordotonal organ. Strong GFP expression in the femur chordotonal organs was observed in the femurs of *IR56a-gal4/UAS-GFP* flies (Figure 5.3 E-H and Table 5.1), similar to that reported for*F-gal4* (Kim et al., 2003; Sehadova et al., 2009) and *IR25a-gal4* (Figure 5.2 B right panel, also see chapter 4). Overall, the number of *IR56a*-positive cells was less than that obtained with the*IR25a-gal4* driver, but they

were located in the same regions of chordotonal organs and most likely represented neurons (Figures5.2 B right panel and Figure 5.3 E-H, L).It therefore appears that the *IR56a-gal4*-expressing cells are subsets of *IR25a-gal4*-expressing ones. However, whether the IR56a-expressing cells overlap with IR25a^{+} neurons still remains to be shown. Besides the expression in the chordotonal organs, like IR25a, IR56a is also highly expressed in the sacculus and some of the olfactory sensory neurons (Figure 5.3 B-D) as well as in the chemosensory neurons located in tibia and tarsal (Figure 5.3I-L). In the central nervous system, IR56a is expressed in SOG (sub-oesophageal ganglion) with visible connection to the VNC (ventral nerve cord) (Sivasubramaniam, unpublished, Figure 5.3M-N). Unlike IR25a, IR56a is not expressed in JO (Figure 5.3 B-D),which indicats that femur chordotonal organ may be more important for temperature entrainment with IR56a as a partner of IR25a.

Table 5.1 analysis of expression pattern of the divergent IRs.

tissues / Gal4	Johnston's organ	3rd antennal segment	Femur Ch organ	Tibia and Tarsus
IR7a	-	-	-	-
IR7c	-	+	-	+
IR10a	-	-	-	-
IR11c	-	-	-	-
IR20a	-	-	-	+
IR25a	+	+	+	+
IR47a	-	-	-	-
IR52b	-	-	-	+
IR52c	+	-	+	-
IR52d	-	-	-	+
IR56a	-	+	+	+
IR56d	+	-	+	+
IR60c	-	-	-	+
IR67a	-	-	-	-
IR68b	-	-	-	-
IR94e	-	-	-	+
IR94h	-	-	-	-

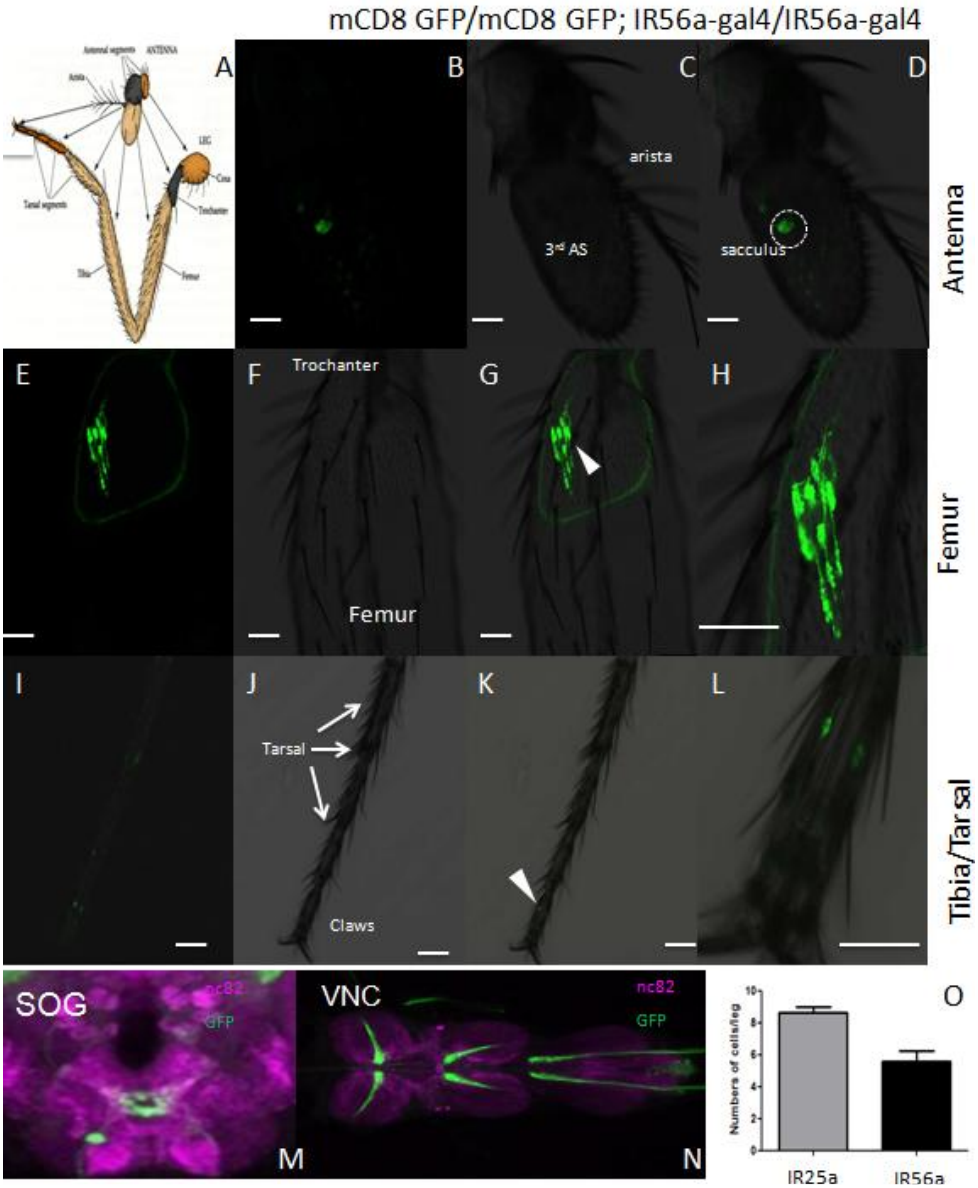

Figure 5.3 Analysis of the spatial expression pattern of IR56a.

(A) Schematic of the anatomical structure of *Drosophila* antenna and legs. The arrows show the portions of the antenna that form specific corresponding portions of the leg (Postlethwait and Schneiderman, 1971).

(B–L) Expression of UAS-mCD8:GFP driven by *IR56a-gal4* in olfactory sensory neurons (OSNs, B-D), in mechanoreceptors neurons of the femur chordotonal organs (Ch organs) (E-H) and in potential chemoreceptors of the legs (I-L). 3rd AS: 3rd antennal segment. The dotted circle in D highlights the sacculus. Arrow heads in G and K indicate the zoomed region in H and L, respectively. (B), (E) and (I) are green florescent channel; (C), (F) and (J) are bright light channel. Scale bar = 20um.

(M, N) Expression of UAS-mCD8:GFP driven by *IR56a-gal4* and co-stained with neuronal marker nc82 in central nervous system (J) and VNC (K) (Sivasubramaniam, unpublished).Genotypesfor(B-L):*UAS-mCD8:GFP/UAS-mCD8:GFP; IR56a-gal4/IR56a-gal4.*

(O) Summary of GFP^{+} cells numbers of the IR25a and IR56a in femur Ch organs. Data for IR25a was taken from chapter 4.

5.2.3 IR56a is not required for temperature synchronization to 25℃: 27℃ in constant light.

To further investigate if IR56a is required for temperature entrainment at the behavioural level, I generated a loss-of-function mutant of IR56a. A fly line with a MIMIC insertion (Minos mediated integration cassette) 1000 bp (base pair) upstream of its coding region (Figure 5.4 A) was obtained from the Bloomington stock centre. With the help of a summer student (Mohammed Karim), I carried out crosses to excise this element and screened approximate 200 independent excision lines. Luckily, one imprecise excision event occurred. In line *IR56a*^{128}(No.128 out of the 200 excision events) about 800 bp of genomic sequence starting at the start codon and including most of the coding region of IR56a (Figure 5.4 A)were deleted. As the *IR56a* gene is inserted between the exon 4 and 5 of the *Drosophila 5-HT1A* gene, the exon 5 of *5-HT1A* has also been deleted in the mutant *IR56a*^{128}.

To confirm that the loss-of-function mutant of *IR56a* has been generated, I characterized the deletion in the *IR56a*^{128} line by genomic PCR (Figure 5.4B) and DNA sequencing. A 3000 bp PCR product was amplified using genomic DNA from wild type flies (Canton-S and the precise excision fly IR56a^{PE} PE: precise excision), whereas an approximate 1200 bp PCR

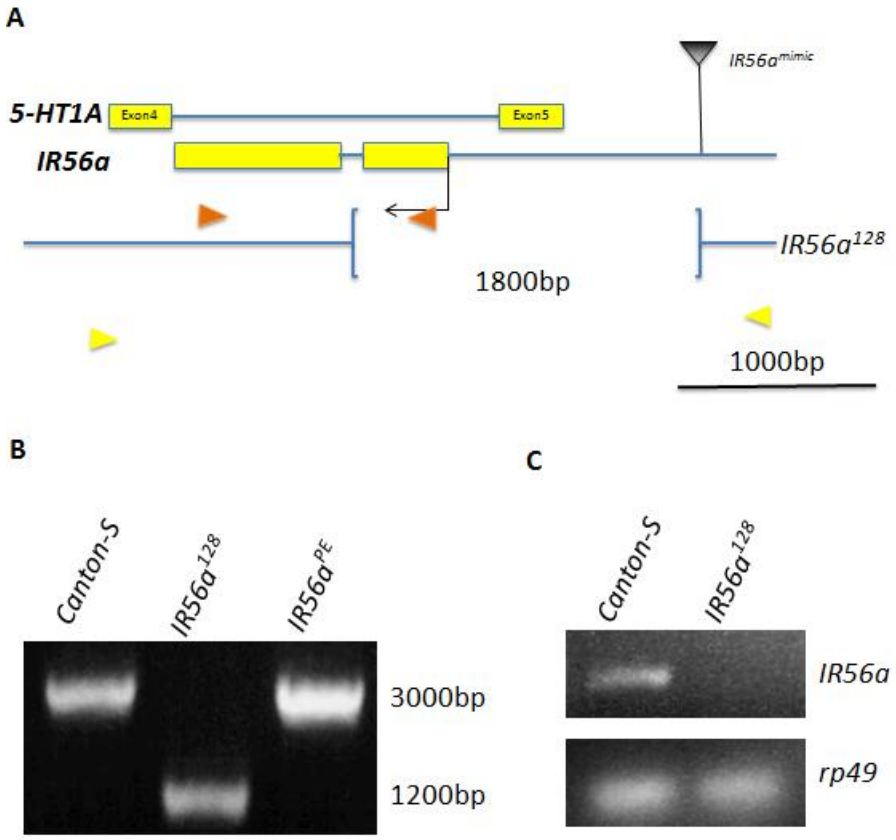

Figure 5.4 Characterization of the deletion in the *IR56a* gene

(A)Schematic representation of the deletion generated by imprecise excision of a MIMIC insertion in the *Drosophila 5-HT1A* gene. Black arrow represents translation start site. A triangle indicates the P element insertion. The pair of yellow triangles indicate a set of primers designed to amplify the region of genomic DNA including *IR56a* and part of *5-HT1A*, and the brown pair were used for RT-PCR. The excised region is represented by a pair of brackets. The yellow blocks represent exons.

(B)Genomic PCR analyses of imprecise excisions were carried out. Canton-S and $IR56a^{PE}$ were used as controls. $IR56a^{128}$ is the imprecise excision line. PE, precise excision.

(C)RT-PCR analysis of the transcription of the mutant flies. Total RNA was extracted from fly legs of wild-type flies (Canton-S), and flies with a *IR56a* deletion ($IR56a^{128}/IR56a^{128}$). PCR reactions for *rp49* transcripts served as controls. Mutant $IR56a^{128}$flies produced normal *rp49* PCR product but no *IR56a* transcript product.

product was amplified from $IR56a^{128}$genomicDNA using the same pair of primers. Around 800bp were deleted from*IR56a* gene region in

IR56a^{128}mutants as determined by sequence alignment after DNA sequencing. To confirm the endogenous expression level of *IR56a* in the femur of wild type and IR56a mutant flies, semi-quantitive RT- PCR experiments using RNA isolated from their femurs respectively (Figure 5.4C). A cDNA band of *IR56a* gene can be amplified by using total RNA from Canton S but not from *IR56a*^{128}flies, indicating that *IR56a* is expressed in the femur of wild type flies, and *IR56a*^{128} is a null mutant of *IR56a* gene.

Next, I accessed if the behavioural patterns of the locomotor activity of *IR56a*^{128}mutant flies were altered in LD and DD. Wild type (*y w*) and *IR56a* mutant flies were initially synchronized to three LD cycles at 25°C followed by 6 days in DD at 25°C. As expected, *IR56a*^{128}mutant flies showed robust bimodal activities during the LD sessions and no significant difference between the wild type and mutant flies in DD were observed (Figure 5.5 upper panel). Moreover, the analysis of the percentage of rhythmic flies, rhythmic strength and the length of period also indicated that *IR56a*^{128}is not required for circadian rhythms in LD and DD(Figure 5.5 lower panel).

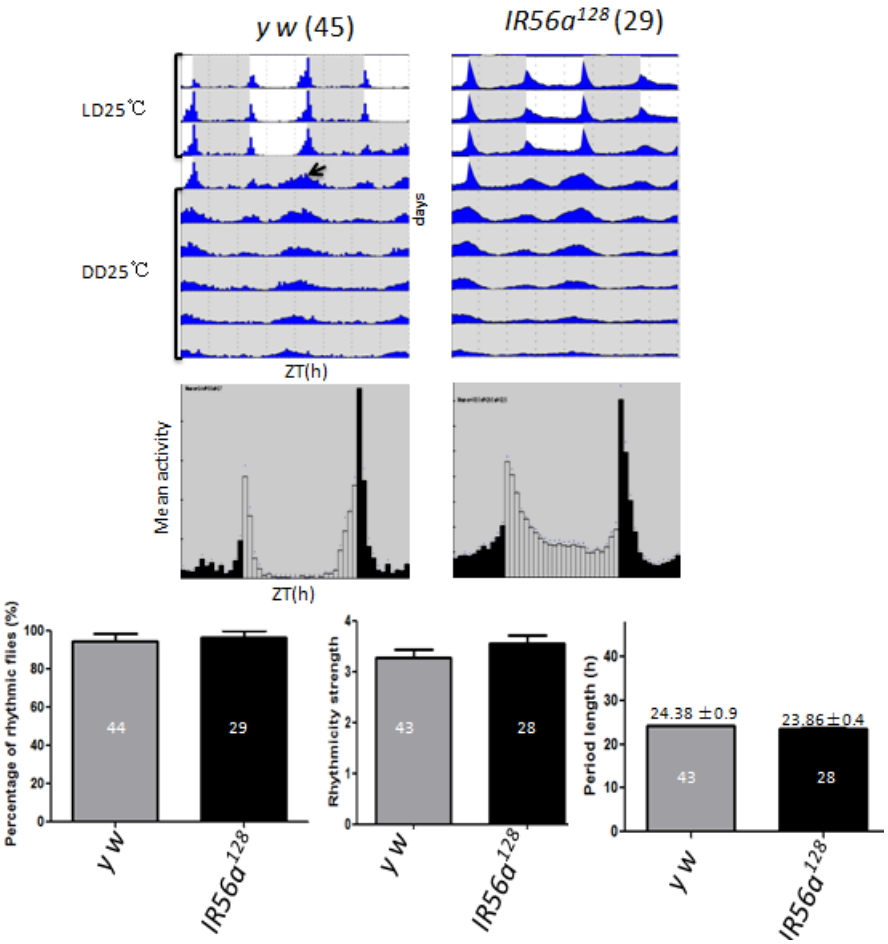

Figure 5.5 Locomotor behaviour of *IR56a*^{128} flies in LD and DD.

Upper panel: Actograms of flies with indicated genotypes were transferred to constant darkness (DD) before 3 days 12h: 12h light: dark cycles (LD). The transition day from LD to DD is represented by a black arrow. Number of individuals tested is indicated in brackets. Middle panel: Daily average activity plots (Histograms) of flies from the indicated genotypes in LD. Lower panel: Percentage of rhythmic flies (left), Rhythmic Strength (R.S.) (center) and Period length (right) of the indicated genotype in DD. For the calculation of Period length, only rhythmic flies (R. S.>1.5) are included. Numbers in the columns indicated the number of tested individuals. Average period and SEM of indicated genotypes is shown above the columns.

The next step was to find out if *IR56a* is involved in temperature synchronization. I used the same conditions (12h: 12h 25°C: 27°C, LL) during which *IR25a* mutants exhibit temperature entrainment defects. Wild type (Canton S) and *IR56a* mutant flies were initially exposed to LL at 25°C for 3 days followed by two 5-day temperature cycles (12h: 12h

25°C: 27°C), each shifted by a delay of 6 hours compared to the previous cycle (Figure 5.6 A). As expected, the positive control (Canton-S)quickly re-synchronize to the first temperature cycle (TC1) and shift their activity peaks almost 6 hours when transferred to TC2 (Figure 5.6 A, left). Synchronization to TCs was evident, indicated by a well-organized activity peak in the second half of the warm phase during the original and shifted TCs (TC1 and TC2). Activity peaks can also be distinguished in the daily average of the histograms (Figure 5.6 B, left) that show the average activity of the last two days of each TCs. Unexpectedly, homozygous *IR56a*^{128} mutants also exhibited a similar behavioural pattern with a discerned activity peak before the onset of cryophase (Figure 5.6 centre panels), suggesting that *IR56a* is not required for temperature entrainment at behavioural level. The phenotype was also confirmed using the transheterozygous *IR56a*^{128} */Df (IR56a)* (Figure 5.6 right panels). Based on these observations, I conclude that *IR56a* is not required for temperature synchronization in 12h: 12h 25°C: 27°C, LL at the behavioural level.

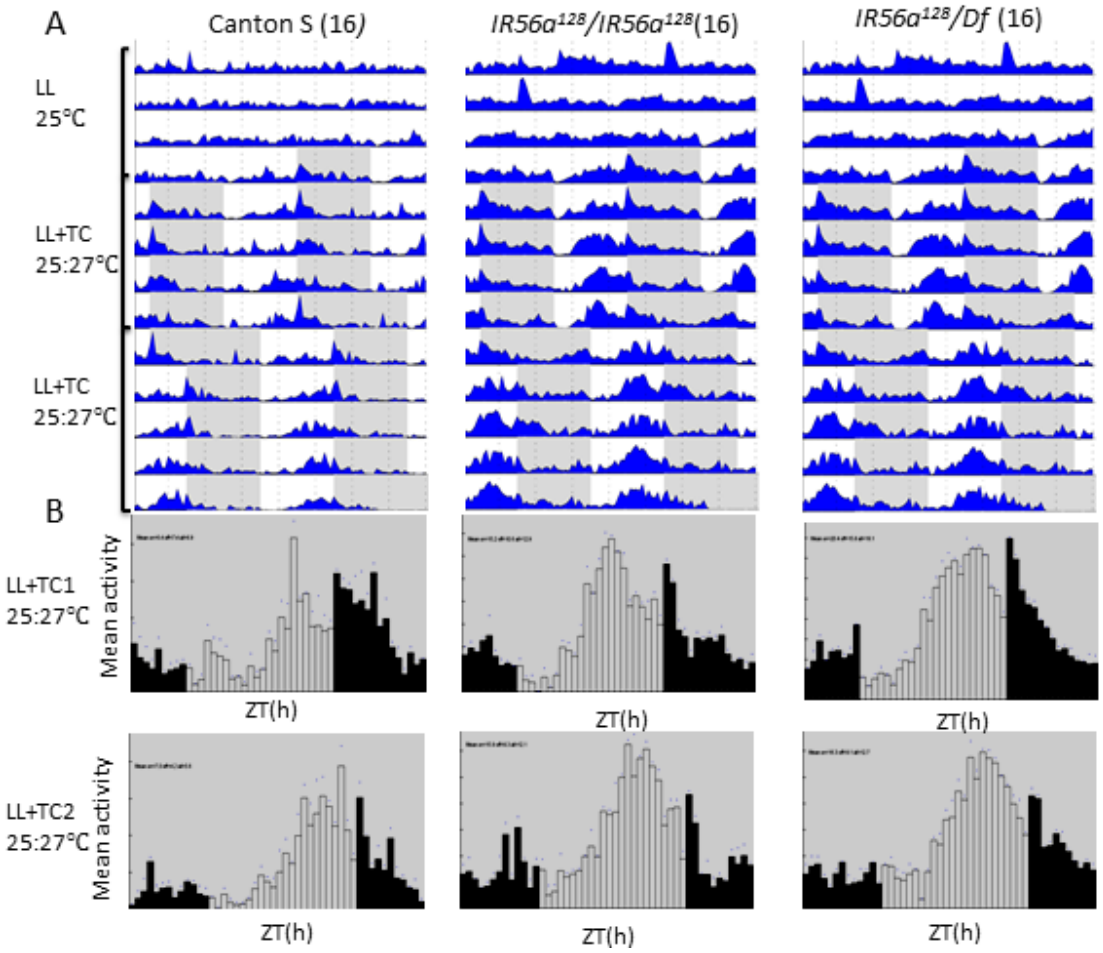

Figure 5.6 IR56a is not required for temperature entrainment.

Actograms (A) and histograms (B) of flies exposed to two temperature cycles (TC1 and TC2). Flies with the indicated genotypes were first exposed to LL for four days (LL and 25℃) and then transferred to two 12h: 12h 25°C: 27°C temperature cycles for another five days. Subsequently, the onset of the warm phase in TC2 was delayed by 6 hours compared to the initial regime (LL + TC1). Number of individuals tested is indicated in parentheses. The Canton S flies served as positive controls.

Discussion

5.3.1 Is IR25a sufficient for the synchronization of circadian behaviour to a temperature cycle of 12h: 12h 25°C: 27°C, LL?

Although previous olfactory studies show that reconstitution of a functional IR olfactory receptors complex need at least one co-receptor (IR8a or IR25a) and a specific IR (Abuin et al., 2011), it is surprising that in temperature entrainment, at least under the condition of 12h: 12h 25°C: 27°C, LL, the second femur chordotonal organ located IR (IR56a), is not required for temperature entrainment, which suggests that IR25a maybe the only receptor located in the femur chordotonal organ and required for synchronization to temperature cycles at this condition (Figure 5.6 A).Interestingly, a recent study in salt sensation revealed that IR76b alone is sufficient to induce salt-evoked responses (Zhang et al., 2013), which could be similar to the situation in temperature entrainment. Thus, a mandatory combination of IRs may be not a 'golden rule' for all the IRs involved in behavioural processes. However, to prove this hypothesis, an experiment showing that IR25a is a functional thermo receptor is required.

5.3.2 Is IR56a a partner of IR25a for entrainment to temperature cycles

with other temperature intervals?

Although it appears that IR56a is not required for temperature entrainment to 12h: 12h 25°C: 27°C, LL, it does not rule out that IR56a is involved in temperature entrainment to other temperature intervals, because IR25a is involved in the synchronization to a very broad temperature range (18°C-27°C). It is possible that IR25a and IR56a together or IR56a alone mediate temperature entrainment under relative lower absolute temperatures (Figure 5.7 B-D). Further behavioural tests are necessary to address this question.
In addition, the interaction between IR25a and IR56a needs to be confirmed biochemically. My work on the *IR56a* project is a starting point and surely, further research will be required to dissect the function of this gene.

5.4 Summary of Main Results

5.4.1 *IR76a* and *IR76b* are not required for temperature entrainment in the temperature cycles of 12h: 12h 25°C: 27°C.

5.4.2 IR56a is expressed in subsets of chordotonal organs.

5.4.3 IR56a is not required for light entrainment and rhythmicity in constant darkness.

5.4.4 IR56a null mutants exhibit normal behavioural locomotor activity patterns under the temperature cycles of 12h: 12h 25°C: 27°C in LL.

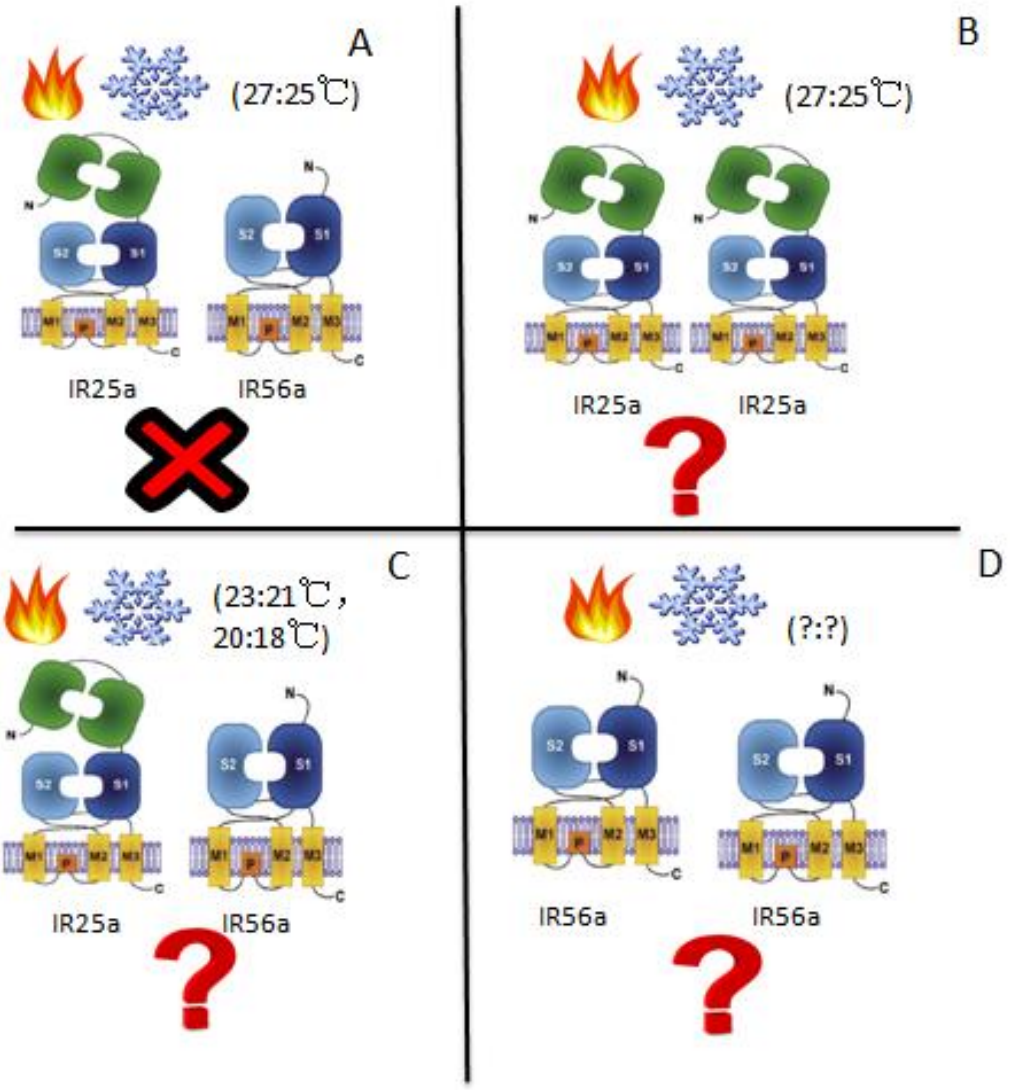

Figure 5.7 Four potential working models for IR25a/IR56a in temperature entrainment.

Chapter6
Summary

Temperature cycles robustly synchronized *Drosophila* circadian clocks and even rescue arrhythmic behaviour in constant light, whereas the mechanisms underlining are poorly understood. The isolation of the first temperature entrainment mutant *nocte* provides us a good opportunity to genetically and functionally dissect the molecular mechanisms of temperature entrainment, which will definitely broaden our knowledge of temperature entrainment. However, after bioinformatical analysis, we couldn't find any homologies to proteins of known function, which slowed down our pace of investigation.

To conquer this difficulty, I applied Co-immunoprecipitation(Co-IP) combined with Mass spectrometry to try to isolate novel proteins interacting with Nocte *in vivo*. I started my PhD with generating Tag fused Nocte transgenic flies, and continued pursuing the protein affinity pull-down. After I successfully isolated 4 potential protein candidates interacting with Nocte, I continued my PhD with focusing on one of them, IR25a (Ionotropic Receptor 25a). Using a series of biochemistry, behavioural test and Immunohistochemistry technique, I was able to show that IR25a is required for synchronizing both central and peripheral

clocks to temperature cycles but not to LD cycles. IR25a is expressed in subsets of chordotonal organs and physically interacts with Nocte. Further investigations suggest the existence of a co-receptor working together with IR25a. I therefore continue my project to isolate the co-receptor of IR25a. I have found another IR (IR56a) that is also expressed in femur Ch organs. However, preliminary behavioural analysis of using IR56a null mutants suggests that IR56a is not required for temperature entrainment with a higher temperature interval (27:25°C), whereas further investigation is required to be performed. Overall, my PhD work demonstrates a novel function of IR25a involved in temperature synchronization.

Based on the data in my work, a hypothetic working model was shown in Figure 6.1. As shown in the olfactory studies, unlike canonical iGLURs, IRs lose their binding ability to internal neurotransmitter such as Glutamate, but may use their ligand binding domain (LBD, Abuin et al., 2011, also reviewed in chapter one) to capture specific temperature molecules, as a co-receptor, IR25a may also recruit other IRs to work as a complex, one potential candidate is IR56a. IR25a physically interacts with Nocte, this interaction may thereby help IR25a to stabilize itself on the membrane. When certain temperature (such as 25: 27℃) pulse actives IR25a, the channel domain of IR25a will be opened, so Ca^{2+} influx can be

transported from extracellular matrix into cytoplasm, which will directly modulate membrane potential or active a serial of signal pathway, which might also include another interesting protein isolated in chapter 3, dSAR (*Drosophila* Sarcalumenin, a protein encoded by *CG9297*). As mentioned in chapter3, dSAR is a sarcoplasmic reticulum (SR) luminal glycoprotein, which is highly abundant in longitudinal SR. Functional analysis revealed that it may be responsible for Ca^{2+} cycling, therefore the unknown downstream signal pathway using Ca^{2+} as second signal messenger will be activated, although more work need to be done to identify them. On the other hand, other receptor independent pathways mediated by Mcm3 and the protein encoded by *CG1440* may also exist, however further investigations are needed.

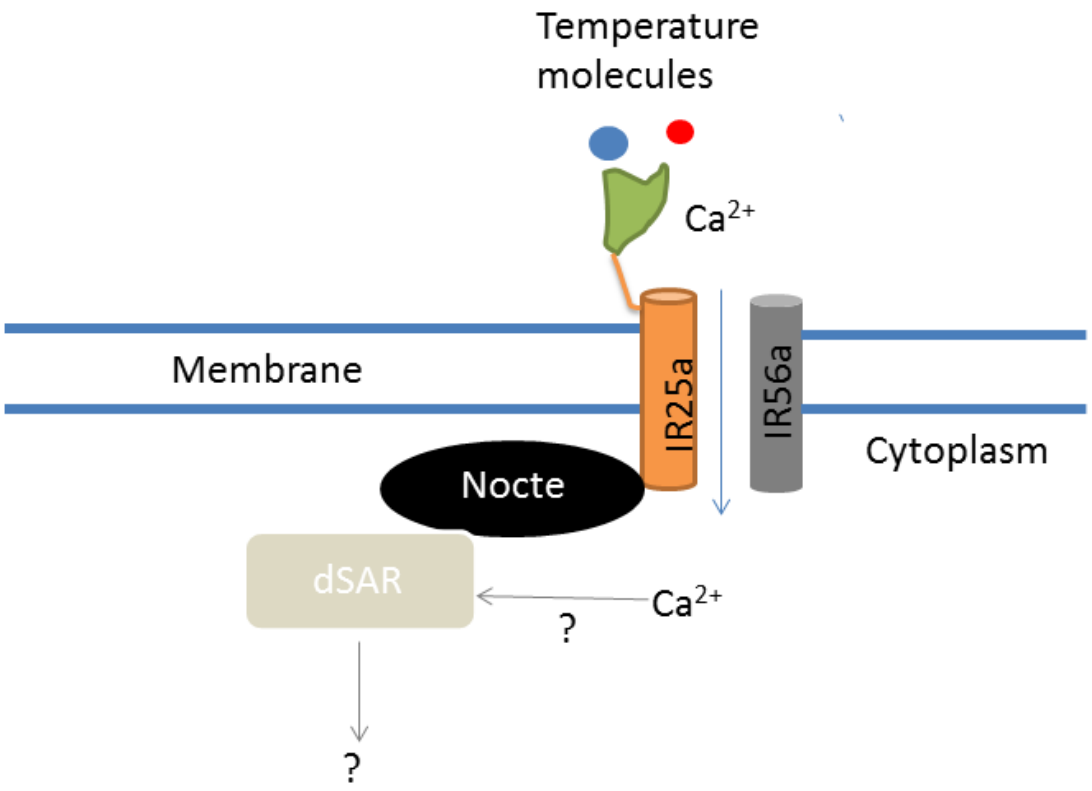

Figure 6.1 predicted working model of IR25a/Nocte.
IR25a (orange) may be stabilized on the membrane by interacting with cytoplasmic protein Nocte. IR25a may capture single cold (blue)/ hot (red) temperature molecue using its ligand binding domain (Green), therefore induce the entry of ca2+. IR56a (Grey column) may work as a potential co-receptor with IR25a. Cytoplasmic ca2+ might bind to dSAR (Drosophila Sarcalumenin, a protein encoded by CG9297, grey square), another potential Nocte interacter and active the downstream unknown signal pathways, which will finally active thermo transduction from Chordotonal organ neurons to clock cells. The grey color indicates the parts haven't been proved.

As a model system, *Drosophila* offers a powerful combination of molecular, genetic, behavioural and cell culture tools, therefore representing an attractive model to explore this issue. Knowledge we achieved from *Drosophila* circadian clock has been used to inspire us to understand the basic mechanism of the biological clock of our own. As discussed in chapter1, the molecular mechanisms underlying central oscillation as well as light entrainment in *Drosophila* is quite conserved

to the ones in mammals. Based on the similarity of phenomenon about temperature entrainment between these two systems, it's very possible that they share the similar mechanisms as well. As a relative simpler model, it will be easier to understand the fundamental principal of temperature entrainment in *Drosophila*, and the knowledge we achieve in temperature entrainment using *Drosophila* may aid our understanding of human temperature entrainment and related diseases. Therefore, even though both Nocte and IR25a don't have homologues in mammals, it's still worth to understand their molecular functions and the related signal pathway they involved in, as they may partially share the same mechanisms in mammals.

References

Abuin L, Bargeton B, Ulbrich MH, Isacoff EY, Kellenberger S, and Benton R. (2011). Functional architecture of olfactory ionotropic glutamate receptors. Neuron. 69: 44-60.

Ai M, Min S, Grosjean Y, Leblanc C, Bell R, Benton R, and Suh GS, (2010). Acid sensing by the Drosophila olfactory system. Nature. 468: 691-695.

Ai M, Blais S, Park JY, Min S, Neubert TA, Suh GS. (2013). Ionotropic glutamate receptors IR64a and IR8a form a functional odorant receptor complex in vivo in Drosophila. J Neurosci. 33:10741-10749

Allada R, White N E, So WV, Hall JC, and Rosbash M. (1998). A mutant Drosophila homolog of mammalian Clock disrupts circadian rhythms and transcription of period and timeless. Cell. 93: 791-804.

Baines RA, Uhler JP, Thompson A, Sweeney ST, and Bate M. (2001). Altered electrical properties in Drosophila neurons devel- oping without synaptic transmission. J. Neurosci. 21: 1523–1531.

Benton R, Vannice KS, Gomez-Diaz C, and Voshall LB. (2009). Variant

ionotropic glutamate receptors as chemosensory receptors in Drosophila. Cell. 136: 149-162.

Boothroyd CE, and Young MW. (2008). The in(put)s and out(put)s of the Drosophila circadian clock. Ann N Y Acad Sci. 1129: 350-357.

Brown SA, Zumbrunn G, Fleury-Olela F, Preitner N, Schibler U. (2007) Rhythms of Mammalian Body temperature can sustain peripheral circadian clocks. Current Biology. 12:1574-1583.

Busza A, Emery-Le M, Rosbash M, Emery P. (2004).
Roles of the two Drosophila CRYPTOCHROME structural domains in circadian photoreception.Science. 4;304(5676):1503-6.

Busza A, Murad A, Emery P. (2007) Interactions between circadian neurons control temperature synchronization of Drosophila behavior. J Neurosci. 27(40): 10722-10733.

Buhr ED, Yoo SH, Takahashi JS. (2010) Temperature as a universal resetting cue for mammalian circadian oscillators. Science. 330:379-385

Camacho F, Cilio M, Guo Y, Virshup DM, Patel K, Khorkova O, Styren S,

Morse B, Yao Z, Keesler GA. (2001). Human casein kinase Idelta phosphorylation of human circadian clock proteins period1 and 2. FEBS Lett. 489: 159-165.

Cary LC, Goebel M, Corsaro BG, Wang HG, Rosen E, Fraser MJ. (1989). Transposon mutagenesis of baculoviruses: analysis of Trichoplusia ni transposon IFP2 insertions within the FP-locus of nuclear polyhedrosis viruses. Virology. 172(1): 156-169.

Cassone VM, Speh JC, Card JP, Moore RY. (1988). Comparative anatomy of the mammalian hypothalamic suprachiasmatic nucleus. J Biol Rhythms. 3: 71-91.

Ceriani MF, Darlington TK, Staknis D, Mas P, Petti AA, Weitz CJ, Kay SA. (1999). Light-dependent sequestration of TIMELESS by CRYPTOCHROME. Science. 284: 760-765.

Chen KF, Peschel N, Zavodska R, Sehadova H, Stanewsky R. (2011). QUASIMODO, a Novel GPI-anchored zona pellucida protein involved in light input to the Drosophila circadian clock. Curr Biol. 21(9): 719-729.

Chen GQ, Cui C, Mayer ML, Gouaux E. (1999). Functional

characterization of a potassium-selective prokaryotic glutamate receptor. Nature. 402(6763): 817-21.

Chiu JC, Vanselow JT, Kramer A, and Edery I. (2008). The phospho-occupancy of anatypical SLIMB-binding site on PERIOD that is phosphorylated by DOUBLETIME controls the pace of the clock. Genes Dev. 22: 1758-1772.

Chung YD, Zhu J, Han Y, Kernan MJ. (2001). nompA encodes a PNS-specific, ZP domain protein required to connect mechanosensory dendrites to sensory structures. Neuron. 29(2): 415-28.

Collingridge GL, Isaac JT, Wang YT. (2004). Receptor trafficking and synaptic plasticity. Nat Rev Neurosci. 5:952–962

Croset V, Rytz R, Cummins SF, Budd A, Brawand D, Kaessmann H, Gibson TJ, Benton R. (2010). Ancient protostome origin of chemosensory ionotropic glutamate receptors and the evolution of insect taste and olfaction. PLoS Genet. 6: e1001684.

Cull-Candy SG, Leszkiewicz DN. (2004). Role of distinct NMDA receptor subtypes at central synapses. Sci STKE. 2004:16.

Cyran SA, Yiannoulos G, Buchsbaum AM, Saez L, Young MW, and Blau J. (2005). The double-time protein kinase regulates the subcellular localization of the Drosophila clock protein period. J Neurosci .25: 5430-5437.

Dunipace L, Meister S, McNealy C, Amrein H. (2001). Spatially restricted expression of candidate taste receptors in the Drosophila gustatory system. Curr Biol. 11(11): 822-35.

Edery I, Zwiebel LJ, Dembinska ME, Rosbash M. (1994). Temporal phosphorylation of the Drosophila period protein.Proc. Natl. Acad. Sci. 91(6): 2260-4.

Emery P, So WW, Kaneko M, Hall JC, Rosbash M. (1998). CRY, a Drosophila clock and light-regulated cryptochrome, is a major contributor to circadian rhythm resetting and photosensitivity. Cell. 95: 669-679.

El Allali K, Achaâban MR, Bothorel B, Piro M, Bouâouda H, El Allouchi M, Ouassat M, Malan A, Pévet P. (2013). Entrainment of the circadian clock by daily ambient temperature cycles in the camel (Camelus

dromedarius).

Emery P, Stanewsky, R, Hall JC, and Rosbash M. (2000). A unique circadian-rhythm photoreceptor. Nature. 404: 456-457.

Am J Physiol Regul Integr Comp Physiol. 304(11): R1044-52.

Fang Y, Sathyanarayanan S, and Sehgal A. (2007). Post-translational regulation of the Drosophila circadian clock requires protein phosphatase 1 (PP1). Genes Dev. 21: 1506-1518.

Fogle KJ, Parson KG, Dahm NA, Holmes TC.(2011). CRYPTOCHROME is a blue-light sensor that regulates neuronal firing rate.Science. 18;331(6023):1409-13.

Freeman M.(1996). Reiterative use of the EGF receptor triggers differentiation of all cell types in the Drosophila eye. Cell. 87(4):651-60.

Forsburg SL. (2004). Eukaryotic MCM proteins: beyond replication initiation. Microbiol Mol Biol Rev. 68(1):109-31.

Gallio M, Ofstad T A, Macpherson L J, Wang JW, and Zuker, C. S.. (2011).

The coding of temperature in the Drosophila Brain. Cell. 144: 614-624.

Gekakis N, Stakins D, Nguyen HB, Davis FC, Wilsbacher LD, King DP, Takahashi JS, Weitz CJ. (1998) Role of the CLOCK protein in the mammalian circadian mechanism. Science. 280:1564-1560

Gentile C, Sehadova H, Simoni A, Chen C, Stanewsky R. (2013). Cryptochrome antagonizes synchronization of Drosophila's circadian clock to temperature cycles. Curr Biol. 23(3):185-95.

Gereau RW, and Swanson GT. (2008). The Glutamate Receptors (Totowa, N.J.: Humana Press).

Giot L, Bader JS, Brouwer C, Chaudhuri A, Kuang B, Li Y, Hao YL, Ooi CE, Godwin B, Vitols E, Vijayadamodar, G, Pochart P, Machineni H, Welsh M, Kong Y, Zerhusen B, Malcolm R, Varrone Z A, Minto M, Burgess S, McDaniel L, Stimpson E, Spriggs F, Mckenna M P, Chat J, and Rothberg J M. (2003). A protein interaction map of Drosophila melanogaster. Science. 302: 1727-1736.

Glaser FT, Stanewsky R. (2005). Temperature synchronization of the Drosophila circadian clock. Curr Biol. 15:1352-63.

Grima B, Chelot E, Xia R, and Rouyer F. (2004). Morning and evening peaks of activity rely on different clock neurons of the Drosophila brain. Nature. 431: 869-873.

Guler AD, Altimus CM, Ecker JL, Hattar S. (2007). Multiple photoreptors contribute to nonimage-forming visual functions predominantly through melanopsin –containing retinal ganglion cells. Cold Spring Harb.Symp.Quant.Biol. 72:509-515.

Hall JC. (2003).Genetics and molecular biology of rhythms in Drosophila and other insects.Adv Genet. 48:1-280.

Hardin PE. (2005). The circadian timekeeping system of Drosophila. Curr Biol. 15: 714-722.

Hardin PE. (2006). Essential and expendable features of the circadian timekeeping mechanism. Curr. Opin. Neurobiol. 16: 686-692.

Hamada FN, Rosenzweig M, Kang K, Pulver SR, Ghezzi A, Jegla T J,and Garrity PA. (2008). An internal thermal sensor controlling temperaturepreference in Drosophila. Nature. 454: 217-220.

Harrisingh MC, Wu Y, Lnenicka GA, Nitabach MN. (2007). Intracellular Ca2+ regulates free-running circadian clock oscillation in vivo. J Neurosci. 27(46): 12489-99.

Harrisingh MC, Nitabach MN. (2008). Circadian rhythms. Integrating circadian timekeeping with cellular physiology. Science. 320(5878):879-80.

Helfrich-Förster C, Edwards T, Yasuyama K, Wisotzki B, Schneuwly S, Stanewsky R, Meinertzhagen IA, Hofbauer A. (2002). The extraretinal eyelet of Drosophila: development, ultrastructure, and putative circadian function. J Neurosci.22(21): 9255-66

.

Helfrich-Forster C, Shafer OT, Wulbeck C, Grieshaber E, Rieger D, and Taghert P. (2007). Development and morphology of the clock-gene-expressing lateral neurons of Drosophila melanogaster. The Journal of comparative neurology. 500: 47-70.

Helfrich-Förster C, Winter C, Hofbauer A, Hall JC, Stanewsky R. (2001). The circadian clock of fruit flies is blind after elimination of all known photoreceptors. Neuron.30(1):249-61.

Jepson JE, Shahidullah M, Lamaze A, Peterson D, Pan H, Koh K. (2012). dyschronic, a Drosophila homolog of a deaf-blindness gene, regulates circadian output and Slowpoke channels. PLoS Genet. 8(4): e1002671.

Jiao, Q ,Hiroshi Takeshima, Yoshihiro Ishikawa and Susumu Minamisawa. (2012).Sarcalumenin plays a critical role in age-related cardiac dysfunction due to decreases in SERCA2a expression and activity. Cell Calcuim. 51: 31-39.

Kaneko M, and Hall JC. (2000). Neuroanatomy of cells expressing clock genes in Drosophila: transgenic manipulation of the period and timeless genes to mark the perikarya of circadian pacemaker neurons and their projections. J Comp Neurol. 422: 66-94.

Kamikouchi A, Inagaki HK, E_ertz T, Hendrich O, Fiala A, Gopfert MC, and Ito K. (2009). The neural basis of Drosophila gravity-sensing and hearing. Nature. 458:165-171.

Kernan, M J. (2007). Mechanotransduction and auditory transduction in Drosophila.Pugers Arch. 454: 703-720.

Kim J, Chung YD, Park DY, Choi S, Shin DW, Soh H, Lee HW, Son W, Yim J, Park CS, Kernan MJ, Kim C. (2003). A TPRV family ion channel required for hearing in Drosophila. Nature. 424: 81-84.

Kim EY, Ko HW, Yu W, Hardin PE, Edery I. (2007). A DOUBLETIME kinase binding domain on the Drosophila PERIOD protein is essential for its hyperphosphorylation, transcriptional repression, and circadian clock function. Mol Cell Biol. 27(13): 5014-28.

Kloss B, Price JL., Saez L, Blau, J, Rothenfluh A, Wesley CS, and Young MW. (1998).The Drosophila clock gene double-time encodes a protein closely related to human casein kinase Iepsilon. Cell. 94: 97-107.

Kloss B, Rothenfluh A, Young MW, and Saez L. (2001). Phosphorylation of period isinfluenced by cycling physical associations of double-time, period, and timeless in the Drosophila clock. Neuron. 30: 699-706.

Ko HW, Jiang J, and Edery I. (2002). Role for Slimb in the degradation of Drosophila Period protein phosphorylated by Doubletime. Nature. 420: 673-678.

Koh K, Zheng X, and Sehgal A. (2006). JETLAG resets the Drosophila

circadian clock by promoting light-induced degradation of TIMELESS. Science. 312: 1809-1812.

Konopka R J. and Benzer S. (1971). Clock mutants of Drosophila melanogaster. Proc. Natl. Acad. Sci. 68: 2112-2116

Krishnan B, Levine JD, Lynch MK, Dowse HB, Funes P, Hall JC, Hardin PE, Dryer SE. (2001). A new role for cryptochrome in a Drosophila circadian oscillator. Nature. 411: 313-317.

Kyriacou, C. P. and Rosato, E. (2000). Squaring up the E-box. J. Biol. Rhythms. 15: 483-490.

Kume K, Zylka MJ, Sriram S, Shearman LP, Weaver DR, Jin X, Maywood ES, Hastings MH, Reppert SM. (1999). mCRY1 and mCRY2 are essential components of the negative limb of the circadian clock feedback loop. Cell. 286: 7680771.

Kurabayashi N, Hirota T, Sakai M, Sanada K, Fukada Y. (2010). DYRK1a and glycogen synthase kinase 3beta, a dual-kinase mechanism directing proteasomal degradation of CRY2 for circadian timekeeping. Mol Cell Biol.

30:1757-1768.

Kwon Y, Shim HS, Wang X, and Montell C. (2008). Control of thermotactic behavior via coupling of a TRP channel to a phospholipase C signaling cascade.Nat. Neurosci. 11: 871-873.

Lefterov IM, Koldamova RP, Lazo JS. (2000). Human bleomycin hydrolase regulates the secretion of amyloid precursor protein. FASEB J. 14(12): 1837-47.

Levine JD, Funes P, Dowse HB, and Hall JC. (2002). Signal analysis of behavioral and molecular cycles. BMC Neurosci. 3: 1.

Lee Y, Montell C. (2013). Drosophila TRPA1 functions in temperature control of circadian rhythm in pacemaker neurons. J Neurosci. 33(16): 6716-25.

Li WZ, Li SL, Zheng HY, Zhang SP, Xue L. (2012). A broad expression profile of the GMR-GAL4 driver in Drosophila melanogaster. Genet Mol Res. 11(3): 1997-2002.

Lin FJ, Song W, Meyer-bernstein E, Naidoo N, Sehgal A. (2001). Photic

signalling by Cryptochrome in the Drosophila circadian system. Molecular and Cellular Biology, 21: 7287-7294.

Lin DM., and Goodman CS. (1994). Ectopic and increased expression of fasciclin II alters motoneuron growth cone guidance. Neuron. 13(3): 507-523.

Lindsley D L, and Zimm GG. (1992). The Genome of Drosophila melanogaster (San Diego, California: Academic Press)

Lowrey PL, Shimomura K, Antoch MP, Yamazaki S, Zemenides PD, Ralph MR, Menaker M, Takahashi JS. (2000).Positional syntenic cloning and functional characterization of the mammalian circadian mutation tau. Science. 288:483-492.

Martinek S, Inonog S, Manoukian AS, and Young MW. (2001). A role for the segmentpolarity gene shaggy/GSK-3 in the Drosophila circadian clock. Cell. 105: 769-779.

Mayer ML. (2006). Glutamate receptors at atomic resolution. Nature. 440: 456–462.

Mayer ML. (2011). Structure and mechanism of glutamate receptor ion channel assembly, activation and modulation. Curr Opin Neurobiol. Apr;21(2):283-90.

Montell C. (2005). Drosophila TRP channels. Pugers Arch. (451): 19-28.

Morin LP. (2007). SCN organization reconsidered. J Biol Rhythms. 22:3-13.

Murali T, Pacifico S, Yu J, Guest S, Roberts GG 3rd, Finley RL Jr . (2010). DroID 2011: a comprehensive, integrated resource for protein, transcription factor, RNA and gene interactions for Drosophila. Nucleic Acids Res. 39: 736-743.

Muskus MJ, Preuss F, Fan JY, Bjes ES, and Price JL. (2007). Drosophila DBT lacking protein kinase activity produces long-period and arrhythmic circadian behavioral and molecular rhythms. Molecular and cellular biology. 27: 8049-8064.

Nässel D, Winther A, (2010) Drosophila neuropeptides in regulation of physiology and behaviour. Progress in Neurobiology. 92(1): 42-104.

Ng FS, Tangredi MM, Jackson FR. (2011).Glial cells physiologically modulate clock neurons and circadian behavior in a calcium-dependent manner. Curr Biol. 21(8):625-34.

O'Neill JS, Reddy AB. (2011). Circadian clocks in human red blood cells. Nature. 469(7331):498-503.

Peschel N, Veleri S, Stanewsky R. (2006). Veela defines a molecular link between Cryptochrome and Timeless in the light-input pathway to Drosophila's circadian clock. Proc. Natl. Acad. Sci. 14;103(46): 17313-8.

Peschel, N. (2008). New Insights into Circadian Photoreception and the Molecular Regulation of the Resetting of Drosophila's Circadian Clock. PhD thesis

Postlethwait J H and Schneiderman HA. (1971). Pattern formation and determination in the antenna of the homeotic mutant Antennapedia of Drosophila melanogaster. Dev. Biol. 25: 606-640.

Price, JL, Blau J, Rothenfluh A, Abodeely M, Kloss B, and Young MW. (1998).double-time is a novel Drosophila clock gene th.at regulates PERIOD protein accumulation. Cell. 94: 83-95.

Przewloka MR, Zhang W, Costa P, Archambault V, D'Avino PP, Lilley KS, Laue ED, McAinsh AD and Glover DM. (2007) Molecular analysis of core kinetochore composition and assembly in Drosophila melanogaster. Plos one. 2: e478.

Rees JS, Lowe N, Armean I M, Roote J, Johnson G, Drummond E, Spriggs H, Ryder E, Russell S, Johnston DS, and Lilley K S. (2011). In Vivo Analysis of Proteomes and Interactomes Using Parallel Affinity Capture (iPAC) Coupled to Mass Spectrometry. Molecular and Cellular Proteomics. 10(6): 23861-238610

Rosato E, Kyriacou CP. (2006). Analysis of locomotor activity rhythms in Drosophila. Nat Protoc. 1(2): 559-68.

Rutila J E, Suri V, Le M, So WV, Rosbash M and Hall J C. (1998). CYCLE is a second bHLH-PAS clock protein essential for circadian rhythmicity and transcription of Drosophila period and timeless. Cell. 93: 805-814.

Sathyanarayanan S, Zheng X, Xiao R, and Sehgal A. (2004). Posttranslational regulation of Drosophila PERIOD protein by protein

phosphatase 2A. Cell. 116: 603-615.

Sehadova H, Glaser F T, Gentile C, Simoni A, Giesecke A, Albert J and Ralf Stanewsky. (2009). Temperature entrainment of Drosophila's circadian clock involves the gene nocte and signaling from peripheral sensory tissues to the brain. Neuron. 64: 251-266.

Sehgal A, Price J L, Man B, and Young MW. (1994). Loss of circadian behavioral rhythms and per RNA oscillations in the Drosophila mutant timeless. Science. 263: 1603-1606.

Silbering F, Rytz R, Grosjean Y, Abuin L, Ramdya P, Jefferis GSXE and Benton R. (2011). Complementary function and integrated wiring of the evolutionarily distinct Drosophila olfactory subsystems. J.Neurosci. 31: 13357-13375.

Siepka SM, Yoo SH, Park J, Song W, Kumar V, Hu Y, Lee C, Takahashi JS. (2007). Circadian mutant Overtime reveals F-box protein FBXL3 regulation of cryptochrome and period gene expression. 129: 1011-1023

Skerra A, Schmidt TG. (2000). Use of the Strep-Tag and streptavidin for detection and purification of recombinant proteins. Methods Enzymol.

326: 271-304.

Smach MA, Charfeddine B, Lammouchi T, Othman LB, Letaief A, Nafati S, Dridi H, Bennamou S, Limem K. (2010) Analysis of association between bleomycin hydrolase and apolipoprotein E polymorphism in Alzheimer's disease. Neurol Sci. 31(6): 687-91.

Sobolevsky AI, Rosconi MP, Gouaux E. (2009). X-ray structure, symmetry and mechanism of an AMPA-subtype glutamate receptor. Nature. 462(7274):745-56.

Stanewsky R. (2002). Clock mechanisms in Drosophila. Cell Tissue Res. 309(1):11-26.

Stanewsky R, Frisch B, Brandes C, Hamblen-Coyle MJ, Rosbash M, and Hall JC. (1997). Temporal and spatial expression patterns of transgenes containing increasing amounts of the Drosophila clock gene period and a lacZ reporter: Mapping elements of the PER protein involved in circadian cycling. J. Neurosci. 17: 676-696.

Stanewsky R, Kaneko M, Emery P, Beretta B, Wager-Smith K, Kay SA, Rosbash M, Hall JC. (1998). The cryb mutation identifies cryptochrome as

a circadian photoreceptor in Drosophila. Cell. 95: 681-692.

Stephan FK, Zuker I. (1972).Circadian rhythms in drinking behavior and locomotor activity of rats are eliminated by hypothalamic lesion. Proc Natl Acad Sci USA. 69: 1583-1586

Stoleru D, Nawathean P, Fernandez MP, Menet JS, Ceriani MF, and Rosbash M. (2007). The Drosophila circadian network is a seasonal timer. Cell. 129: 207-219.

Stoleru D, Peng Y, Agosto J, and Rosbash M. (2004). Coupled oscillators control morning and evening locomotor behaviour of Drosophila. Nature. 431: 862-868.

Silbering A F, Rytz R, Grosjean Y, Abuin L, Ramdya P, Jefferis G. S. X. E., Benton R. (2011). Complementary Function and Integrated Wiring of the Evolutionarily Distinct Drosophila Olfactory Subsystems. J. Neurosci. 38: 13357-13375.

Sun Y, Liu L, Ben-Shahar Y, Jacobs JS, Eberl DF, and Welsh MJ. (2009). TRPA channels distinguish gravity sensing from hearing in Johnston's organ. Proc. Natl. Acad. Sci. U.S.A. 106: 13606-13611.

Syed S, Saez L, and Young MW. (2011). Kinetics of doubletime kinase-dependent degradation of the Drosophila period protein. The Journal of biological chemistry. 59: 128-134.

Szular J, Sehadova H, Gentile C, Szabo G, Chou WH, Britt SG, Stanewsky R. (2012). Rhodopsin 5- and Rhodopsin 6-mediated clock synchronization in Drosophila melanogaster is independent of retinal phospholipase C-β signaling. J Biol Rhythms. 27(1): 25-36

Tang X, Platt MD, Lagnese CM, Leslie JR, Hamada FN.(2013). Temperature integration at the AC thermosensory neurons in Drosophila. J. Neurosci. 33, 894–901.

Taghert PH, Shafer OT. (2006).Mechanisms of clock output in the Drosophila circadian pacemaker system. J Biol Rhythms. 21(6):445-57. Review.

Tauber E, Zordan M, Sandrelli F, Pegoraro M, Osterwalder N, Breda C, Daga A, Selmin A, Monger K, Benna C, et al. (2007). Natural selection favors a newly derived timeless allele in Drosophila melanogaster. Science (New York), NY. 316: 1895-1898.

Venken KJ, Schulze KL, Haelterman NA, Pan H, He Y, Evans-Holm M, Carlson JW, Levis RW, Spradling AC, Hoskins RA, Bellen HJ. Nat Methods. (2011). MiMIC: a highly versatile transposon insertion resource for engineering Drosophila melanogaster genes. Nat Methods. 8(9):737-43.

Veraksa, A., Bauer, A., Artavanis-Tsakonas, S. (2005). Analyzing protein complexes in Drosophila with tandem affinity purification-mass spectrometry. Developmental dynamics. 232: 827-834.

Veleri S, Brandes C, Helfrich-Förster C, Hall JC, Stanewsky R. (2003). A self-sustaining, light-entrainable circadian oscillator in the Drosophila brain. Curr Biol. 13(20): 1758-67.

Veleri S, Rieger D, Helfrich-Förster C, Stanewsky R. (2007). Hofbauer-Buchner eyelet affects circadian photosensitivity and coordinates TIM and PER expression in Drosophila clock neurons. J Biol Rhythms. 22(1): 29-42.

Vidalain PO, Boxem M, Ge H, Li S, and Vidal M.. (2004). Increasing specificity in high-throughput yeast two-hybrid experiments. Methods. 32: 363-370.

Wang JY, and Hardin PE. (2006). Circadian oscillation of Drosophila and mammals. Journal of Cell Science. 119: 4793-4795.

Weber F, and Kay SA. (2003). A PERIOD inhibitor buffer introduces a delay mechanism for CLK/CYC-activated transcription. FEBS letters. 555: 341-345.

Wheeler DA, Hamben-Coyle MJ, Dushay MS, and Hall, J. C. (1993). Behavior in light-dark cycles of Drosophila mutants that are arrhythmic, blind, or both. J.Biol. Rhythms 8, 67-94.

Xia S, Miyashita T, Fu TF, Lin WY, Wu CL, Pyzocha L, Lin IR, Saitoe M, Tully T, Chiang AS. (2005) NMDA receptors mediate olfactory learning and memory in Drosophila. Curr Biol. 15(7):603-15.

Xu K, Zheng X, and Sehgal A. (2008). Regulation of Feeding and Metabolism by Neuronal and Peripheral Clocks in Drosophila. Cell Metabolism. 8: 289-300.

Yorozu S, Wong A, Fischer BJ, Dankert H, Kernan MJ, Kamikouchi A, Ito K, Anderson DJ. (2009) Distinct sensory representations of wind and

near-field sound in Drosophila brain. Nature. 12: (458) 201-205.

Yoshii T, Heshiki Y, Ibuki-Ishibashi T, Matsumoto A, Tanimura T, Tomioka K. (2005). Temperature cycles drive Drosophila circadian oscillation in constant light that otherwise induces behavioural arrhythmicity. Eur J Neurosci. 22(5):1176-84.

Yoshii T, Todo T, Wülbeck C, Stanewsky R, Helfrich-Förster C. (2008). Cryptochrome is present in the compound eyes and a subset of Drosophila's clock neurons. J Comp Neurol. 508(6):952-66.

Yu, H., Braun, P., Yildirim, M. A., Lemmens, I., Venkatesan, K., Sahalie, J., Hirozane-Kishikawa, T., Gebreab, F., Li, N., Simonis, N., Hao, T., Rual, J.F., Dricot, A., Vazquez, A., Murray, R. R., Barabasi, A. L., Tavernier, J., Hill, D. E., and Vidal, M. (2008). High-quality binary protein interaction map of the yeast interactome network. Science. 322 (5898): 104-110.

Yuan Q, Joiner WJ, Sehgal A. (2006). A sleep-promoting role for the Drosophila serotonin receptor 1A. Curr Biol. 16(11): 1051-62.

Zhang J, Schulze KL, Hiesinger PR, Suyama K, Wang S, Fish M, Acar M, Hoskins RA, Bellen HJ, Scott MP. (2007). Thirty-one flavors of Drosophila

rab proteins. Genetics. 176(2): 1307-22.

Zhang Y. V., Ni J., Montell C. (2013). The Molecular Basis for Attractive Salt-Taste Coding in Drosophila Science. 340: 1334-1338.

Zimmerman WF, Pittendrigh CS, Pavlidis T. (1968). Temperature compensation of the circadian oscillation in drosophila pseudoobscura and its entrainment by temperature cycles. J Insect Physiol. 14(5): 669-84.